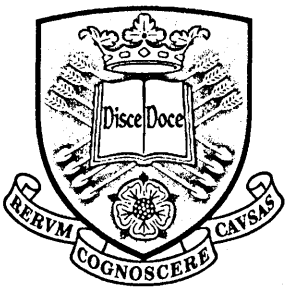


The University Of Sheffield.

# Analysis and Control of FES-Assisted Paraplegic Walking with Wheel Walker

by

**Rozita Jailani**

A thesis submitted to the University of Sheffield for the degree of
**Doctor of Philosophy**

Department of Automatic Control and Systems Engineering
The University of Sheffield
Mappin Street
Sheffield, S1 3JD
United Kingdom

**May 2011**

## DEDICATION

I dedicate this work to my beloved husband, Zamali Zamin, my daughter Nur Alya Farzana, my son, Muhammad Ammar Luqman and my mother Rahmah Sayed Jonid, and to the memory of my father Jailani Ismail.

# Abstract

The number of people with spinal cord injury (SCI) is increasing every year and walking has been found to be the most exciting and important prospect to these patients to improve their quality of life. Many individuals with incomplete SCI have the potential to walk and every one of them wants to try. Unfortunately up to now, there is less than one third of patients could walk again after SCI. Residual function, the orthotic support, energy expenditure, patient motivation and control technique are some of the factors that influence the walking outcome of spinal cord injured people. In this thesis, a series of studies are carried out to investigate the possibility of enhancing the performance of the functional electrical stimulation (FES) assisted paraplegic walking with wheel walker through the development and implementation of intelligent control technique and spring brake orthosis (SBO) with full utilization of the voluntary upper body effort. The main aim of this thesis is to enable individuals with complete paraplegia to walk again with maximum performance and the simplest approach as possible.

Firstly, before simulation of the system can be made, it is important to select the right model to represent the actual plant. In this thesis, the development of a humanoid and wheel walker models are carried out using MSC.visualNastran4D (vN4D) software and this is integrated with Matlab Simulink® for simulation. The newly developed quadriceps and hamstrings muscle models from the series of experiments are used to represent subject muscles after comparison and validation with other two well-known muscle models are performed.

Several experiments are conducted to investigate the effect of stimulation frequency and pulse-width in intermittent stimulation with isometric measurement from paraplegic subjects. The results from this work can serve as a guidance to determine the optimum stimulation parameters such as frequency and pulse-width to reduce muscle fatigue during FES application. The ability test is introduced to determine

the maximum leg force that can be applied to the specific paraplegic subject during FES functional task with minimum chance of spasm and leg injury.

Investigations are carried out on the control techniques implemented for FES walking with wheel walker. PID control and fuzzy logic control (FLC) are used to regulate the electrical stimulation required by the quadriceps and hamstrings muscles in order to perform the FES walking manoeuvre according to predefined walking trajectory. The body weight transfer is introduced to increase the efficiency of FES walking performance. The effectiveness of body weight transfer and control strategy to enhance the performance of FES walking and reduce stimulation pulses required is examined.

Investigations are carried out on the effectiveness of spring brake orthosis (SBO) for FES assisted paraplegic walking with wheel walker. A new concept in hybrid orthotics provides solutions to the problems that affect current hybrid orthosis, including knee and hip flexion without relying on the withdrawal reflex or a powered actuator and foot-ground clearance without extra upper body effort. The use of SBO can also eliminate electrical stimulation pulses required by the hamstrings muscle for the same FES walking system.

Further improvement of the FES walking system is achieved by introducing finite state control (FSC) to control the switching time between springs, brakes and electrical stimulation during FES assisted walking with wheel walker with the combination of FLC to regulate the electrical stimulation required for the knee extension. The results show that FSC can be used to accurately control the switching time and improve the system robustness and stability.

# Acknowledgements

In the name of Allah, the Most Merciful and Most Gracious. Praise is for Allah, Lord of the world, Guide of the bewildered and joiner of those who are severed; Whose help we seek in worldly matters and in religion. May His blessings and peace be upon our noblest of Prophets and Messengers, Prophet Muhammad S.A.W, the Truthful and Trustworthy, and upon his Family, and Companions, and all those who excel in following them until the Day of Reckoning.

I am deeply indebted to my supervisor, Dr. M. Osman Tokhi for the many helpful suggestions and excellent discussions to improve the thesis in many ways. I also would like express my sincere gratitude to Dr. Samad Gharooni for his help.

This appreciation also includes my fellow research colleagues and all staffs in the Department of Automatic Control and System Engineering, University of Sheffield for their advice and assistance during the execution of the project. Thanks go to the Malaysian Government and Universiti Teknologi MARA for the financial support during my PhD.

Lastly, it would not be possible for me to complete this project without the moral support from my loving husband, Zamali Zamin, my daughter, Nur Alya Farzana and my son, Muhammad Ammar Luqman. They have sacrificed a lot due to my study abroad.

Last but not least, my special thanks to my loving mother, Rahmah Sayed Jonid, my sisters and brothers, all my family members and my friends for their understanding, support and encouragement through the years.

# Table of Contents

# List of Figures

# List of Tables

# Chapter 1

# Introduction

## 1.1 Overview

Paraplegia is impairment in motor and/or sensory function of the lower extremities. It is usually the result of spinal cord injury (SCI) which affects the neural elements of the spinal canal. The prevalence of SCI is not well known in many countries. In some countries, such as Sweden and Iceland, registries are available. According to new data initiated by the Christopher & Dana Reeve Foundation, there are nearly 1 in 50 people living with paralysis; approximately 6 million people. That number is nearly 33% higher than previously estimated in 2007 (CDRF, 2010). In the United Kingdom, incident of SCI are 10 to 15 per million people per annum which are 600 to 900 new cases per year (Swain and Grundy, 2002). Sisto et al. (2008) reported that more than 200,000 people in the United States (US) suffer from SCI and each year more than 10,000 new cases occur while in China there are approximately 60, 000 new cases per year (Qiu, 2009).

The majority of SCI (61%) comprise of male population and 39% are female. The average age for spinal cord injuries is 48 years old. These injuries result from motor vehicle accidents (24%), work-related accidents (28%), sport/recreation accidents (16%), falls (9%), natural disaster (1%), birth defect (3%), victim violence (4%) and unknown reason (9%) (CDRF, 2010). Quadriplegia is slightly more common than paraplegia.

Brown-Triolo et al. (1997) found that 51% of SCI subjects defined mobility in terms of life impact and autonomy, and gait was found to be perceived as the first choice in possible technology applications. Their subjects also indicated willingness

to endure time intensive training and undergo surgery operation if mobility is guaranteed. Therefore, solutions to mobility loss were seen as an exciting prospect to these patients.

## 1.2 Spinal Cord Injury

A SCI usually begins with a sudden, damage or traumatic blow to the spinal cord that fractures or dislocates vertebrae and results in a loss or impaired function causing reduced mobility or/and feeling (Apparelyzed, 2010). The damage begins at the moment of injury when displaced bone fragments, disc material, or ligaments bruise or tear into spinal cord tissue. Instead, an injury is more likely to cause fractures and compression of the vertebrae, which then crush and destroy the axons, extensions of nerve cells that carry signals up and down the spinal cord between the brain and the rest of the body. An injury to the spinal cord can damage a few, many, or almost all of these axons. Some injuries will allow almost complete recovery but others will result in complete paralysis (NIND, 2010).

Spinal cord injury can occur from many causes, common causes of damage are trauma (automobile crashes, gunshot, falls, sports injuries, war injuries, etc.) or disease (Transverse Myelitis, Vascular malformations, development disorders, Ischemia, Tumor, Polio, Spina Bifida, Friedreich's Ataxia, etc.). The spinal cord does not have to be severed in order for a loss of function to occur. In most people with SCI, the spinal cord is intact, but the cellular damage to it results in loss of function.

SCIs are classified as either complete or incomplete. An incomplete injury means that the ability of the spinal cord to convey messages to or from the brain is not completely lost. In an incomplete injury, some sensation and/or movement below the level of the injury is retained. A person with an incomplete injury may be able to move one limb more than another, may be able to feel parts of the body that

cannot be moved, or may have more functionality on one side of the body than the other. With the advances in acute treatment of SCI, incomplete injuries are becoming more common. Recent evidence suggests that over 95% of people with incomplete SCI recover some locomotor function. On the other hand, a complete injury is indicated by a total lack of voluntary movement, sensory and motor function below the level of injury. Both sides of the body are equally affected. Recent evidence suggests that less than 5% of people with complete SCI recover locomotion. People who survive on SCI will most likely have medical complications such as chronic pain and bladder and bowel dysfunction, along with an increased susceptibility to respiratory and heart problems. Successful recovery depends upon how well these chronic conditions are handled every day (Apparelyzed, 2010).

The spinal cord is about 18 inches long and extends from the base of the brain, down the middle of the back, to about the waist. The nerves that lie within the spinal cord are upper motor neurons (UMNs) and their function is to carry the messages back and forth from the brain to the spinal nerves along the spinal tract. The spinal nerves that branch out from the spinal cord to the other parts of the body are called lower motor neurons (LMNs). These spinal nerves exit and enter at each vertebral level and communicate with specific areas of the body. The sensory portions of the LMN carry messages about sensation from the skin and other body parts and organs to the brain. The motor portions of the LMN send messages from the brain to the various body parts to initiate actions such as muscle movement (Apparelyzed, 2010).

Generally, the higher in the spinal column the injury occurs, the more dysfunction a person will experience. Figure 1.1 shows the level of injury and extent of paralysis. Cervical SCI's usually cause loss of movement and sensation in all four limbs, both arms and legs resulting in quadriplegia. It usually occurs as a result of injury at T1 or above. Quadriplegia also affects the chest muscles and injuries at C4 or above affects the respiratory muscles and the ability to breathe where it requires a mechanical breathing machine (ventilator). The twelve vertebras in the chest are

called the Thoracic Vertebra. The first thoracic vertebra, T1, is the vertebra where the top rib attaches. Injuries in the thoracic region usually cause loss of movement and sensation in the lower half of the body affecting the chest, right and left legs and is called paraplegia. The sacral vertebra runs from the Pelvis to the end of the spinal column. Injuries to the five Lumbar vertebra (L1 - L5) and similarly to the five Sacral Vertebra (S1 - S5) may affect nerve and muscle control to the bladder, bowel, and legs.

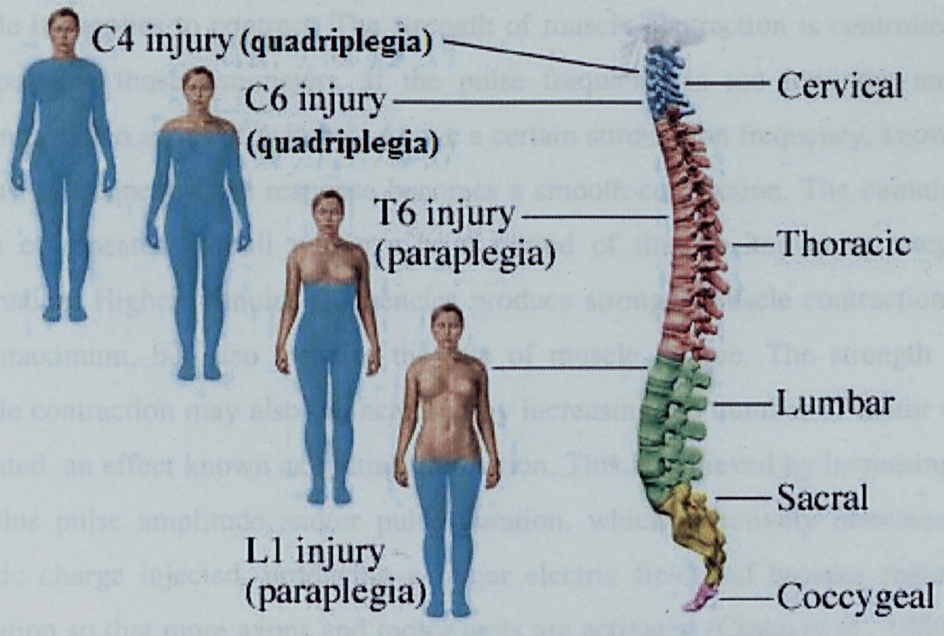


**Figure 1.1: Levels of injury and extend of paralysis (Hassan, 2009)**

## 1.3 Functional Electrical Stimulation

Functional electrical stimulation (FES) is a safe technique that produces contractions in muscles by means of small electrical stimulation to stimulate the physical or bodily functions lost through nervous system impairment, caused by paralysis resulting from SCI, head injury, stroke or other neurological disorders. FES has been used widely in rehabilitation for therapy, function restoration and

maintenance of vital function in muscle weakness and/or paralysis. It was first introduced as functional electrotherapy by Liberson in 1961 to correct foot drop in people with stroke and later with people with multiple sclerosis from 1977 (Liberson et al., 1961). A year later, Moe and Post (IFESS, 2010) changed the name to functional electrical stimulation and the name remains so until now.

Stimulation is delivered as a waveform of electrical current pulses, which are characterized by three parameters: pulse frequency, amplitude, and duration. Figure 1.2 shows that the nerve sends a message received from 2 FES electrodes to the muscle it supplies to contract. The strength of muscle contraction is controlled by manipulating those parameters. If the pulse frequency is too low, the muscle responds with a series of twitches. Above a certain stimulation frequency, known as the fusion frequency, the response becomes a smooth contraction. The cumulative effect of repeated stimuli within a brief period of time is known as temporal summation. Higher stimulus frequencies produce stronger muscle contractions up to a maximum, but also increase the rate of muscle fatigue. The strength of a muscle contraction may also be increased by increasing the number of motor units activated, an effect known as spatial summation. This is achieved by increasing the stimulus pulse amplitude and/or pulse duration, which effectively increases the electric charge injected, producing a larger electric field and broader region of activation so that more axons and motor units are activated (Crago et al., 1980). In most neuroprostheses, the strength of muscle contraction is controlled by modulating the pulse amplitude or pulse duration, and the stimulus frequency is set constant and as low as possible to avoid fatiguing the muscle prematurely.

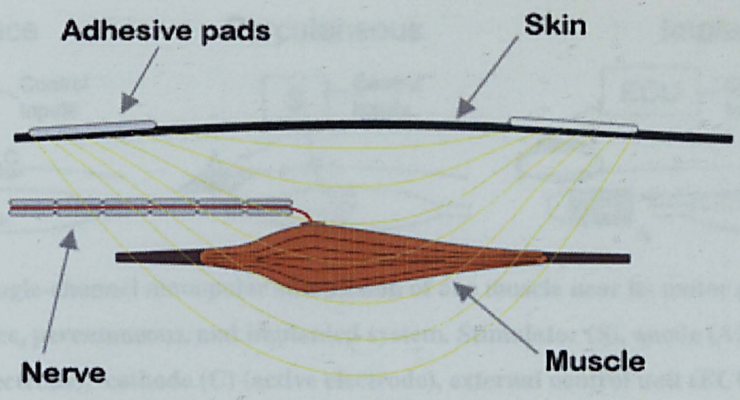


**Figure 1.2: Muscle contraction using FES (FESNW, 2010)**

The electrical stimulation may be delivered using surface, percutaneous, or implanted systems (Figure 1.3). Surface systems, sometimes referred to as transcutaneous systems, utilize electrodes that are placed on the skin and are connected with flexible leads to a stimulator that may be worn around the waist, the arm, or the leg. Usually, a sensor or switch that controls the stimulation is also connected to the stimulator. Surface electrodes are readily available in a variety of sizes from many manufacturers.

The electrodes are placed on the skin over the nerves or over the motor points of muscles to be activated. The advantages of surface systems are that they are non-invasive and relatively technologically simple. Therefore, these systems are easily applied in the clinic, easily reversible, and relatively inexpensive, making them especially well utilized in therapeutic applications. However, the repeated placement of electrodes in appropriate locations to get the desired response requires skill and patience. Also, it can be difficult to achieve isolated contractions or activate deep muscles.

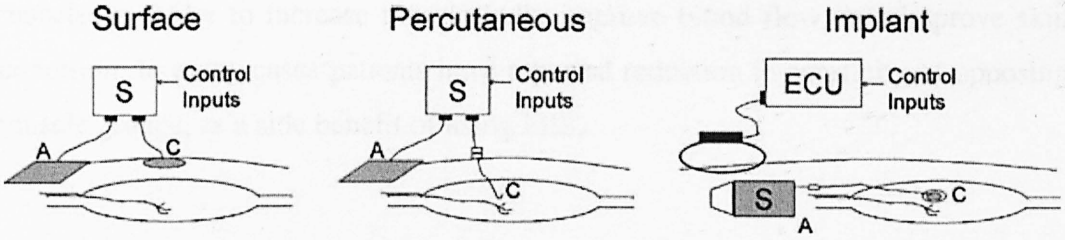


**Figure 1.3: Single-channel monopolar stimulation of one muscle near its motor point is shown for a surface, percutaneous, and implanted system. Stimulator (S), anode (A) (reference electrode), cathode (C) (active electrode), external control unit (ECU).**

Percutaneous systems make use of intramuscular electrodes that pass through the skin and are implanted into the muscle to be activated. Percutaneous electrodes can activate deep muscles, can provide isolated and repeatable muscle contractions, and are less likely to produce pain during stimulation because they bypass the sensory afferents in the skin. An electrode is inserted through the skin and implanted in the muscle using a hypodermic needle. The electrode leads exit the skin and are connected to external stimulation equipment. A large surface electrode is used as the return electrode. The percutaneous interface on the skin is protected by placing a junction connector over the skin surface where the electrodes exit. Percutaneous systems provide a minimally invasive technique for investigating the feasibility of restoring functional muscle contractions without having to prematurely subject research participants to implantable system surgery.

Implanted neuroprosthetic systems are designed for long-term use. Unlike surface and percutaneous systems, the stimulator is implanted, eliminating the need for wiring outside of the body to an external stimulator. The implanted electrodes are connected by leads under the skin to the implanted stimulator. Thus, the electrodes can be made with larger and more durable leads because they do not pass through the skin. They are often connected to the stimulator using in-line connectors, which permit the surgical removal and replacement of individual electrodes if necessary.

Currently, applications of FES include standing, walking, cycling, rowing, ambulation, grasping, male sexual assistance, bowel-and-bladder function control and respiratory control. FES can also be used as an exercise system for paralysed

muscles in order to increase muscle bulk, improve blood flow, and improve skin condition. In many cases patients have reported reduction in spasticity of opposing muscle groups, as a side benefit of using FES.

## 1.4 FES-assisted Walking

The vital aim of lower extremity FES systems is to enable individuals with complete paraplegia to walk again. Walking involves a translation of the body's centre of gravity through a space in a safe manner along a pathway requiring the least energy. Paraplegics are physically disabled in most cases and some people may be able to walk to a certain extent. One way to accomplish this task is to provide them with assistive devices, such as crutches (Bajd et al., 1992, 1994; Zefran et al., 1996), walker (Dutta et al., 2008; Hu et al., 2004; Popovic et al., 1999; Scheiner et al., 1994; Zhaojun et al., 2006), braces (Marsolais and Mansor, 1992), orthosis (Hendershot and Philips, 1988; Jaspers et al., 1996; Solomonow et al., 1992) and walk trainer (Bouri et al., 2006).

The physiological benefits of standing and walking for persons with paraplegia were first mentioned by Abrahamson in 1948 (Abrahamson, 1948), who stated that an hour of standing each day will prevent osteoporosis in the lower limbs and will help to prevent urinary calculi and genitourinary infections. Walking for paraplegics also can increase their physical fitness, bone mass density, independence and quality of life. Kralj and Bajd (1989) introduced the technique of eliciting a flexion withdrawal reflex of the hip, knee and ankle by stimulating the peroneal nerve using a single electrode, to produce lower extremity motion toward the swing phase of walking gait. Graupe and Kohn (1998) introduced Parastep™ that uses four to six channels of bilateral surface stimulation of quadriceps, proneal nerves and if necessary the glutei to enable paraplegia to walk for a short distance with help of walker. Before that, they used EMG signals as a feedback to control the FES stimulation for the same purpose (Graupe, 1989, Graupe et al., 1982,

1989).

Quigley M. J. (1977) reported that only about two percent paraplegic will reach the level of household ambulation. The main reason is that paraplegic needs more energy to ambulate using orthosis and the procedure for most orthoses is difficult and time consuming. Clinkingbeard et al. (1964) found that a paraplegic expends nine times more energy per meter than a normal person walking at a comfortable speed. Moreover, Mikelberg and Reid (1981) in their 5 years study found that 50% of patients for whom orthoses were prescribed did not use them. Therefore, a new orthosis design which can reduce the energy expenditure, is safe and practical is aimed to improve the acceptance of orthoses. Similar to the hybrid FES activity, the performance of FES-assisted walking gait can be enhanced through the implementation of an efficient control strategy. Suitable electrical stimulation to the muscle is required in achieving a smooth and well coordinated walking gait.

## 1.5 Research Objectives

The main aim for this research is to develop a reliable, effective, safe and affordable FES-assisted paraplegic walking with wheel walker. In order to achieve this aim successfully, several research objectives are set as follows:

1. To develop the humanoid and wheel walker models that duplicate the subject and actual wheel walker used in this research as accurate as possible using suitable software.

2. To optimize the subject's leg properties based on pendulum test using evolutionary algorithms to complete the humanoid model developed in 1.

3. To carry out a muscle fatigue test to investigate the effect of stimulation parameters on the subject's muscle fatigue. Also, to perform tests to examine the subject's leg limitation.

4. To develop a muscle model based on experimental data obtained from the subject. This will ensure that the developed model representing the subject's muscle is as accurate as possible.

5. To develop intelligent control strategies for FES-assisted walking with wheel walker that is able to deliver correct amount of electrical stimulation to the muscle to achieve smooth and safe walking gait.

6. To minimize the electrical stimulation applied to the quadriceps and hamstrings muscle by introducing a body weight transfer technique and a novel spring brake orthosis to assist walking process so that it is more efficient, effective, smooth, safe and reliable.

## 1.6 Contributions

The main contributions of the research can be highlighted as follows:

**Modelling the dynamic humanoid FES-walking with wheel walker:** In this study, the wheel walker and humanoid are modelled using dynamic computer aided software called MSC.visualNastran4D (vN4D). The humanoid model is built up using anthropometric data obtained from the subject used in this research while the wheel walker model is duplicated from a real wheel walker available in the market. The vN4D combines CAD, motion, physics-based animation and finite element analysis (FEA) simulation into a single functional modelling system. The vN4D enables engineers to simulate how a design behaves under real world conditions

without having to solely rely on costly physical prototypes. This is a new method of simulating the system performance without placing the subject to risk.

**Optimizing subject leg's stiffness and damping:** In this study, evolutionary algorithms, genetic algorithm (GA) and particle swarm optimisation (PSO) are used to optimize stiffness and damping of subject leg based on passive pendulum test output obtained from the subject. This will make the model developed imitate the subject used as accurate as possible. The current method of obtaining these parameters is by using mathematical equations, so far the use of evolutionary algorithm approach to estimate these parameters has not been reported yet.

**Novel muscle model:** This research has successfully developed a novel muscle model for paraplegic. The muscle model is developed based on experimental data obtained from the paraplegic. The muscle model has been compared with two well-known muscle models developed previously by other researchers.

**Investigation of the effect of FES on paraplegic muscle fatigue:** In this research, the effect of FES on muscle fatigue has been examined. The results from this study indicate the best selection of stimulation parameters that can be used for the particular functional task. A simple rule has also been introduced to calculate paraplegic maximum ability that can be used to avoid leg spasm or/and leg injury during and after stimulating paraplegic leg. The main contributions in this area are the identification of leg performance and optimum stimulation parameters. So far, there is no publication available to obtain optimum stimulation parameters of FES for the paraplegic and most of the previous research obtain stimulation parameters.

**Intelligent control of FES-walking:** In this research, intelligent control techniques using fuzzy logic and PID control are proposed to regulate the stimulation pulse width required by the quadriceps and hamstrings muscles in order to perform a smooth walking gait. Both controllers are able to track predefined walking trajectories thoroughly but fuzzy logic control uses less electrical stimulation

compared to PID control. In this respect, the effectiveness of these two controllers is investigated.

**Body weight transfer technique to reduce electrical stimulation:** In this research, a new body weight transfer (BWT) technique is introduced. This technique can improve the paraplegic walking performance by reducing the electrical stimulation required. BWT is practical technique that can be applied to paraplegic walking with wheel walker.

**Spring brake orthosis for FES-walking:** In this research, a new methodology for paraplegic gait, based on exploiting natural dynamics of human gait, is introduced. The work is a first effort towards restoring natural like swing phase in paraplegic gait through a new hybrid orthosis, referred to as spring brake orthosis (SBO). This mechanism simplifies the control task and results in smooth motion and more-natural like trajectory produced by the flexion reflex for gait in spinal cord injured subjects. SBO was first introduced in 2001 by Gharooni for leg swing and in this thesis the work is extended to increase paraplegic walking performance using SBO.

**Finite state control for FES-walking with SBO:** In this research, finite state control is developed for the implementation of intention detection and activity co-ordination levels of hierarchical control in FES-walking and SBO mechanism. The finite state control is proposed to automatically control the output from the fuzzy logic used to control the stimulation pulse widths required by the quadriceps muscles and control the switch of the brake used in SBO while the subject voluntarily performs the upper body part manoeuvre with the help of wheel walker. This study proposes a novel approach which is used to increase the stability and efficiency of FES-walking with SBO.

## 1.7 Thesis Outlines

**Chapter 1:** This chapter defines SCI and introduces the theory and brief history of FES for person with SCI. Moreover, this chapter defines the problem and significance of FES for paraplegic mobility. Additionally, the objectives and contributions of the research are described in detail. Finally, the list of publications and achievement arising from this research work are provided.

**Chapter 2:** This chapter illustrates the process of modelling of humanoid and wheel walker using the vN4D environment. This chapter describes the optimisation process of leg's passive parameters using evolutionary algorithms. Two different evolutionary algorithms used are genetic algorithm (GA) and particle swarm optimisation (PSO). Results from both algorithms are compared with the measurement and estimation made using mathematical equations published earlier. The best results obtained are then used to complete the humanoid model.

**Chapter 3:** This chapter describes the anatomy and physiology of the human skeletal muscle. This chapter also presents the development of paraplegic quadriceps and hamstrings muscle model using adaptive neuro-fuzzy inference system (ANFIS). A series of experiments using FES with different stimulation frequency, pulse width and pulse duration to investigate the behaviour of output muscle torque is conducted. The data thus collected is used to develop the paraplegic muscle model.

**Chapter 4:** This chapter compares isometric performance and paraplegic muscle fatigue using two different protocols: pulse-width modulation and frequency modulation. Muscle performance is assessed by measuring percent decline in peak force and maximum muscle force for different stimulation frequencies and pulse widths. A simple rule is introduced to avoid spasm or injury to the leg during FES application.

**Chapter 5:** This chapter describes a simulation of bipedal locomotion to generate stimulation pulses for activating muscles for paraplegic walking with wheel walker using FES. The study is carried out with a model of humanoid with wheel walker using the vN4D dynamic simulation software. The developed stimulated muscle models of quadriceps and hamstrings discussed in chapter 3 are used for knee extension and flexion. Proportional-integral-derivative (PID) and fuzzy logic control (FLC) are designed in Matlab/Simulink to regulate the muscle stimulation pulse-width required to drive FES-assisted walking gait and the computed motion is visualised in graphic animation from vN4D. The body weight transfer (BWT) technique is introduced to improve the paraplegic walking performance.

**Chapter 6:** This chapter introduces a new methodology for paraplegic gait, based on exploiting natural dynamics of human gait. The work is a first effort towards restoring natural like swing phase in paraplegic gait through a new hybrid orthosis, referred to as spring brake orthosis (SBO). This mechanism simplifies the control task and results in smooth motion and more-natural like trajectory produced by the flexion reflex for gait in spinal cord injured subjects. Stimulated muscle model of quadriceps is need for knee extension. A comparison of performance of FLC and PID control for knee extension using SBO is provided and the best controller is obtained.

**Chapter 7:** This chapter investigates the effectiveness of finite state control (FSC) to control walking gait and SBO switching sequences. This technique can reduce the need for sensor in SBO alone. The results obtained are discussed.

**Chapter 8:** This chapter summarizes the thesis with highlight remarkable achievements and concludes the work. Future research directions and recommendations are also presented.

## 1.8 Publications

The lists of publications arising from this research work that are either published, accepted or under review are listed below. Further publications are currently at the writing stage.

**Refereed Journals**

1. **Jailani, R.**, Tokhi, M.O., Gharooni, S.C. and Ibrahim, B.S.K.K., (2010). FES-assisted walking with spring brake orthosis: Simulation studies, *Journal of Applied Bionics and Biomechanics*, IOS Press, Vol. 8, ISSN: 1176-2322. *In press.*

2. **Jailani, R.**, Tokhi, M.O. and Gharooni, (2010). Hybrid Orthosis: The Technology for spinal cord injury, *Journal of Applied Sciences*, Asian Network for Scientific Information, Vol. 10, Num. 21, pp 1-8, 2010. ISSN: 1812-5654.

3. **Jailani, R.**, Tokhi, M.O., Gharooni, S.C. and Hussain Z., (2009). A novel approach in development of dynamic muscle model for paraplegic with functional electrical stimulation, *Journal of Engineering and Applied Science*, Medwell Journals, Vol. 4, Num. 4, pp 272-276, 2009. ISSN: 1816-949x, 1818-7803.

**Refereed Conferences Proceedings**

1. **Jailani, R.**, Tokhi, M.O. and Gharooni, S.C., Finite state control of FES-assisted walking with spring brake orthosis. *Proceedings of the 13th International Conference on Computer Modelling and Simulation (UKSim2010),* 30 March – 1st April 2011, Cambridge, United Kingdom, ISBN 978-0-7695-4376-5.

2. **Jailani, R.**, Tokhi, M.O. and Gharooni, S.C., Fuzzy logic control of knee extension for FES-assisted walking with spring brake orthosis. *The 2010 IEEE International Conference on Systems, Man, and Cybernetics (SMC 2010),* 10-13 October 2010, Istanbul, Turkey.

3. **Jailani, R.**, Tokhi, M.O., Gharooni, S.C. and Joghtaie, M., (2010). The effectiveness of spring brake orthosis for FES-assisted walking with wheel walker. *13th International Conference on Climbing and Walking Robots and the Support Technologies for Mobile Machines (CLAWAR2010),* 31 August-3 September 2010, Nagoya, Japan.

4. **Jailani, R.**, Tokhi, M.O. and Gharooni, S.C., (2010). Spring brake orthosis for FES-assisted walking with wheel walker. *Proceedings of International Conference on Modelling and Simulation in Engineering, Economics and Management (MS'2010),* 15-17 July 2010, Barcelona, Spain. World Scientific Publishing Company, Singapore, pp. 677 – 685. ISBN: 13 978-981-4324-43-4, 10 981-4324-43-4.

5. **Jailani, R.**, Tokhi, M.O. and Gharooni, S.C., (2010). Fuzzy and PID controls of FES-assisted walking with body weight transfer: Simulation studies. *Proceedings of International Conference on Modelling and Simulation in Engineering, Economics and Management (MS'2010),* 15-17 July 2010, Barcelona, Spain. World Scientific Publishing Company, Singapore, pp. 581 – 588. ISBN: 13 978-981-4324-43-4, 10 981-4324-43-4.

6. **Jailani, R.**, Tokhi, M.O. and Hussain, Z., (2010). PID control of knee extension for FES-assisted walking with spring brake orthosis. *The 4$^{th}$ Asia Modelling Symposium (AMS2010),* 26-28 May 2010, Kota Kinabalu, Malaysia.

7. **Jailani, R.**, Tokhi, M.O. and Hussain, Z., (2010). The effectiveness of body weight transfer in FES-assisted walking with wheel walker. *Proceedings of the 12th International Conference on Computer Modelling and Simulation (UKSim2010),* 24-26 March 2010, Cambridge, United Kingdom, pp 206-211, ISBN 978-0-7695-4016-0.

8. **Jailani, R.**, Tokhi, M.O., Gharooni, S.C. and Hussain, Z., (2010). Development of dynamics muscle model with functional electrical stimulation. *Proceedings of the International Conference on Complexity in Engineering (COMPENG2010)*, 22–24 February, Roma, Italy, pp 132-134, ISBN 978-0-7695-3974-4.

9. **Jailani, R.**, Tokhi, M.O., Gharooni, S.C., Joghtaei, M. and Hussain, Z., (2009). The investigation of the simulation frequency and intensity on paraplegic muscle fatigue. *Proceedings of 14th Annual Conference of the International Functional Electrical Stimulation Society (IFESS2009)*, 13–17 September, Seoul, Korea.

10. **Jailani, R.**, Tokhi, M.O., Gharooni, S.C. and Hussain, Z., (2009). Passive stiffness and viscosity of dynamic leg model: Comparison between GA and PSO. *Proceedings of CLAWAR 2009: The Twelfth International Conference on Climbing and Walking Robots and the Support Technologies for Mobile Machines,* Istanbul, Turkey, 09 – 11 September 2009, World Scientific Publishing Company, Singapore, pp. 1128 – 1136. ISBN: 13 978-981-4291-26-2, 10 981-4291-26-9.

11. **Jailani, R.**, Panogiostis, K., Tokhi, M.O., Hussain, Z., Huq, M.S. and Ibrahim, B.S.K.K., (2009). Proportional derivative like fuzzy logic control of dynamic walking with crutches. *Proceedings of CLAWAR 2009: The Twelfth International Conference on Climbing and Walking Robots and the Support Technologies for Mobile Machines,* Istanbul, Turkey, 09 – 11

September 2009, World Scientific Publishing Company, Singapore, pp. 1137 – 1144. ISBN: 13 978-981-4291-26-2, 10 981-4291-26-9.

12. **Jailani, R.**, Tokhi, M.O., Gharooni, S.C., Hussain, Z., Joghtaei, M. and Ibrahim, B.S.K.K., (2009). Estimation of passive stiffness and viscosity in paraplegic: A dynamic leg model in visual nastran. *Proceedings of the 14th International Conference on Methods and Models in Automation and Robotics (MMAR2009)*, 19–21 August, Międzyzdroje, Poland.

13. **Jailani, R.**, Hussain, Z., Tokhi, M.O. and Huq, M.S., (2009). Dynamic simulation of walking with crutches for paraplegics. *Proceedings of the 2nd International Conference on Control, Instrumentation and Mechatronics Engineering (CIM2009)*, pp. 727–731, 2–3 June, 2009, Malacca, Malaysia.

**Award**

1. Best Paper Award
   The 14th IEEE International Conference on Methods and Models in Automation and Robotics (MMAR 2009), Miedzyzdroje, Poland, 19-21 August 2009.

# Chapter 2

# Modelling of Humanoid with Wheel Walker and Identification of Passive Leg Parameters

## 2.1 Introduction

In order to simulate a system and control its operation accurately, it is important to choose the right model for the plant. This chapter illustrates the way humanoid with wheel walker using MSC.visualNastran 4D (vN4D) is modelled. The vN4D software is selected for this project where it combines computer aided design (CAD), motion, finite element analysis (FEA) and control technologies into a single functional modelling system. It can be linked to Matlab/Simulink control system within a single program. The Matlab/Simulink software is chosen to build the control system and simulate the system in real-time.

This chapter also presents investigations into pendulum test to measure passive knee motion from a paraplegic subject. The test is used to evaluate changes in the knee angular displacement, passive stiffness and damping. Then, genetic algorithm (GA) and particle swam optimisation (PSO) are used with vN4D to optimise passive stiffness and damping values for modelling the paraplegic leg. The best passive leg's values obtained from GA and PSO are used to complete the leg model integrated with vN4D. Therefore, the humanoid with wheel walker together with passive stiffness and damping represent the actual paraplegic subject that has been used throughout this thesis.

## 2.2 Modelling of Humanoid with Wheel Walker

### 2.2.1 Visual Nastran Software

The MSC.visualNastran 4D (vN4D) software is for design and engineering professional development of products involving assemblies of three dimensional (3D) parts. It is an engineering tool that will resolve design problems, reduce failures and warranty costs, turn around designs faster and work with existing Window® based 3D computer-aided design (CAD) systems. The vN4D combines CAD, motion, physics-based animation and finite element analysis (FEA) simulation into a single functional modelling system (MSC visualNastran, 2011).

The vN4D is a physical testing tool in a virtual environment and consists four main parts, namely *draw it, move it, break it* and *control it*. The *draw it* associates and integrates with virtually every 3D CAD system and provides photo realistic rendering of images, animations, and mark-up. The *move it* provides 3D rigid body dynamics and kinematics, ability to check the moving interferences or clearances, measures velocity, force, torque, friction, gravity, acceleration and other meters and always to obtain contact, collision and response. The *break it* comprises integrated dynamic and static stress analyses, automatic calculation of loads & stresses throughout assembly, stress and strain, deflection, vibration, factor of safety and thermal analyses. The *control it* integrates vN4D with the control systems testing and visualization with Simulink®, formula language, Excel, and C++/VB OLE control (MSC visualNastran, 2011).

The vN4D's versatility allows users to complete models in several ways. The general idea is to firstly define the geometry of the model, mesh this geometry, load & constrain the mesh and lastly analyse this model. Figure 2.1 shows the basic idea behind modelling with vN4D.

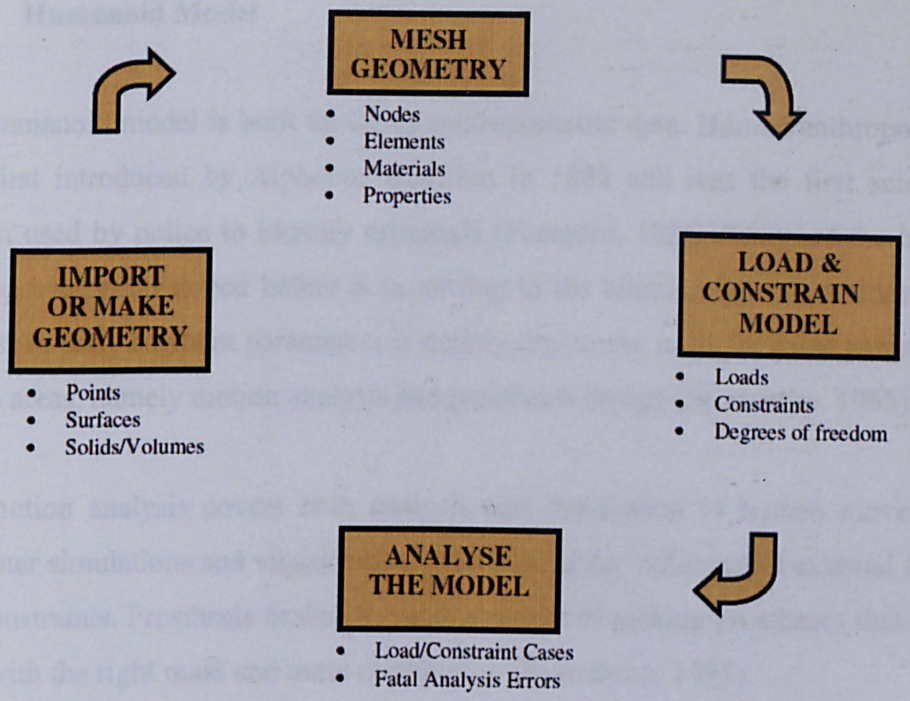


**Figure 2.1: Basic modelling steps for vN4D for windows**

The vN4D enables engineers to simulate how a design behaves under real world conditions without having to solely rely on costly physical prototypes. There are many successful works done using vN4D. Cŏte (2004) used vN4D for dynamic and static modelling of piezoelectric composite structures while Acosta-Marquez (2005) used vN4D to model the exoskeleton for gait analysis. Keith (2010), a technical specialist at ColTech Inc., confirmed that vN4D saved several fundamental mistakes in their internal combustion engine test, which could have caused four months delay. In addition, they would have scrapped two or three engine sets before discovering the problems if they did not run the simulation using vN4D. Wang (2001) used vN4D to investigate the strength of composite honeycomb structures and found that results from both computation and experiment indicated good agreement. These prove that vN4D software for modelling and simulation is reliable, accurate and suitable for non linear systems.

### 2.2.2 Humanoid Model

The humanoid model is built up using anthropometric data. Human anthropometry was first introduced by Alphonse Bertillon in 1883 and was the first scientific system used by police to identify criminals (Pheasant, 1886). Many of the human anthropometry developed before is according to the human origin. Nowadays, the interest in body segment parameters is mainly due to the need for these parameters in two areas, namely motion analysis and prosthesis design (Bjørnstrup, 1995).

The motion analysis covers both analysis and description of human movement, computer simulations and visualization of motion under influence of external forces and constraints. Prosthesis design is partly a matter of making prostheses that looks right with the right mass and mass distribution (Bjørnstrup, 1995).

In this study, well-known human anthropometry that has been developed in 1966 by Drillis and Contini (1966) and obtained from Winter (1990) is chosen to make sure that the same procedures can be duplicated for subject from different origin. Human body is characterized by three main planes and directions with planes crossing in the centre of the body gravity. The length and mass of each body segment is expressed according to the overall weight and height of the humanoid. The physical measurements of the body segment vary with body build, sex and racial origin. This technique demonstrates that the corresponding anthropometric data is obtained as fractions of body height or weight. These segment proportions serve as good approximation in the absence of better data, preferably measured directly from the individual. Figure 2.2 shows the average set of segment length that is expressed as a fraction of body height, H. The corresponding segment length used for the humanoid is given in Table 2.1, which corresponds to fraction of body height. The humanoid developed in this work is based on an available paraplegic subject whose height (H) is 1.73m. This is to make sure the simulation results can be validated with experimental results from the same paraplegic subject.

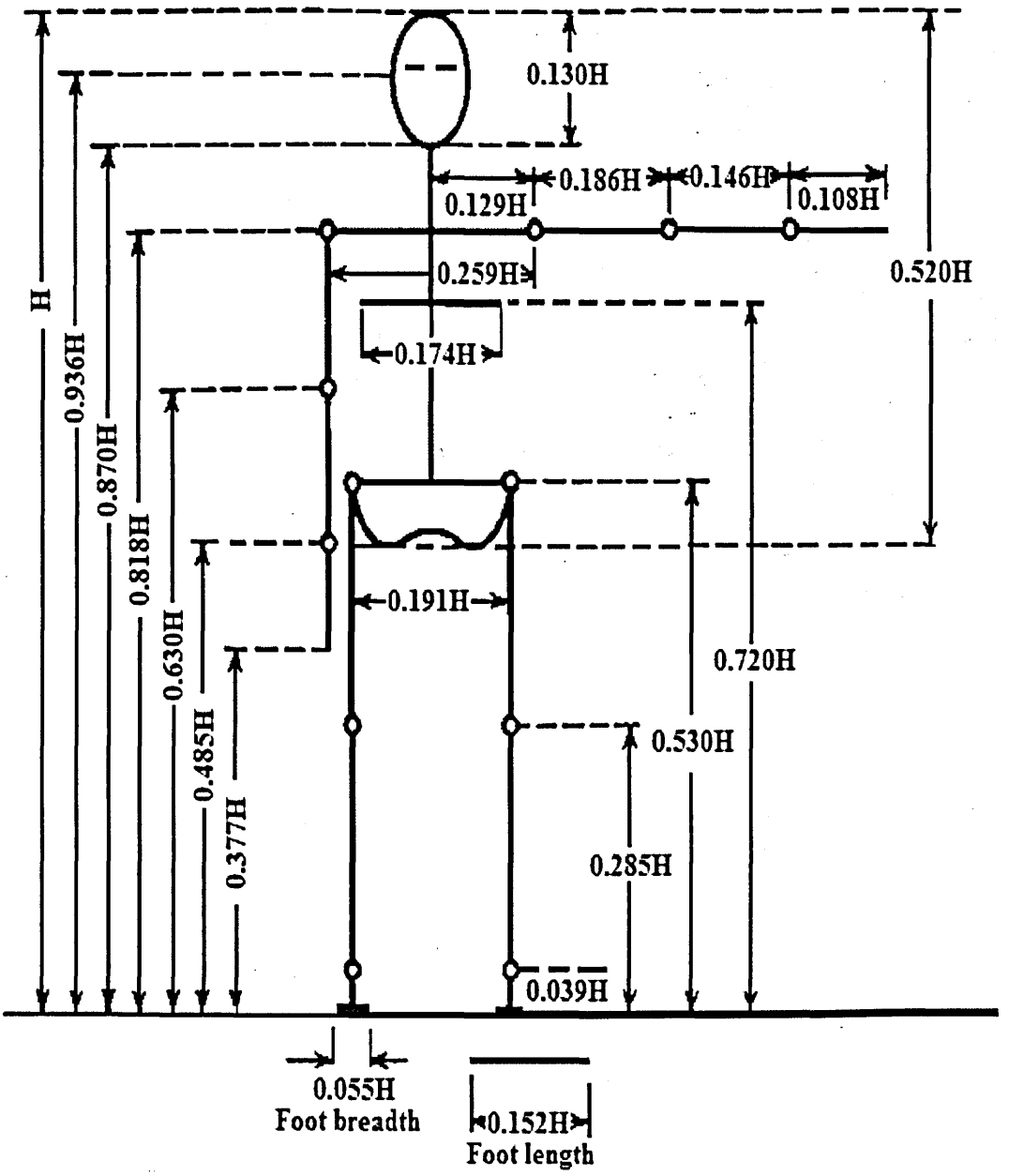


Figure 2.2: Human dimensions (Winter, 2005)

**Table 2.1: Body segment length**

| Body segments | Segment Length, Fraction of height (H) | Segment Length (m) |
|---|---|---|
| Foot height | 0.039H | 0.06747 |
| Foot breadth | 0.055H | 0.09515 |
| Foot Length | 0.152H | 0.26296 |
| Shank | 0.246H | 0.42558 |
| Thigh | 0.245H | 0.42385 |
| Trunk | 0.288H | 0.49824 |
| Hand | 0.108H | 0.18684 |
| Lower arm | 0.146H | 0.25258 |
| Upper arm | 0.186H | 0.32178 |
| Neck | 0.052H | 0.08996 |
| Head | 0.13H | 0.2249 |

The same anthropometric data was used to determine the mass of each body segment. Table 2.2 lists the mass of each segment related to total body mass based on the same paraplegic subject body weight of 80kg. In order to determine an appropriate shape for each of the body segment, the location of the centre of mass of the segment is required. The locations of the centre of mass together with segment density were also obtained from anthropometric data of the same source. The density of each body segment was used to determine its volume which then determined their segment width. Table 2.3 lists both location of the centre of mass and segment density. The location of the centre of mass is measure from the top of the each of the body segment.

**Table 2.2: Body segment mass**

| Body segments | Segment Mass, Fraction of weight (M) | Segment Mass (kg) |
|---|---|---|
| Foot | 0.0145M | 1.16 |
| Shank | 0.0465M | 3.72 |
| Thigh | 0.1M | 8.00 |
| Trunk | 0.497M | 39.76 |
| Hand | 0.006M | 0.48 |
| Forearm | 0.016M | 1.28 |
| Upper arm | 0.028M | 2.24 |
| Head & Neck | 0.083M | 6.64 |

**Table 2.3: Location of segment centre of mass, density and volume for humanoid**

| Body segment | Centre of mass proximal (m) | Density (kg/l) | Volume ($m^3$) |
|---|---|---|---|
| Hand | 0.09454 | 1.16 | 0.0004 |
| Lower arm | 0.10861 | 1.13 | 0.0011 |
| Upper arm | 0.14029 | 1.07 | 0.0021 |
| Foot | 0.12300 | 1.10 | 0.0011 |
| Shank | 0.18427 | 1.09 | 0.0034 |
| Thigh | 0.18353 | 1.05 | 0.0076 |
| Head and Neck | 0.31486 | 1.11 | 0.0003 |
| Trunk | 0.24912 | 1.03 | 0.0386 |

The body segments are linked with humanoid joint. Table 2.4 shows the developed humanoid joints, their types, axes of rotation and degree of freedom. The most important joints are the knee and hip joints as they contribute significantly to FES assisted paraplegic mobility. The elbow and shoulder are also considered to be important as they provide voluntary upper body movement assisting the walking gait.

**Table 2.4: Properties of the humanoid joints**

| Body segment | Number of segment | Type of joint | Axis of rotation | Control parameter | Degree of freedom |
|---|---|---|---|---|---|
| Head | 1 | Rigid | NA | NA | 0 |
| Neck | 1 | Rigid | NA | NA | 0 |
| Shoulder | 2 | Revolute | Y | NA | 1 |
| Elbow | 2 | Revolute | Y | NA | 1 |
| Wrist | 2 | Revolute | Y | NA | 1 |
| Hip | 2 | Revolute | X | NA | 1 |
| Knee | 2 | Revolute Motor | X | Torque | 1 |
| Ankle | 2 | Revolute | X | NA | 1 |

The humanoid developed using the anthropometric data and appropriate joint properties under vN4D software are shown in Figure 2.3. The developed model will be used together with wheel walker.

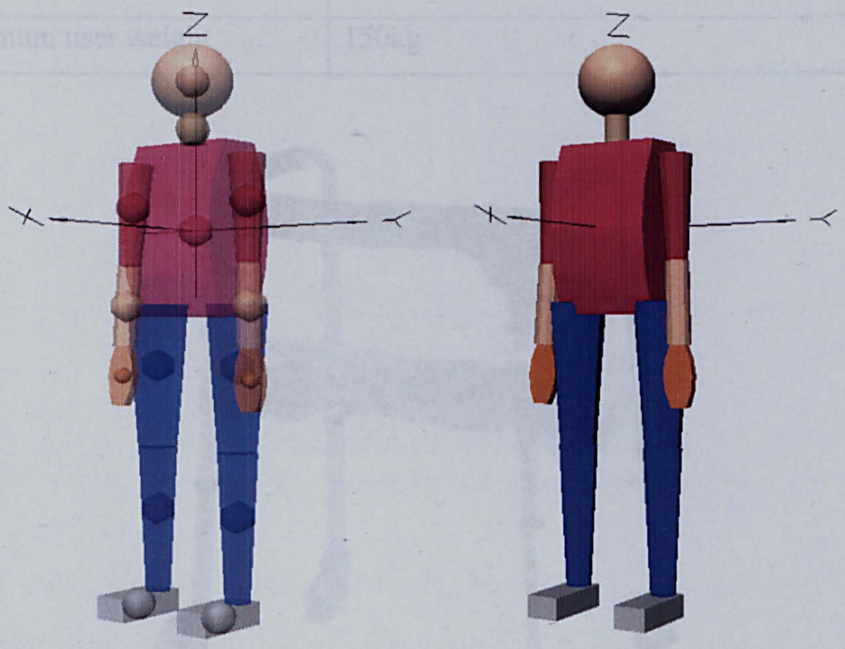


(a) (b)

**Figure 2.3: Humanoid using vN4D (a) with and (b) without the position of centre of gravity**

### 2.2.3 Wheel Walker Model

The wheel walker model is developed using vN4D software based on the design of a wheel walker sold by Pines Discount Pharmacy™, see Figure 2.4. The model developed incorporates all the basic parts of the real machine. Table 2.5 shows specifications of the wheel walker used in this research. The material, dimensions and weight are duplicated from a real wheel walker available in the market (Anonymous, 2010). Figure 2.5 shows the developed wheel walker using vN4D.

**Table 2.5: Specification of wheel walker model**

| Part | Specification |
|---|---|
| Frame | Material: Anodized aluminium<br>Depth: 49 cm<br>Width: 64 cm<br>Height: min 82cm, max 98cm<br>Weight: 2.4 kg<br>Radius 2.5 cm |
| Maximum user weight | 150kg |

**Figure 2.4: Wheel walker (Anonymous, 2010)**

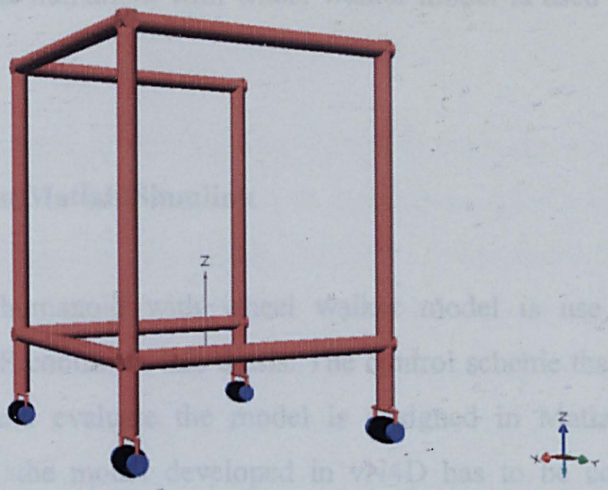

**Figure 2.5: Wheel walker model using vN4D**

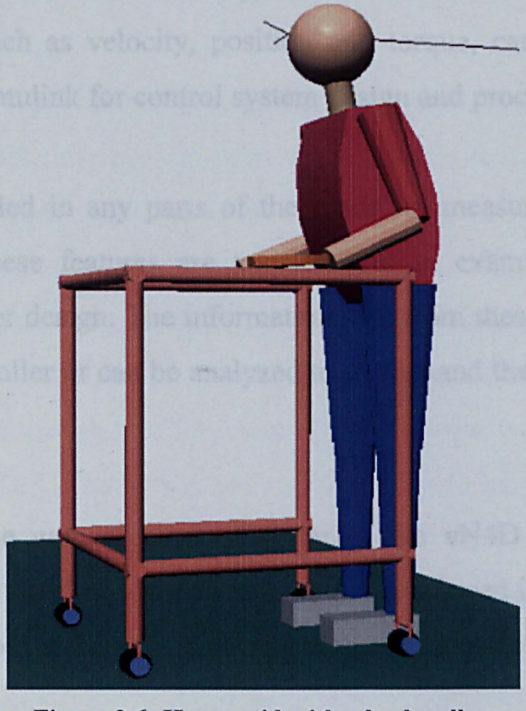

**Figure 2.6: Humanoid with wheel walker**

The final stage of the development of the humanoid with wheel walker model incorporated is the combination of both models. It is important to make sure that the humanoid is attached to the wheel walker model at the right position and right joint. The complete model of the humanoid with wheel walker using vN4D is

shown in Figure 2.6. This humanoid with wheel walker model is used throughout this thesis.

### 2.2.4 Visual Nastran in Matlab/Simulink

The completed vN4D humanoid with wheel walker model is use for futher investigation such as FES control in this thesis. The control scheme that is applied to the system to test and evaluate the model is designed in Matlab/Simulink environment. Therefore, the model developed in vN4D has to be connected to Matlab/Simulink. The advantage of the vN4D is that it is easily linked to Matlab/Simulink. A block representing the vN4D model can be inserted into Simulink obtained from Simulink library for further evaluation. The parameters in the vN4D model, such as velocity, position and torque, can be linked between vN4D and Matlab/Simulink for control system design and processing.

Meters can be installed in any parts of the model to measure position, velocity, acceleration, etc. These features are very helpful in examining the model for structural or controller design. The information sent from these meters can be used as inputs to the controller or can be analyzed to understand the structural behaviour as required.

Figure 2.7 shows the general block diagram of the vN4D model controller in Maltlab/Simulink. In this thesis, the muscle model developed in Matlab/Simulink is linked to the humanoid walking with wheel walker model developed in vN4D for model evaluation.

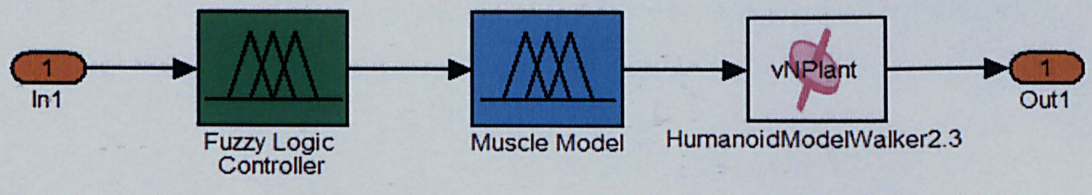


**Figure 2.7: Block diagram of vN4D model in Matlab/Simulink**

## 2.3 Identification of Passive Leg Parameters

The vN4D is four-dimension software that can be used to represent normal human body and its movement accurately. However, to develop paraplegic leg model is very difficult since there are many parameters that have to be considered. Riener and Edrich (1997;1999) and Riener et al. (1996) presented a simple mathematical model that describes passive elastic joint properties of hip, knee and ankle. They used healthy subjects in their experiments, and later (Edrich et al., 2000) they used six paraplegics and ten healthy subjects and found that passive elastic properties of the joints in the healthy subjects can be adopted to model the lower extremities of paraplegic. So far, the literature lacks publication on development of joint model to represent paraplegic leg, specifically using vN4D software.

The trajectory of the oscillating leg from passive pendulum test provides a set of kinematic parameters such as peak angular values, useful to monitor the changes in the range of knee motion. Lin and Rymer (1991) and Fee (1994, 1995a, b) used this test to understand the underlying neurophysiological disturbances in spasticity. The kinematic outcome depends on a combination of forces acting at the joint. Among these forces, stiffness and damping represent the passive resistances provided by the articular and periarticular tissues to the angular motion. While stiffness is the resistance of an elastic body to resist deformation, damping is related to the friction between adjacent layers of tissues. Thus, both parameters may influence the range of motion of knee joint affecting angular displacement and both are important parameters to represent the properties of the leg. Ferrarin and Pedotti (2000) used these parameters obtained from their passive pendulum test together with data from FES trials to develop their dynamic joint torque model.

## 2.4 Optimisation Techniques

Recently, GA and PSO techniques appeared as promising approaches for handling various optimization problems. These techniques are finding popularity within the research community as design tools and problem solvers because of their versatility and ability to perform optimization in complex multimodal search spaces (Panda and Padhy, 2007). GA can be viewed as a general-purpose search method, an optimization method, or a learning mechanism, based on principles of biological evolution, reproduction and "the survival of the fittest" (Goldberg, 1989). GA is well suited to and has been extensively applied to solve complex design optimization problems because it can handle both discrete and continuous variables, nonlinear objective and constrained functions without requiring gradient information (Abdel-Magid and Abido, 2003). PSO is inspired by the ability of flocks of birds, schools of fish, and herds of animals to adapt to their environment, find rich sources of food, and avoid predators by implementing an information sharing approach. The PSO technique was invented in the mid 1990s while attempting to simulate the choreographed, graceful motion of swarms of birds as part of a sociocognitive study investigating the notion of collective intelligence in biological populations (Kennedy and Eberhart, 1995).

In this chapter, passive knee stiffness, damping and relaxation indexes are measured using Wartenberg's technique (Wartenberg, 1951). Relaxation indexes represent the subject's leg relaxation level during experiment. These indexes are for monitoring purposes. GA and PSO are used with vN4D to find the stiffness and damping, and the results are assessed in comparison to one another. Stiffness and damping thus found are validated by results from the experiment while results from Wartenberg technique are for comparison purposes so that the final results can be accurately used to develop paraplegic passive leg model using vN4D.

### 2.4.1 Genetic Algorithm

Genetic algorithm is a robust intelligent optimisation technique with powerful global searching ability in complex spaces (Goldberg, 1989) based on the principle of natural evolution and population genetics without the need of derivative information. It was initiates by Holland (1975) where computational models that mimic natural evolution to solve problems in a wide variety of domains were introduced. Additionally, no continuous conditions of the objective function and design space are needed. GA is implemented as a computer simulation in which a population of abstract representations of candidate solutions to an optimization problem evolves toward better solutions.

A simple GA that has given good results in a variety of engineering problems is composed of three operators; selection, crossover and mutation. These operators are implemented by performing the basic tasks of copying strings, exchanging portion of strings and generating random numbers. These tasks are easily performed on a computer. Selection is simply a process by which strings with large fitness values, good solutions to the problem at hand, receive correspondingly large numbers of copies in the new population while strings exchange information via probabilistic decisions by the second operator called crossover. Crossover provides a mechanism for strings to mix and match their desirable qualities through a random process. The third operator, mutation enhances the ability of the GA to find near optimal solutions. Mutation is the occasional alteration of a value at a particular string position. Figure 2.8 shows the flowchart of the working principle of GA.

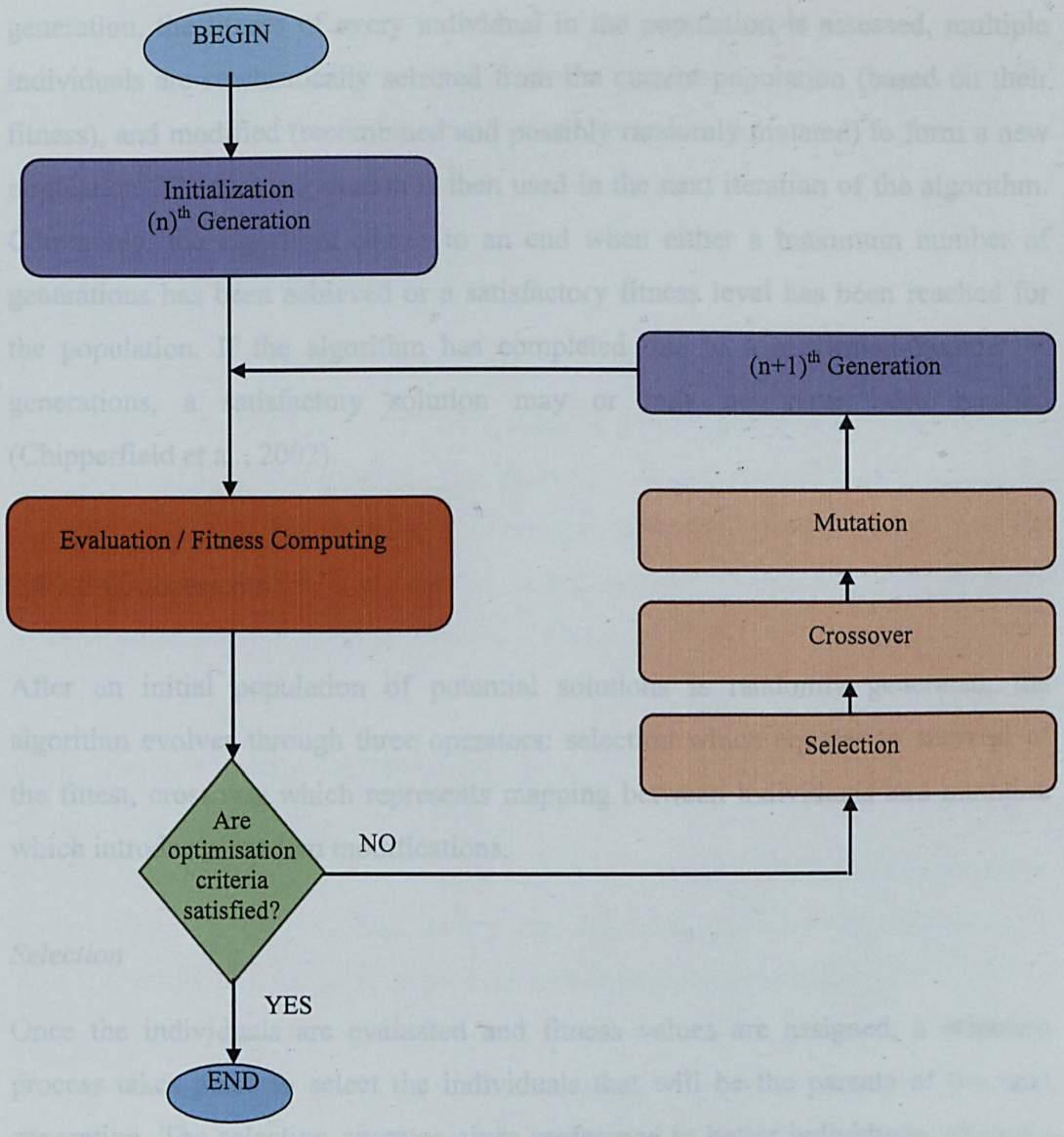


**Figure 2.8: Flowchart of the working principle of genetic algorithm**

2.4.1.1 GA operation

Genetic algorithm is implemented in a computer simulation in which a population of representations (chromosomes) of candidate solutions (individuals) to an optimization problem evolves toward better solutions. The solutions are signified in binary as strings of 0s and 1s, but other encodings are also possible. The evolution normally starts from a population of randomly produced individuals. In each

generation, the fitness of every individual in the population is assessed, multiple individuals are stochastically selected from the current population (based on their fitness), and modified (recombined and possibly randomly mutated) to form a new population. The new population is then used in the next iteration of the algorithm. Commonly, the algorithm comes to an end when either a maximum number of generations has been achieved or a satisfactory fitness level has been reached for the population. If the algorithm has completed due to a maximum number of generations, a satisfactory solution may or may not have been reached (Chipperfield et al., 2002).

#### 2.4.1.2 GA operators

After an initial population of potential solutions is randomly generated, the algorithm evolves through three operators: selection which equates to survival of the fittest, crossover which represents mapping between individuals and mutation which introduces random modifications.

*Selection*

Once the individuals are evaluated and fitness values are assigned, a selection process takes place to select the individuals that will be the parents of the next generation. The selection operator gives preference to better individuals, allowing the individuals to pass on the genes to the next generation. The goodness of each individual depends on its fitness. Fitness may be determined by an objective function or by a subjective judgement (Goldberg, 1989).

*Crossover*

Crossover is the prime distinguished factor of GA from other optimization techniques. It is the operation responsible for producing new chromosome in the GA. Once the selection operator has selected two individuals from the population, the crossover operator exchanges part of the genetic information to produce new

chromosome. The exchange points are randomly chosen. The two new offspring created from this mating are put into the next generation of the population. By recombining portions of good individuals, this process is likely to create even better individuals (Chipperfield et al., 2002).

*Mutation*

Mutation is another important genetic operator that introduces new genetic structure in the population. With some low probability, a portion of the new individuals will have some of their bits flipped. The purpose is to maintain diversity within the population and inhibit premature convergence. Mutation alone induces a random walk through the search space. Mutation and selection (without crossover) create parallel, noise-tolerant and hill-climbing algorithms (Chipperfield et al., 2002).

### 2.4.2 Particle Swarm Optimisation

The PSO method is a member of wide category of swarm intelligence methods for solving optimization problems. It is a population based search algorithm where each individual is referred to as particle and represents a candidate solution. Each particle in PSO flies through the search space with an adaptable velocity that is dynamically modified according to its own flying experience and also the flying experience of other particles. Figure 2.9 shows a flowchart of the working principle of PSO.

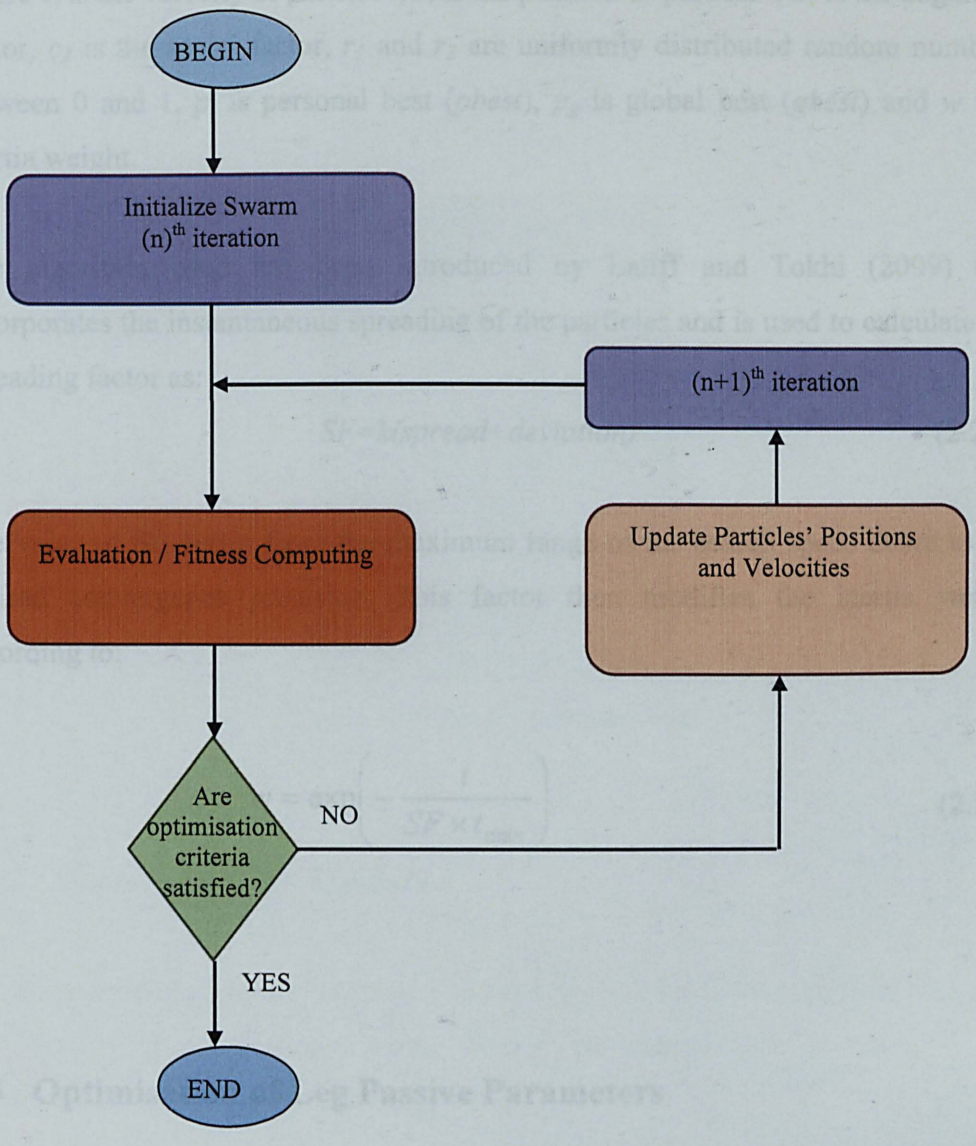


**Figure 2.9: Flowchart of working principle of particle swarm optimization**

In PSO each particle strives to improve itself by imitating traits from its successful peers. Further, each particle has a memory and hence it is capable of remembering the best position in the search space ever visited by it. The position corresponding to the best fitness is known as *pbest* and the overall best out of all the particles in the population is called *gbest* (Panda and Padhy, 2007; Brandstatter and Baumgartner, 2002). The update velocity equation used is

$$v_{id} = wv_{id} + c_1 r_1 (p_{id} - x_{id}) + c_2 r_2 (p_{gd} - x_{gd}) \qquad (2.1)$$

where $v_i$ is the velocity of particle $i$, $x_i$ is the position of particle $i$, $c_1$ is the cognition factor, $c_2$ is the social factor, $r_1$ and $r_2$ are uniformly distributed random numbers between 0 and 1, $p_i$ is personal best (*pbest*), $p_g$ is global best (*gbest*) and $w$ is a inertia weight.

The algorithm used has been introduced by Latiff and Tokhi (2009) that incorporates the instantaneous spreading of the particles and is used to calculate the spreading factor as:

$$SF=k(spread+deviation) \tag{2.2}$$

The value of SF varies from the maximum range of the search space down to the desired convergence precision. This factor then modifies the inertia weight according to:

$$w = \exp\left(-\frac{t}{SF \times t_{\max}}\right) \tag{2.3}$$

## 2.5 Optimisation of Leg Passive Parameters

### 2.5.1 Passive Pendulum Test

During the experiment, a paraplegic subject is placed in a semi-upright sitting position (45° to 60°) with the lower legs hanging over the edge of a table (see Figure 2.10). The thigh is tightened with strap to the table to make it stay in a stationary condition. To avoid any modification to the passive characteristic of the knee due to ankle movements, plastic ankle foot orthosis (AFO) is used to keep the ankle at 90°. The subject's shank is raised and held until the knee muscle is completely relaxed. This may take about 10 to 15 seconds. Then the subject's leg is

allowed to swing freely and the leg movement is recorded until the shank reaches its final resting position.

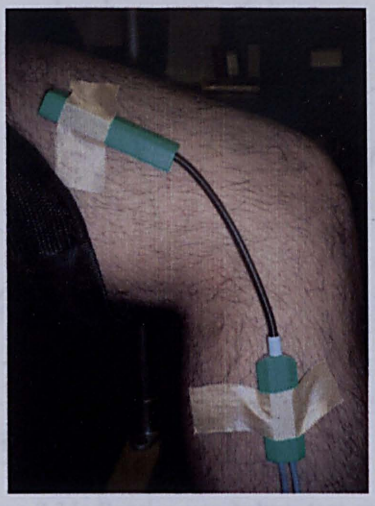

**Figure 2.10: Passive pendulum test**

### 2.5.2 Measurement and Estimation

There are several variables that could be derived from kinematics of pendulum test. The following displacement and timing parameters are measured using Wartenberg's technique (Wartenberg, 1951):

1. Start angle, onset angle *(OA)*
2. Resting angle *(RA)*
3. First 3 peak flexion angles *($F_1$, $F_2$, $F_3$)*
4. First 3 peak extension angles *($E_1$, $E_2$, $E_3$)*
5. Amplitude of initial flexion, $F_{1amp}=F_1-OA$
6. Amplitude of initial extension, $E_{1amp}=F_1-E_1$
7. Plateau amplitude, $PA=RA-OA$
8. Relaxation index, $RI=F_{1amp}/PA$
9. Extension relaxation index, $ERI=E_{1amp}/PA$
10. Period of the first cycle, $T$

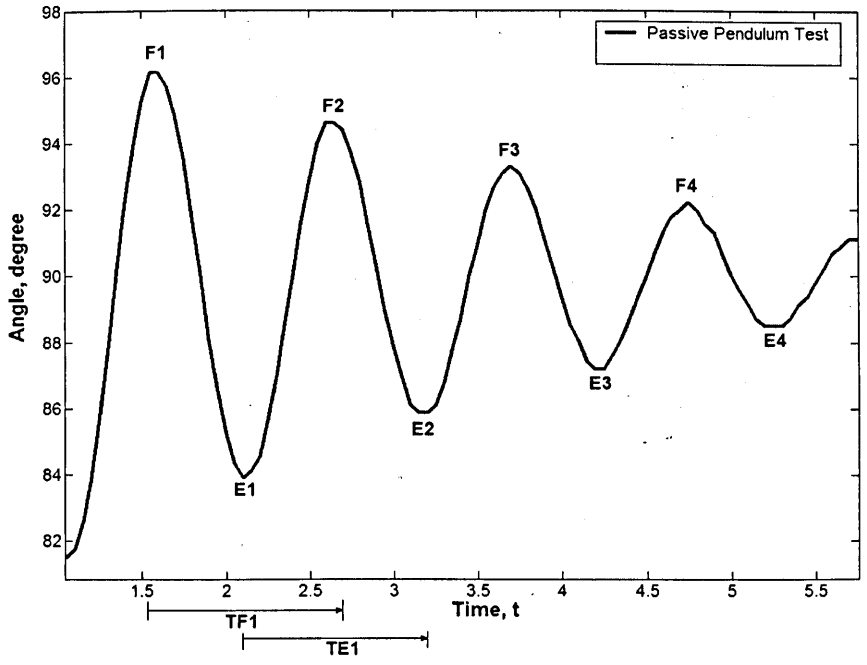


**Figure 2.11: Passive pendulum test output**

Figure 2.11 shows the measurement and estimation of Wartenberg's equation applied to the passive pendulum test output. The high peak represents the knee flexion and low peak represents the knee extension. The stiffness and damping are measured for every cycle of knee flexion and extension.

Knee stiffness *(K)* and damping *(B)* were estimated by computing the damping ratio $(\zeta)$ and the natural frequency $(\omega_n)$ obtained from the test data. The following equations as reported by Lin and Rymer (1991) are used:

$$\zeta = \frac{B}{2\sqrt{JK'}} = \sqrt{\frac{(\ln D)^2}{4\pi^2 + (\ln D)^2}} \tag{2.4}$$

where

$$D = \frac{F_1}{F_2}, \frac{F_2}{F_3}, \frac{F_3}{F_4}, \frac{E_1}{E_2}, \frac{E_2}{E_3}, \frac{E_3}{E_4}$$

where $J$ represents the sagittal moment of inertia applied to the leg-foot complex rotation around the knee axis, $m$ is the leg-foot complex mass, $g$ is the acceleration due to gravity, $l$ leg-foot length from the knee axis and $T$ is time for one complete cycle.

The estimation for $J$, $m$ and $l$ were obtained for the subject according to Winter (1990). Using equations (2.4) and (2.5) the values of damping and stiffness were obtained as follows:

$$\omega_n = \sqrt{\frac{K'}{J}} = \frac{2\pi}{T} \tag{2.5}$$

$$B = 2 \times \zeta \times \omega_n \times J \tag{2.6}$$

$$K = K' - \frac{mgl}{2} \tag{2.7}$$

### 2.5.3 Visual Nastran Leg Model

The vN4D can give an accurate prediction of product performance. In this section, a leg model is built using the anthropometric data discussed in Section 2.3. The corresponding segment length used for the leg model is given in Table 2.2, which corresponds to fraction of body height. Using the anthropometric data above, the leg model was developed using the vN4D. Figure 2.12 shows the developed leg model.

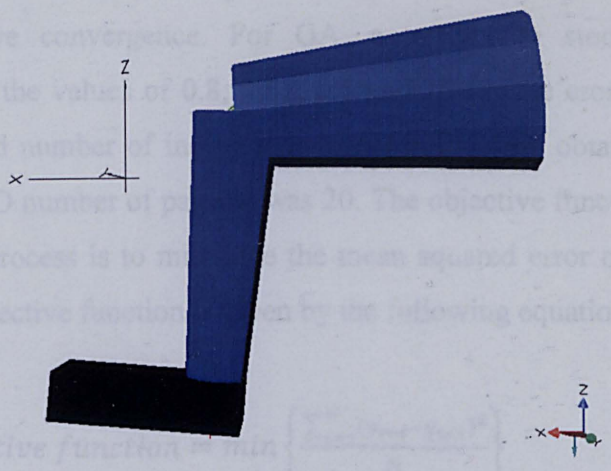


**Figure 2.12: vN4D leg model**

### 2.5.4 Parameter Optimisation

Two algorithms; GA and PSO are used with vN4D to find the passive stiffness and damping values of paraplegic leg. These values are then used to develop paraplegic leg model as shown in Figure 2.13.

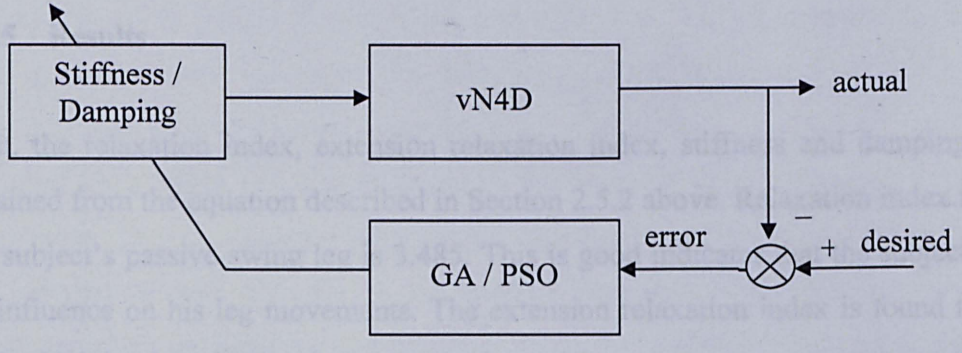


**Figure 2.13: Block diagram of GA/PSO parameter optimization applied to the vN4D leg model**

The use of vN4D to evaluate the individuals' fitness and GA/PSO to optimise the design variables, allows solving complex problems. This approach can be implemented as follows: the variable information of the individuals/particles for each generation in GA/PSO is put into vN4D software automatically in order, the vN4D carries the simulation analysis and the results of the relative individuals'

UNIVERSITY
OF SHEFFIELD
LIBRARY

fitness are output to GA/PSO program. GA/PSO executes to create new individuals particle to achieve convergence. For GA, according to stochastic universal sampling method, the values of 0.8, 0.01, 0.8 and 20 for the crossover, mutation, generation gap and number of individuals respectively were obtained by trial and error while for PSO number of particle was 20. The objective function specified for the optimization process is to minimize the mean squared error of the knee angle trajectory. The objective function is given by the following equation:

$$objective\ function = min\left\{\frac{\sum_{i=1}^{N}(y_{ref}-y_{act})^2}{N}\right\} \quad (2.8)$$

where $y_{ref}$ is the desired knee angle trajectory, $y_{act}$ is actual knee angle trajectory and N is number of sample values.

Under such conditions, the GA and PSO searches well, in a stable manner and without pre-mature convergence. In this chapter, the interface between vN4D and GA/PSO is completed. Then the results from GA and PSO are validated with experimental data.

### 2.5.5 Results

First, the relaxation index, extension relaxation index, stiffness and damping are obtained from the equation described in Section 2.5.2 above. Relaxation index from the subject's passive swing leg is 3.485. This is good indicator that the subject has no influence on his leg movements. The extension relaxation index is found to be 1.83 which is normal value for a paraplegic.

Figure 2.14 shows that the stiffness was maintained about 0.32 Nm/deg from second flexion and above and it was less than 0.32 Nm/deg for the first flexion and extension. This indicates that the maximum passive stiffness for the subject's leg was 0.32 Nm/deg.

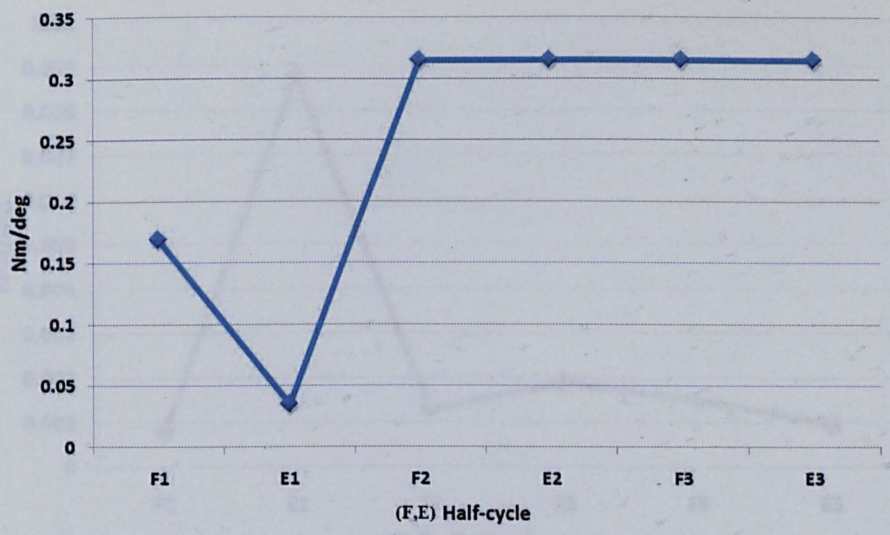


**Figure 2.14: Stiffness computed from the subject during first six half-cycle. F is the stiffness in flexion; E is the stiffness in extension**

Figure 2.15 shows that damping for leg flexion was less than damping for leg extension. However, the damping found from the experimental data by calculation was between 0.0009 Nms/deg and 0.009 Nms/deg.

During the GA optimisation session, it was found that the best performance of the vN4D leg model can be achieved with the optimum values of the damping and the stiffness equal to 0.0031055 Nms/deg and 0.024244 Nm/deg respectively while PSO gave optimum values of the damping and the stiffness equal to 0.0031 Nms/deg and 0.0242 Nm/deg respectively. From these results, stiffness and damping found from GA and PSO are in the range of values obtained from the calculation. These values are obtained by considering all leg movements' cycles and adaptation with the vN4D leg model. Therefore, these experiments are important when the stiffness and damping values for the vN4D leg model may be inaccurate to obtained using calculation.

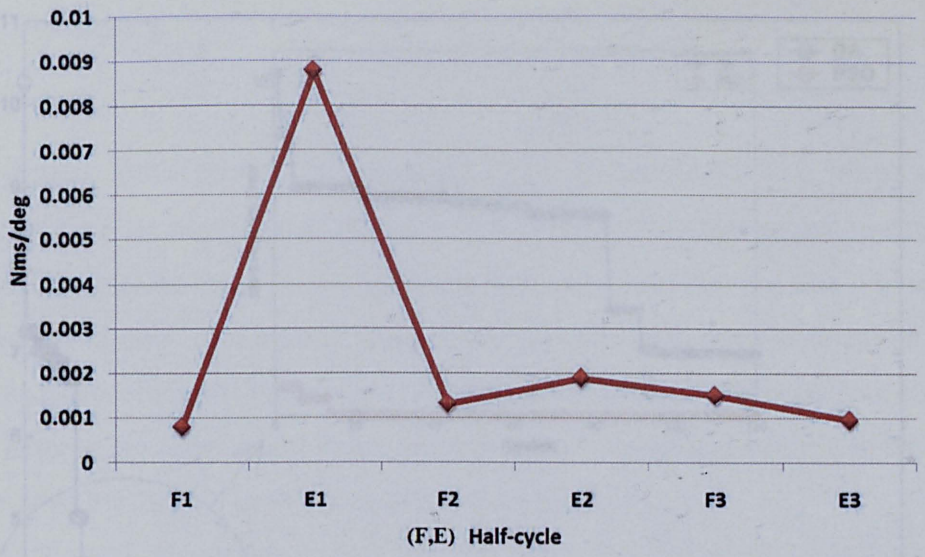


**Figure 2.15: Damping computed from subject during first six half-cycle. F is the damping in flexion; E is the damping in extension**

The convergence rate of the objective function of the system with the number of iterations for GA and PSO are shown in Figure 2.16. From the figure, it is clear that PSO converged at earlier iteration (at 18$^{th}$ iteration) compared to GA which converged at 930$^{th}$ generation. This means that PSO was faster than GA in terms of processing time. Using the damping and stiffness obtained from GA, the modelling gave a satisfactory result for the given experimental data. The percentage of this model accuracy is found to be 98.1 percent while model accuracy obtained from PSO is 0.2 percent less. In this case, both results were good and acceptable because both algorithms gave almost similar values of stiffness and damping. Figure 2.17 shows a comparison between experimental data and data from vN4D leg model with parameters from GA and PSO.

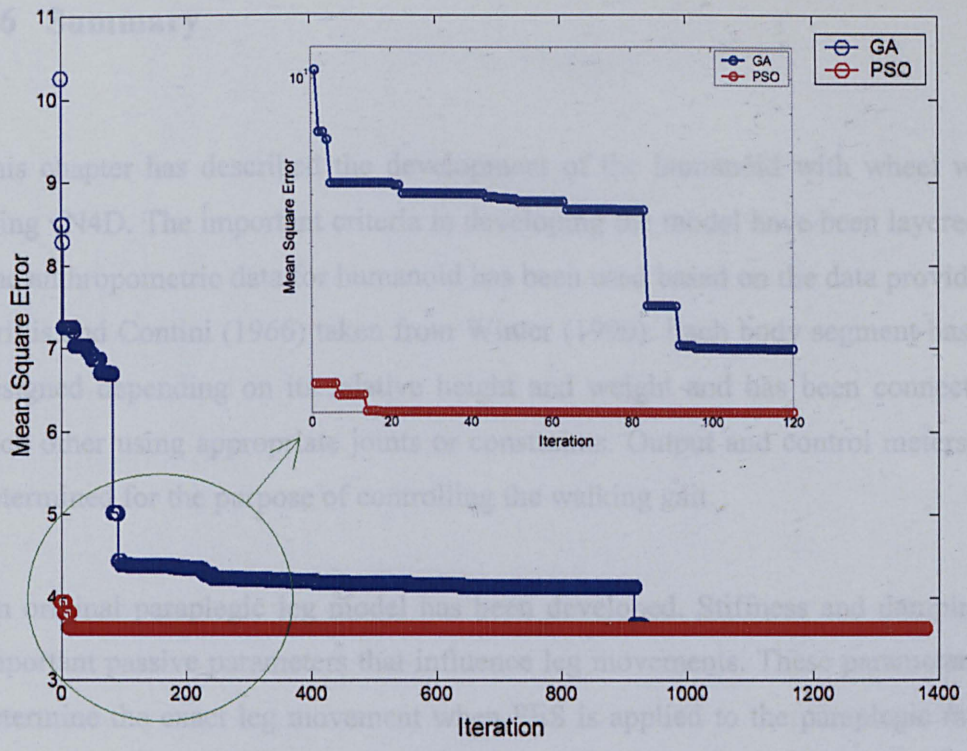


**Figure 2.16: Convergence curve for GA and PSO**

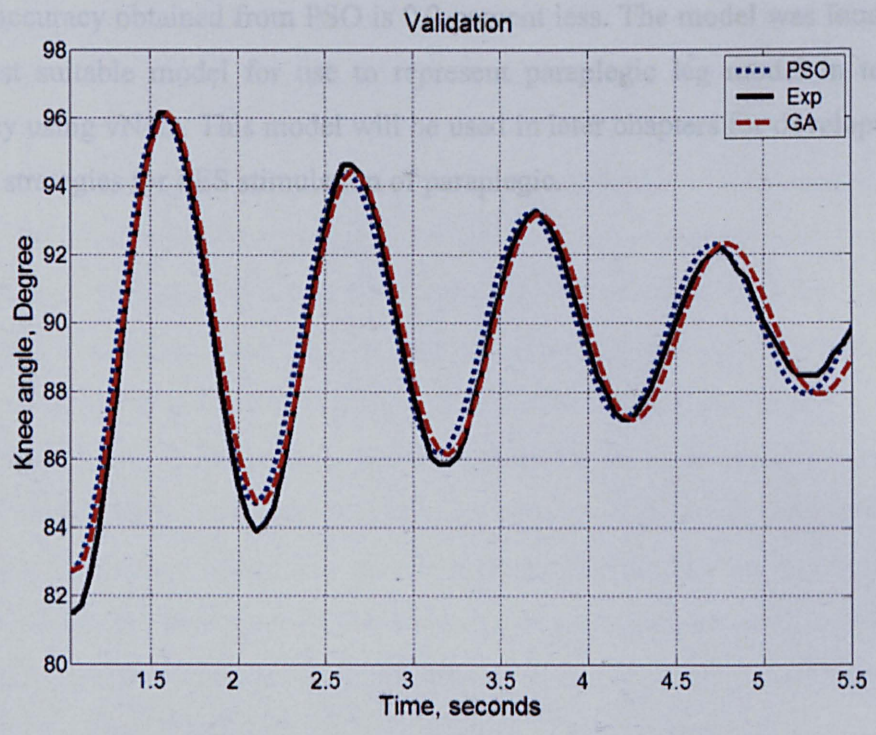


**Figure 2.17: Comparison between the knee angle measured during the passive pendulum test (solid line), simulated by vN4D with parameters from GA (dashed line) and simulated by vN4D with parameters from PSO (dashed-dotted line)**

## 2.6 Summary

This chapter has described the development of the humanoid with wheel walker using vN4D. The important criteria in developing the model have been layered out. The anthropometric data for humanoid has been used based on the data provided by Drillis and Contini (1966) taken from Winter (1990). Each body segment has been designed depending on its relative height and weight and has been connected to each other using appropriate joints or constraints. Output and control meters were determined for the purpose of controlling the walking gait.

An original paraplegic leg model has been developed. Stiffness and damping are important passive parameters that influence leg movements. These parameters will determine the exact leg movement when FES is applied to the paraplegic muscle. The performance of the model, at their respective most optimally tuned set of parameters, the percentage of GA model accuracy is found to be 98.1 percent while model accuracy obtained from PSO is 0.2 percent less. The model was found to be the most suitable model for use to represent paraplegic leg model in terms of accuracy using vN4D. This model will be used in later chapters for development of control strategies for FES stimulation of paraplegic.

# Chapter 3

# Muscle Model

## 3.1 Introduction

This chapter presents the development of paraplegic quadriceps and hamstrings muscle model using adaptive neuro-fuzzy inference system (ANFIS). A series of experiments using functional electrical stimulation (FES) with different stimulation frequencies, pulse width and pulse duration to investigate the behaviour of output muscle torque is conducted. Then these clinical data are used to develop the paraplegic quadriceps and hamstrings muscle models. 500 training data and 300 testing data set are used in the quadriceps muscle model development while 588 training data and 220 testing data set are used for the hamstrings muscle model development. The quadriceps muscle model developed has been validated with clinical data from one of the paraplegic subject and for quadriceps muscle model it also has been validated with two other known muscle models. In other words, the hamstrings muscle model is only validate using testing data set since there are no other hamstrings muscle model developed so far for comparison. In the quadriceps muscle model, the ANFIS muscle model developed is found to be the most accurate muscle model representing paraplegic quadriceps muscle model compared to the other two well known quadriceps muscle models. The established models are then used to predict the behaviour of the underlying system and are used subsequently for the design and evaluation of various intelligent control strategies throughout this thesis.

## 3.2 Physiology of Human Muscle

There are 40% to 60% of the total human body weight is comprise by muscles. Muscle is an organ specializing in the transformation of chemical energy into movement. There are many types of muscles, but they fall into three categories: skeletal, cardiac, and smooth muscles. Their function is to produce force and cause motion by contraction. Cardiac and smooth muscle contraction occurs without conscious thought and is necessary for survival. It is able to function for a century or more, without ever taking a break. Smooth muscle lines the walls of the arteries to control blood pressure, or pushes food through the digestive system while skeletal muscle is responsible for locomotion and can be finely controlled. Examples of skeletal muscles are, movements of the eye, or gross movements like the quadriceps muscle of the thigh. In this thesis, only the skeletal muscle is considered since it is used to affect skeletal movement such as locomotion and maintaining posture. Though this postural control is generally maintained as a subconscious reflex, the muscles responsible react to conscious control like non-postural muscles. As percentage of body mass, an average adult male is made up of 42% of skeletal muscle and an average adult female is made up of 36%.

Muscle is mainly composed of muscle cells. Within the cells are myofibrils; myofibrils contain sarcomeres, which are composed of actin and myosin. Figure 3.1 shows the structure and different levels of skeletal muscle. Individual muscle fibres are surrounded by endomysium. Muscle fibres are bound together by perimysium into bundles called fascicles; the bundles are then grouped together to form muscle, which is enclosed in a sheath of epimysium.

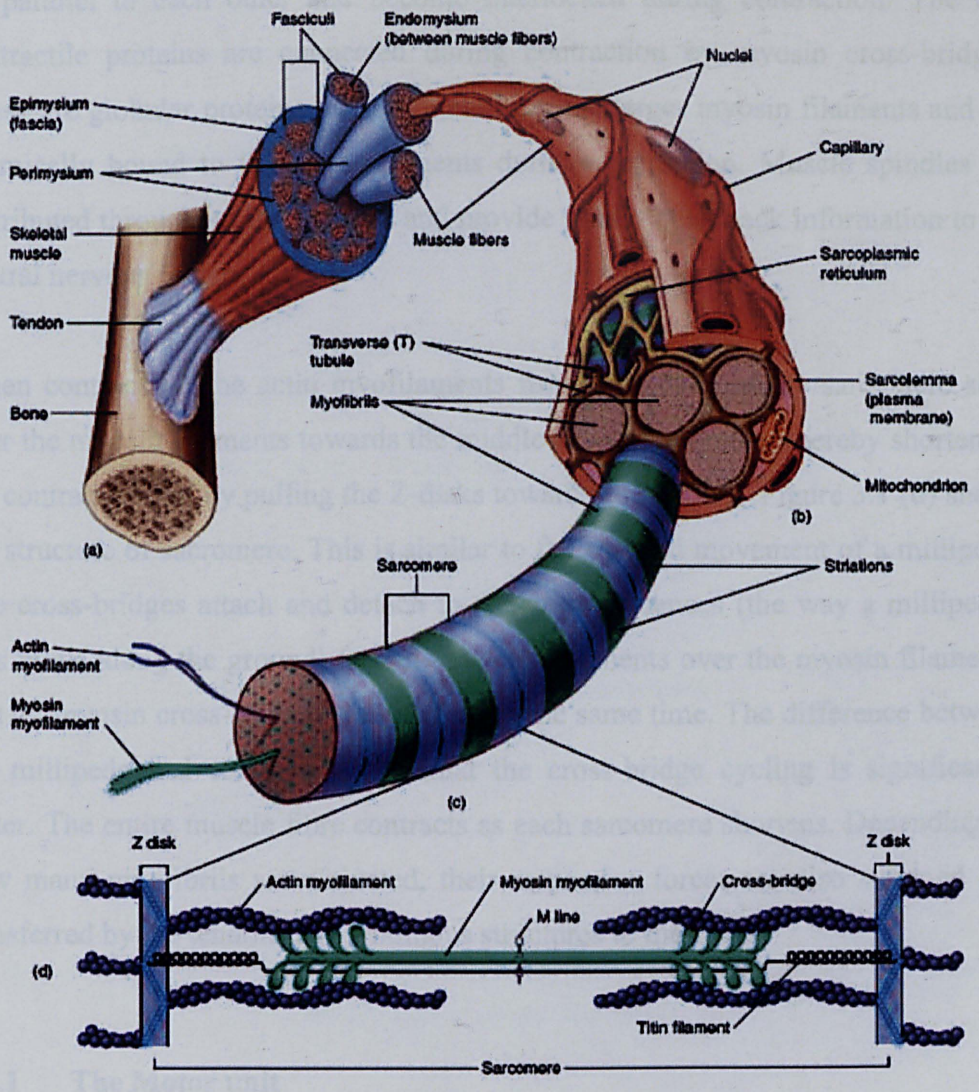


**Figure 3.1: Structural and organisational levels of skeletal muscle (Anonymous, 2010)**

Each muscle is comprised of numerous fibres, each of these in turn consists of many myofibrils, which form the functional units of muscle and affect the contraction and relaxation process. The functional part of the myofibrils consists of numerous contractile units, called sarcomere connected in series. Each sarcomere is composed of different muscle proteins, in particular the two main contractile proteins, myofilaments called actin and myosin. Myosin filaments are thick contractile proteins and remain relatively stationery during contraction. Actin filaments are thin contractile proteins that are drawn towards each other from both ends of the sarcomere during muscle contraction. The actin and myosin filaments

lie parallel to each other and become interlocked during contraction. The two contractile proteins are connected during contraction by myosin cross-bridges. These are globular proteins that originate from the larger myosin filaments and are chemically bound to the actin filaments during contraction. Muscle spindles are distributed throughout the muscles and provide sensory feedback information to the central nervous system.

When contracting, the actin myofilaments from both ends of the sarcomere slide over the myosin filaments towards the middle of the sarcomere, thereby shortening the contractile unit by pulling the Z-disks towards each other. Figure 3.1 (d) shows the structure of sacromere. This is similar to the forward movement of a millipede. The cross-bridges attach and detach in different sequences (the way a millipede's legs move along the ground) to pull the actin filaments over the myosin filaments. Not all myosin cross-bridges are attached at the same time. The difference between the millipede and cross-bridges is that the cross-bridge cycling is significantly faster. The entire muscle fibre contracts as each sarcomere shortens. Depending on how many myofibrils are activated, their respective forces are also summed and transferred by the tendons and tendinous structures to the bones.

### 3.2.1 The Motor unit

Each fibre of a muscle can contribute to force production only if it is recruited by the brain. One motor nerve can branch into tens, hundreds, or even a thousand branches, each one terminating on a different muscle fibre. One motor nerve plus all of the fibres that it innervates is called a motor unit. Figure 3.2 shows how motor unit is activated by the signal from the brain sent through the spinal cord. A single muscle can consist of hundreds of motor units. For example, rectus femoris (one of the 4 quadriceps muscles) might contain 1 million muscle fibres, controlled by 1000 motor nerves. So on average, each motor unit contains 1000 fibres. The fibre type composition of a single motor unit will always be homogeneous. So a single motor unit will consist entirely of either type I (slow twitch) or type II (fast twitch)

fibres. The composition of the entire muscle will be heterogeneous. Every muscle will contain some combination of slow and fast motor units.

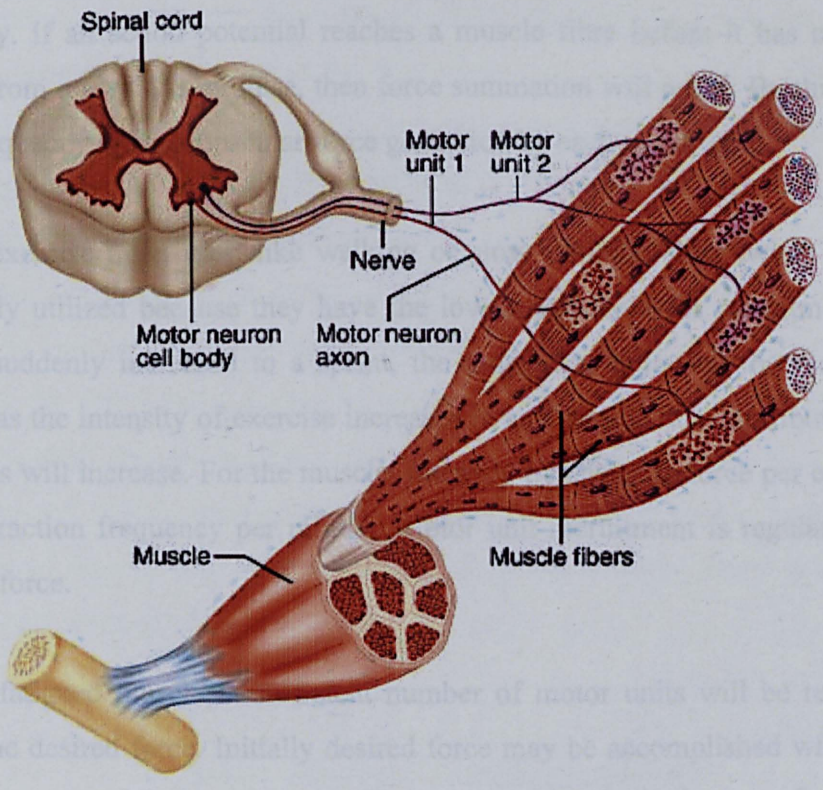


**Figure 3.2: Motor unit activate the muscle fibers by receive the signal from the brain through the spinal cord (Bailey Bio, 2010)**

The brain combines two control mechanisms to regulate the force a single muscle produces. The first is called recruitment. The motor units that make up a muscle are not recruited in a random fashion. Motor units are recruited according to the size principle. Smaller motor units (fewer muscle fibres) have a small motor neuron and a low threshold for activation. These units are recruited first. As more force is demanded by an activity, progressively larger motor units are recruited. This has great functional significance. When requirements for force are low, but control demands are high (writing, playing the piano) the ability to recruit only a few muscle fibres gives the possibility of fine control. As more force is needed the impact of each new motor unit on total force production becomes greater. It is also important to know that the smaller motor units are generally slow units, while the larger motor units are composed of fast twitch fibres. The second method of force

regulation is called rate coding. Within a given motor unit there is a range of firing frequencies. Slow units operate at a lower frequency range than faster units. Within that range, the force generated by a motor unit increases with increasing firing frequency. If an action potential reaches a muscle fibre before it has completely relaxed from a previous impulse, then force summation will occur. By this method, firing frequency affects muscular force generated by each motor unit.

At low exercise intensities, like walking or slow running, slow twitch fibres are selectively utilized because they have the lowest threshold for recruitment. If the pace is suddenly increased to a sprint, the larger fast units will be recruited. In general, as the intensity of exercise increases in any muscle, the contribution of the fast fibres will increase. For the muscle, intensity translates to force per contraction and contraction frequency per minute. Motor unit recruitment is regulated by the required force.

In an unfatigued muscle, a sufficient number of motor units will be recruited to supply the desired force. Initially desired force may be accomplished with little or no involvement of fast motor units. However, as slow units become fatigued and fail to produce force, fast units will be recruited as the brain attempts to maintain the desired force production by recruiting more motor units. Consequently, the same force production in fatigued muscle will require a greater number of motor units. This additional recruitment brings in fast, fatiguable motor units. Therefore, fatigue will be accelerated toward the end of long or severe bouts due to the increased lactate produced by the late recruitment of fast units. During continuous contractions, some units are firing while others recover, providing a built in recovery period. Unfortunately in FES, the same motor units are fired with the same number of pulse width and frequency used. The switching motor unit phenomena do not happen during FES stimulation. These will make the muscle fatigue very quickly and only by stopping the FES stimulation gives muscle time to recover. Muscle fatigue is a very important topic to be explored while dealing with FES for paraplegic. Therefore, chapter 4 will discuss the effect of FES stimulation parameters on muscle fatigue.

## 3.3 Muscle Model

An important step required before the implementation of the movement synthesis and associated control strategy is the development of muscle model. Many muscle models have been developed and the first was pioneered by Hill (1938). The Hill model assumes a muscle to be combination of linear springs and nonlinear contractile element. Figure 3.3 shows the Hill model. It is composed of 3 elements. 2 elements are arranged in series; an elastic element $E_S$ which represents the mechanical isometric response of the muscle, and a contractile element $E_C$ which represents the active force generating capacity derived from chemical free energy stores. The third element is elastic element $E_P$ and is joined in parallel with the two series elements, which account for the resistance of passive muscle to stretch. The properties of these 3 elements are defined in terms of force-length property and force-velocity property (Vignes, 2004).

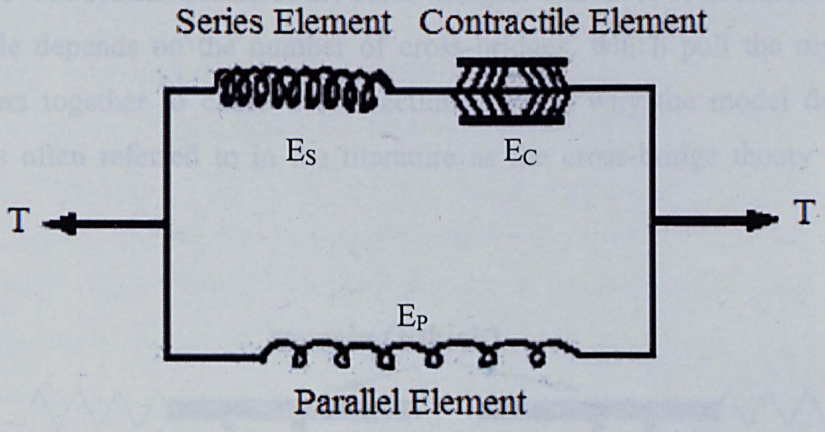


**Figure 3.3: Hill Model (Vignes, 2004)**

For 50 years the Hill (1938) model dominated the field. In this period many ideas have been added to the model in order to accommodate newly discovered facts (Epstein, 1998). Originally rather simple, the model became more and more complicated and lost its appeal. However, the simplest version is still used today to simulate the mechanical behaviour of muscles. However, Hill's model does not

provide insight into the mechanism of the production of force. Since the introduction of Hill model, various modifications have been made to more accurately incorporate further complexities and increase the model's accuracy.

Before 1954, most theories of muscle contraction were based on the idea that shortening and force production were the results of some kind of folding or coiling of large protein molecules. In 1954, Huxley and Hansen (1954) as well as Huxley and Niedergerke (1954) demonstrated that muscle contraction is not associated with any change of length inside the microstructure. These authors postulated that the force is generated through the interaction of actin and myosin filaments. Based on this understanding, Huxley (1957) developed a new theory of muscle contraction by considering the physical and chemical interactions in one muscular unit called a sarcomere. Figure 3.4 shows that the sarcomere consists of four physical components; thick myosin fibers, thin actin filaments, cross-bridges which link the actin to myosin and external matrix to hold the muscle together. Although the myosin fibers provide passive strength of the muscle, active control from the central nervous system occurs in the cross-bridges. The level of neural activation in the muscle depends on the number of cross-bridges, which pull the myosin and actin fibers together to cause a contraction. This is why the model devised by Huxley is often referred to in the literature as the cross-bridge theory (Zahalak, 1990).

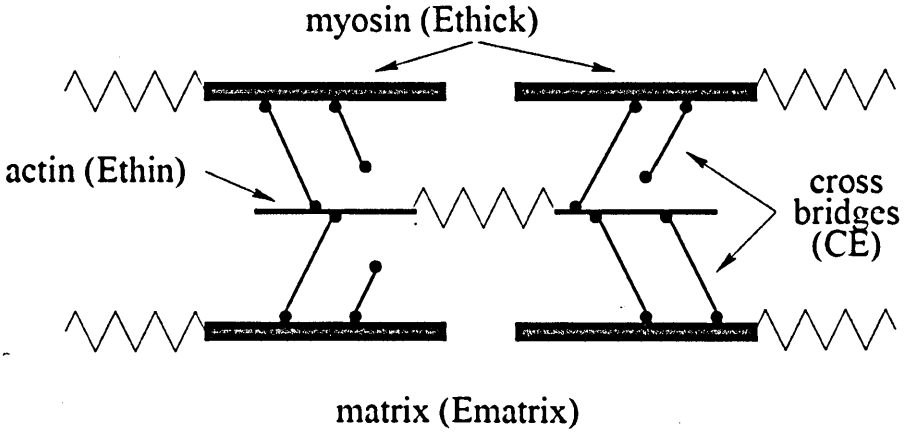


**Figure 3.4: The physical model of sarcomere introduced by Huxley (1957)**

Figure 3.5 shows the Huxley model in which behaviour of the cross-bridge is represented by a non linear contractile element (CE). This component generates a force which depends on the sacromere length, contractile velocity and level of neural activation. The myosin and actin fibers connect in series with the cross-bridges. Since these are inherently passive elastic structures, they are depicted by linear springs. The myosin fibers (*Ethick*) are significantly thicker than the actin filaments (*Ethin*) meaning that the lumped stiffness is approximated by the stiffness of the myosin alone. Finally, the matrix (*Ematrix*) lies in parallel with the rest of the sarcomere, holding the entire system together. This parallel spring usually has a comparatively small stiffness, except for large strains (Winters, 1990).

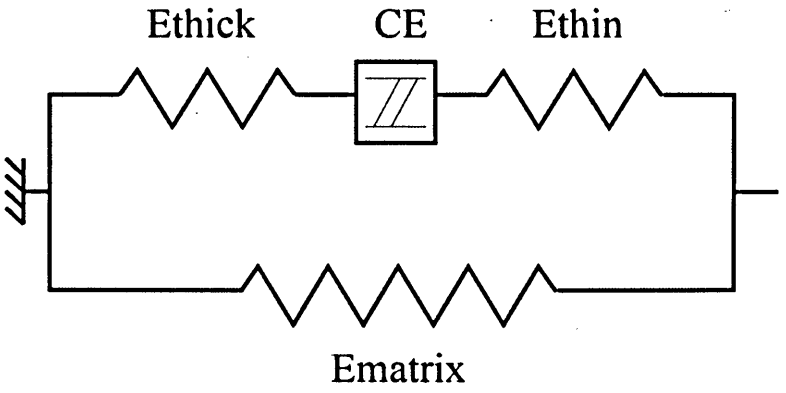


**Figure 3.5: Huxley model (Winter, 1990)**

Another notable muscle model has been reported by Zajac et al. (1986). Zajac introduced the tendon connection and accounted for the muscle fibre pennation angle in the model. The model is shown in Figure 3.6.

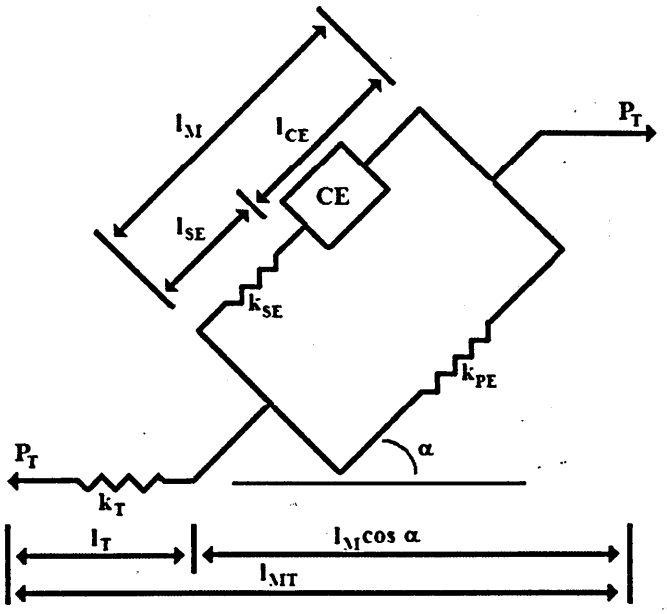


**Figure 3.6: Zajac Model (Zajac, 1986)**

Ferrarin and Pedotti (2000) developed a model that is capable of relating electrical stimulus to dynamic joint torque. The optimal model is described by a simple one pole transfer function that relates the stimulus pulse-width and active muscle torque that was identified by means of parametric approach that considered the family of ARX models and using least squares method on the error between the real data and the output of the model. More complex models have been developed by researchers (Ferrarin et al., 2001; Riener et al., 1996; Riener and Fuhr, 1998) to increase the model accuracy, describing the physiologically based interpretation that capture activities under microscopic and macroscopic levels such as muscle fatigue, calcium dynamics and cross bridge interaction. They introduced a muscle model composed of three parts, activation dynamics, contraction dynamics and body segmental dynamics. Activation dynamics provide the activation needed by the muscle to generate force. It is computed as a function of pulse width and frequency with first order relation and includes the effect of muscle fatigue by introducing the fitness function and a linear second order calcium dynamics (Riener and Fuhr, 1998).

Makssoud et al. (2004) developed a muscle model composed of two parts, activation model and mechanical model. The activation model depends on the parameter of the stimulation intensity, pulse-width and frequency whereas the mechanical model deals with the mechanical behaviour. The model developed is based on physiological operation condition through the implementation of macroscopic muscle model designed by Huxley (1957) who provided an explanation of the interaction of cross bridge phenomena and thus can be linked to the microscopic muscle model introduced by Hill (1938). The drawback of Makssoud et al. (2004) muscle model is that the important component of physiological based muscle model such as muscle fatigue and calcium dynamics are not accounted. Therefore, this research will develop a new muscle model from a series of experimental data, and then the model developed will be compared and validated with the experimental data and two other famous muscle models developed by Ferrarin et al. (2001) and Riener and co-workers (Riener et al., 1996; Riener and Fuhr, 1998).

### 3.3.1 Riener's Muscle Model

One of the famous muscle models has been developed by Riener and co-workers, where their first article was published in 1996 and then in 2000 the complete muscle model was reported. Their muscle model consists of four main components. These are muscle activation, maximum isometric force, force velocity relation, and force-length relation. Figure 3.7 shows that the resultant muscle force can be calculated by multiplying these components.

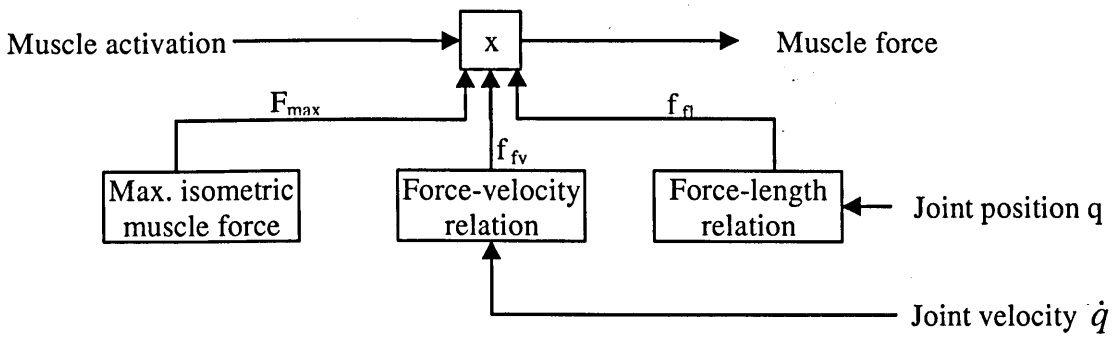


**Figure 3.7: Muscle contraction Model (Riener et al., 1998)**

### 3.3.1.1 Muscle Activation

The muscle activation model comprises four main mechanisms. These are shown as blocks in Figure 3.8. Each block can be considered as a sub-model of the activation dynamics.

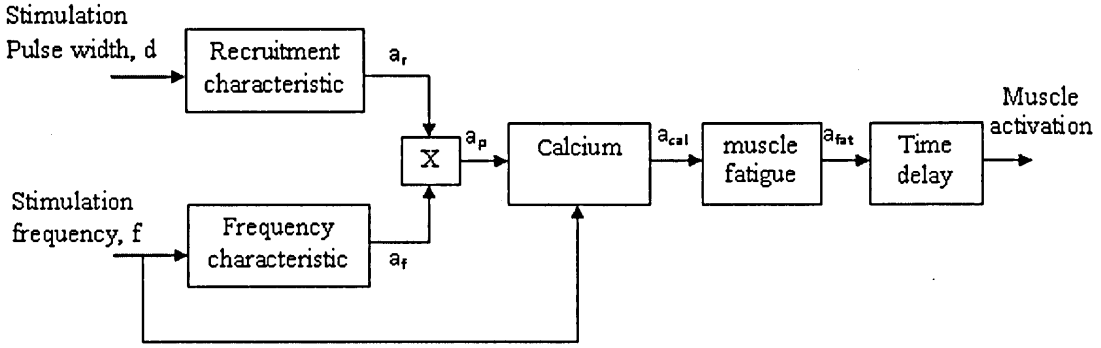


**Figure 3.8: Muscle activation model**

The recruitment level ($a_r$) is the percentage of the recruited motor units, which is computed on the basis of muscle recruitment curve. For constant stimulation amplitude the recruitment level can be approximated as follows:

$$a_r(d) = c_1\left\{(d-d_{thr})\tan^{-1}\left[k_{thr}(d-d_{thr})\right]-(d-d_{sat})\tan^{-1}\left[k_{sat}(d-d_{sat})\right]\right\}+c_2 \quad (0.1)$$

where $0 \le a_r \le 1$, $a_r$ is calculated as a function of the pulse-width, $d_{thr}$ and $d_{sat}$ are pulse-width values corresponding to the threshold and saturation, respectively. The

curvatures of the recruitment curve in the area of threshold and saturation can be adjusted by changing $k_{thr}$ and $k_{sat}$, respectively. The constants $c_1$ and $c_2$ can be chosen to satisfy the conditions $a_r(0)=0$ and $a_r(d)_{d\to\infty} \to 1$.

The muscle force is controlled by adjusting the stimulation pulse-width or pulse amplitude, and pulse frequency. For low frequencies active muscle force drops between successive stimulation pulses, resulting in rippled joint motion, thus long inter-pulse intervals make it difficult to control movements with FES (Riener et al., 1996a). The normalized amount of activation $a_f$ $(0 \le a_f \le 1)$ in a single motor unit is expressed as a function of stimulation frequency $f$.

$$a_f(f)=\frac{(\alpha f)^2}{1+(\alpha f)^2} \qquad (0 \le a_f \le 1) \tag{3.2}$$

This function has been introduced by Riener and Fuhr (1998) and captures the force frequency characteristics of an artificially stimulated muscle.

3.3.1.2 The calcium dynamics

The release of calcium ions from the sarcoplasmic reticulum as a function of the membrane depolarization, as well as the re-accumulation process of the calcium ion pump is modelled by two first order transfer functions in cascade.

$$y(s)=\left(\frac{1}{\tau_{ca}s+1}\right)\cdot\left(\frac{1}{\tau_{ca}s+1}\right)a_p(s) \tag{3.3}$$

The input into the calcium dynamics model is $a_p$ while the output is the activation of a non fatiguing muscle, $a_{cal}$.

3.3.1.3 Muscle Fatigue

The fitness function $fit(t)$ is used to describe the effect of muscle fatigue and recovery, which affect the amount of calcium ions released by the sarcoplasmic reticulum. This is described as:

$$\frac{dfit}{dt} = \frac{(fit_{\min} - fit)a\lambda(f)}{T_{fat}} + \frac{(1-fit)(1-a\lambda(f))}{T_{rec}} \tag{3.4}$$

The minimum fitness is given by $fit_{\min}$, the time constant for fatigue is $T_{fat}$ and for recovery it is $T_{rec}$. The term $\lambda(f)$ is a function of stimulation frequency, while β is a shape factor. $\lambda(f)$has been introduced by Riener et al. (1996) to better account for the fact that muscle fatigue rate strongly depends on the stimulation frequency. The fitness function equation constitutes a general approach which can be applied to any shape of stimulation input. The activation of the fatigued muscle is given as:

$$a_{fat}(t) = a(t)\, fit(t) \tag{3.5}$$

3.3.1.4 Force-velocity relation

The force-velocity relation is given as:

$$f_{fv} = 0.54\tan^{-1}(5.69\bar{v} + 0.51) + 0.745 \tag{3.6}$$

where $\bar{v}$ is the muscle velocity normalized with respect to the maximum contraction velocity of the muscle, $v_m$, of the muscle, ($\bar{v} = v/|v_m|$) and $v=dl/dt$ and $v<0$ for muscle contraction. The velocity, $v_i$ of the muscle group, $i$ is determined using the following expression:

$$v_i = \sum_j \dot{\varphi}_j ma_{ij}(\varphi_j) \tag{3.7}$$

where $ma_{ij}$ is the moment arm of the muscle group, $i$, around joint, $j$ and $\dot{\varphi}_j$ is the angular velocity of the joint.

Force-velocity relation for rectus femoris is given as:

$$f_{fv}(rectus - femoris) = 0.54\tan^{-1}(5.69\frac{v_r}{0.51} + 0.51) + 0.745 \tag{3.8}$$

Force-velocity relation for vasti is given as:

$$f_{fv}(vasti) = 0.54\tan^{-1}(5.69\frac{v_v}{0.48} + 0.51) + 0.745 \tag{3.9}$$

3.3.1.5 Force-length relation

The force-length relation is given as:

$$f_{fl} = \exp\left[-\left(\frac{\bar{l}-1}{\varepsilon}\right)^2\right] \tag{3.10}$$

where $\bar{l}$ is the muscle length normalized with respect to the optimal muscle length $l_{opt}$ and $\varepsilon$ is a shape factor. In order to evaluate $f_{fl}$ in equation (3.10), $\bar{l}$ has to be calculated.

3.3.1.5 Maximum isometric muscle force

Maximum isometric force is the maximum voluntary forces produced by apparently asymptomatic subjects exerting with some muscle actions against opposite direction. Average maximum isometric force for normal subjects is 185N and about 330N for knee flexion and knee extension respectively (Andrews et al., 1996). Meanwhile, for paraplegic subjects, Levy et al. (1990) report that the mean of quadriceps maximum isometric force is between 5N to 30N depending on the level of injury. This value is small because a paraplegic is unable to put the force against opposite force to maintain the leg position. In this muscle model, this value has to be set before it can be used to conduct an experiment on the respective subject.

### 3.3.2 Ferrarin's Muscle Model

Pedotti et al. (1996) have developed a mathematical model for the lower limb that describes the dynamic equilibrium of the moments acting on the knee joint in the sagittal plane. The lower limb model is a swinging leg composed of two rigid segments: the thigh and the shank-foot. The ankle joint is fixed at 90° by a plastic ankle foot orthosis (AFO). Only flexion-extension knee movements are considered as illustrated in Figure 3.9. The passive behaviour of the knee joint depends on the knee joint elastic moment ($M_s$) and the viscous moment ($M_d$). Considering the inertial ($M_i$) and gravitational ($M_g$) moments along with active knee torque ($M_a$) resulting from quadriceps stimulation, a moment balance equation can be written as:

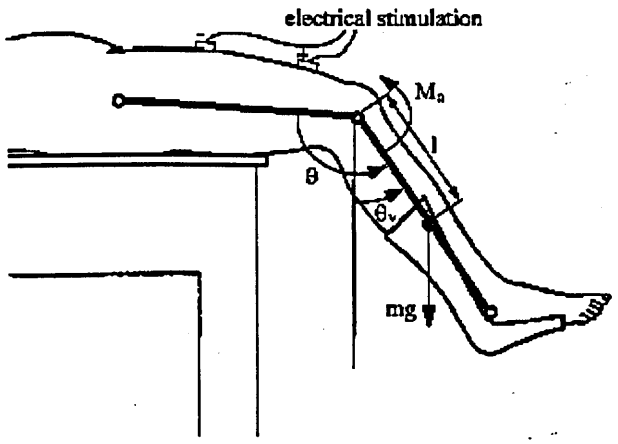


**Figure 3.9: Schematic representation of a free swinging leg , with surface stimulation of the quadriceps muscle (Ferrarin and Pedotti, 2000)**

$$M_i = M_g + M_s + M_d + M_a \tag{3.11}$$

therefore

$$J \cdot \ddot{\theta}_v = -m \cdot g \cdot l \cdot \sin(\theta_v) + M_s - B \cdot \dot{\theta} + M_a \tag{3.12}$$

where $J$ is the inertia of shank-foot complex, $\theta$ is the angle between shank and thigh in the sagittal plane, $\dot{\theta}$ is the knee joint angular velocity, $\theta_v$ is the angle between the shank and the vertical direction of the sagittal plane, $\ddot{\theta}_v$ is the angular acceleration of the shank, $m$ is the mass of foot-shank complex, $g$ is the gravitational acceleration, $l$ is the distance between knee and centre of mass of shank-foot complex, and $B$ is the viscous coefficient.

According to Ferrarin and Pedotti (2000), the damping component of the knee is a linear term with a constant viscous coefficient $B$. The stiffness component is calculated using

$$M_s = -\lambda \cdot e^{-E\theta}(\theta - \omega) \tag{3.13}$$

where, $\lambda$ and $E$ are the coefficients of the exponential term, and $\omega$ is the resting elastic knee angle. The negative sign is due to the choice of the positive extensor torque. The nonlinear component of the knee elasticity is represented by the exponential term.

The passive parameters of the leg model were obtained during passive pendulum trials done by Ferrarin and Pedotti (2000). Once the viscous-elastic parameters were substituted in the following equation, the active torque produced by the stimulated muscle can be calculated at each stimulation frequency;

$$M_a = J \cdot \ddot{\theta}_v + m \cdot g \cdot l \cdot \sin(\theta_v) - M_s + B \cdot \dot{\theta} \tag{3.14}$$

A transfer function between electrical stimulation and the resultant knee torque was identified by means of a parametric approach that considered the family of ARX models and using a least square method on the error between real data and the output of the model. The muscle model obtained is a first order model (one pole only) given as:

$$H(s) = \frac{G}{1 + s\tau} \tag{3.15}$$

where $\tau$ is time constant and $G$ is static gain.

Ferrarin and Pedotti (2000) found that $\tau$ is independent of the stimulation frequency, but is strongly dependent on the shape of the stimulus pulse (step and ramp stimulation). The static gain G is directly dependent on the stimulation frequency, because a higher pulse repetition frequency corresponds to greater electric charge delivered to the muscle, resulting in an increase in muscle contraction and therefore higher values of active joint torque.

## 3.4 Adaptive Neuro-Fuzzy inference System

Performance of FES control systems depends greatly on the accessibility of an accurate muscle model. However, muscle model is known as a highly complex, time varying and nonlinear dynamic system. Therefore, it is necessary to develop the muscle model using a suitable approach that can cope with the complexity and uncertainty of the model. Adaptive neuro-fuzzy inference system (ANFIS) is well known by its ability to undertake this kind of problems.

### 3.4.1 ANFIS Architecture

Sugeno model output membership functions are either linear or constant. If a fuzzy system under consideration has two inputs $x$ and $y$ and one output $f$, then for a first order Sugeno fuzzy model, a common rule set with two fuzzy if-then rules is as follows:

*Rule 1: If x is $A_1$ and y is $B_1$, then $f_1=p_1x+q_1y+r_1$*

*Rule 2: If x is $A_2$ and y is $B_2$, then $f_2=p_2x+q_2y+r_2$*

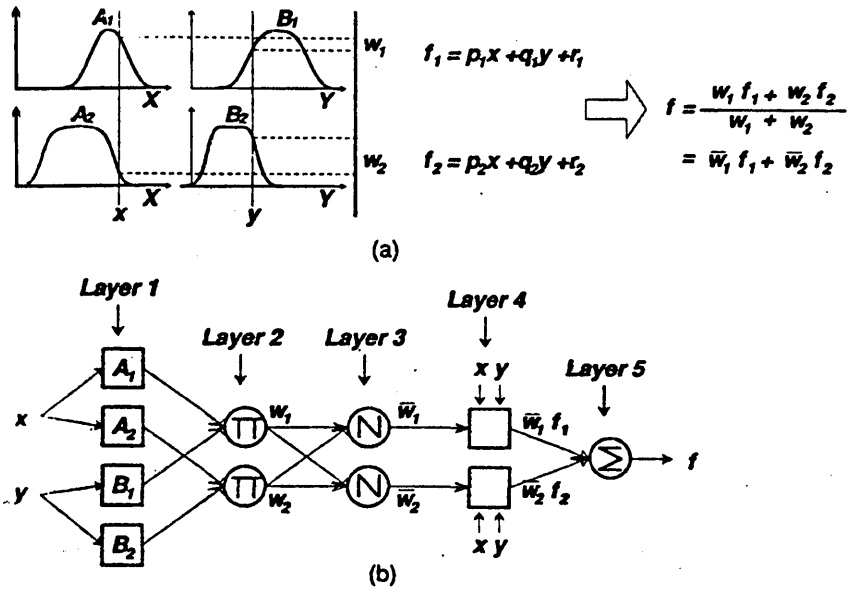


**Figure 3.10: (a) A two-input first order Sugeno fuzzy model with two rules; (b) Equivalent ANFIS architecture.**

Figure 3.10(a) illustrates the reasoning mechanism for the Sugeno model discussed above while the corresponding ANFIS architecture is as shown in Figure 3.10(b), where nodes of the same layer have similar functions. A node represented by a square has parameters and it is called adaptive node while the circle shape one has none and it is called fixed node. The ANFIS architecture consists of five layers with the output of the nodes in each respective layer represented by $O_{i,l}$ where $i$ is the $i$th node of layer $l$ (Denai et al., 2007; Mahfouf, 2004).

Layer 1: The membership function layer. The output of any node in this layer gives the membership degree of an input (crisp);

$$O_{1,i} = \mu_{A_i}(x), \qquad i = 1,2 \; or \tag{3.16}$$
$$O_{1,i} = \mu_{B_{i-2}}(y), \qquad i = 3,4$$

where $x$ (or $y$) is the input to the node and $A_i$ (or $B_{i-2}$) is the fuzzy set associated with this node such as the generalized bell function

$$\mu_{Ai}(x) = \frac{1}{1+\left[\left((x-c_i)/a_i\right)^2\right]^{b_i}} \tag{3.17}$$

where $\{a_i, b_i, c_i\}$ is the parameter set referred to as premise parameters.

Layer 2: Multiplication layer. Every node here multiplies the inputs of membership degrees and produces the firing strength of the rule or the degree with which the corresponding rule is fired.

$$O_{2,i} = w_i = \mu_{A_i}(x) \times \mu_{B_i}(y), \quad i = 1,2 \tag{3.18}$$

Layer 3: Normalization layer. It calculates a ratio of the particular rule-firing degree to the sum of all rule fitting degrees;

$$O_{3,i} = \bar{w}_i = \frac{w_i}{w_1 + w_2}, \; i = 1,2 \tag{3.19}$$

Layer 4: This layer applies Sugeno's processing rule and is therefore an output calculating one.

$$O_{4,i} = \bar{w}_i f_i = \bar{w}_i (p_i x + q_i y + r_i) \tag{3.20}$$

where $\{p_i, q_i, r_i\}$ is the consequent parameters

Layer 5: Calculates the overall output as the sum of all incoming signals;

$$O_{5,i} = \sum_i \bar{w}_i f_i = \frac{\sum_i w_i f_i}{\sum_i w_i} \tag{3.21}$$

Hence, the artificial neural network (ANN) architecture has been built so that it can operate exactly like a Sugeno-type fuzzy system.

### 3.4.2 Hybrid Learning Algorithm

The hybrid learning algorithm is a combination of least square and backpropagation method. In the least square method, the output of a model $y$ is given by the parameterised expression

$$y = \theta_1 f_1(u) + \theta_2 f_2(u) + \cdots + \theta_n f_n(u) \tag{3.22}$$

where $u = [u_1, \ldots u_n]^T$ is the models input vector, $f_1, \ldots f_n$ are known function of $u$, and $\theta_1, \ldots \theta_n$ are unknown parameters to be optimised. To identify these unknown parameters $\theta_1$, usually a training data set of data pairs $\{(u_i, y_i), i = 1, \ldots m\}$ is taken; substituting each data pair in equation (3.22) a set of linear equations is obtained, which can be written as

$$A\theta = y \tag{3.23}$$

in matrix form, where $A$ is an $m$x$n$ matrix

$$A = y\begin{bmatrix} f_1(u_1) & \cdots & f_n(u_1) \\ \vdots & \ddots & \vdots \\ f_1(u_m) & \cdots & f_n(u_m) \end{bmatrix} \tag{3.24}$$

$\theta$ is an $n$x$1$ unknown parameter vector

$$\theta = \begin{bmatrix} \theta_1 \\ \vdots \\ \theta_n \end{bmatrix} \tag{3.25}$$

$y$ is an $m$x$1$ output vector

$$y = \begin{bmatrix} y_1 \\ \vdots \\ y_m \end{bmatrix} \tag{3.25}$$

Since generally $m>n$, instead of exact solution of equation (3.23) an error vector $e$ is introduced to account for the modelling error as

$$A\theta + e = y \tag{3.26}$$

and search for $\theta = \hat{\theta}$ which minimises sum of squared error

$$E(\theta) = \sum_{i=1}^{m}(y_i - a_i^T\theta)^2 = e^T e \tag{3.27}$$

where $E(\theta)$ is called the objective function. The squared error in equation (3.27) is minimised when $\theta = \hat{\theta}$, called least squares estimator (LSE) that satisfies the normal equation

$$A^T A\hat{\theta} = A^T y \tag{3.28}$$

If $A^TA$ is non singular, $\hat{\theta}$ is unique and is given by

$$\hat{\theta} = (A^TA)^{-1}A^Ty \tag{3.29}$$

In case of backpropagation learning rule the central part concerns how to recursively obtain a gradient vector in which each element is defined as the derivative of an error measure with respect to a parameter. Assuming that a given feedforward adaptive network has $L$ layers and layer $l$ has $N(l)$ nodes, then the output function of node $i$ in layer $l$ can be represented as $x_{l,i}$ and $f_{l,i}$ respectively. For the node function $f_{l,i}$

$$x_{l,i} = f_{l,i}(x_{l-1,1}, \ \dots \ x_{l-1,N(l-1)}, \alpha, \beta, \gamma, \dots) \tag{3.30}$$

where $\alpha, \beta, \gamma$, etc are the parameters of this node. Assuming that the given training data set has $P$ entries, an error measure can be defined for the $p^{th}(1 \leq p \leq P)$ entry of the training data set as the sum of squared errors:

$$E_p = \sum_{k=1}^{N(L)}(d_k - x_{L,k})^2 \tag{3.31}$$

where $d_k$ is the $k^{th}$ component of the $p^{th}$desired output vector and $x_{L,k}$ is the $k^{th}$ component of the actual output vector produced by presenting the $p^{th}$ input vector to the network. The task here is to minimise an overall error measure, which is defined as $E = \sum_{p=1}^{P} E_p$. The basic concept in calculating the gradient vector is to pass a form of derivative information starting from the output layer and going backward layer by layer until the input layer is reached. To facilitate the discussion the error signal $\epsilon_{l,i}$ is defined as

$$\epsilon_{l,i} = \frac{\partial E_p}{\partial x_{l,i}} \tag{3.32}$$

This is actually ordered derivative and is different from ordinary partial derivative. For $i^{th}$ output node (at layer $L$)

$$\epsilon_{L,i} = \frac{\partial E_p}{\partial x_{L,i}} \tag{3.33}$$

$$\therefore \epsilon_{L,i} = -2(d_i - x_{L,i}) \tag{3.34}$$

For the internal node at the $i^{th}$ position of layer $l$, the error signal can be derived iteratively by the chain rule:

$$E_{l,i} = \frac{\partial E_p}{\partial x_{l,i}} = \sum_{m=1}^{N(l+1)} \frac{\partial E_p}{\partial x_{l+1,m}} x \frac{\partial f_{l+1,m}}{\partial x_{l,i}} \tag{3.35}$$

$$= \sum_{m=1}^{N(l+1)} \epsilon_{l,i} x \frac{\partial f_{l+1,m}}{\partial x_{l,i}}$$

The gradient vector is defined as the derivative of the error measure with respect to each parameter. If $\alpha$ is a parameter of the $i^{th}$ node at layer $l$, then

$$\frac{\partial E_p}{\partial \alpha} = \frac{\partial E_p}{\partial x_{l,i}} x \frac{\partial f_{l,i}}{\partial \alpha} = \epsilon_{l,i} \frac{\partial f_{l,i}}{\partial \alpha} \tag{3.36}$$

The derivative of the overall error measure $E$ with respect to $\alpha$ is

$$\frac{\partial E}{\partial \alpha} = \sum_{p=1}^{P} \frac{\partial E_p}{\partial \alpha} \tag{3.37}$$

Accordingly, for simplest steepest descent without line minimisation, the update formula for generic parameter $\alpha$ is

$$\Delta\alpha = -\eta \frac{\partial E}{\partial \alpha} \tag{3.38}$$

in which $\eta$ is the learning rate. So, for parameter $\alpha$ it may be written as

$$\alpha_{new} = \alpha_{old} + \Delta\alpha \qquad (3.39)$$
$$= \alpha_{old} - \eta\frac{\partial E}{\partial \alpha}$$

In this type of learning, the update action occurs only after the whole set of training data pair is presented. This process of presentation of whole set of training data pair is called epoch or iteration.

It is assumed that *'S'* is the total set of parameters and *'$S_1$'* and *'$S_2$'* are the sets of input and output parameters respectively. For hybrid learning algorithm, each iteration consists of a forward pass and a backward pass. In the forward pass, when a vector of input data pair is presented, the node outputs of the system are calculated layer by layer till the corresponding row in matrices $A$ and $y$ of equation (3.23) are obtained. The process is repeated for all the training data pair to form the matrices $A$ and $y$ completely. Then the output parameters of set $S_2$ are calculated according to equation (3.29). After this, the error measure for each training data pair is to be calculated. The derivative of those error measures with respect to each node output are calculated using equation (3.33) and equation (3.35). Thus the error signal is obtained. In the backward pass, these error signals propagate from the output end towards the input end. The gradient vector is found for each training data entry. At the end of the backward pass for all training data pairs, the input parameters are updated by steepest descent method as given by equation (3.39).

## 3.5 Development of The Muscle Model

### 3.5.1 Quadriceps Muscle Model

Throughout the experiments, a paraplegic subject is placed in a semi-upright sitting position (45° to 60°) with the thigh hanging using thigh support at a frame to avoid any constraint on the leg movement. Velcro straps are used to stabilise the subject's upper trunk, waist and thigh. The isometric force output of the quadriceps muscle is recorded via a force transducer (PCE-FM200, PCE Group Company, Deutschland) placed aligned with the anterior aspect of the leg, about 5cm proximal to the lateral malleolus. The position of the leg is recorded instantaneously using Matlab software through analogue to digital converter (ADC) card and serial connection. Meantime, the force and torque are also recorded simultaneously.

Electrical stimulation is delivered via two MultiStick™ gel surface electrodes (Pals platinum, Axelgaard Mfg. Comp, USA, 50mm x 90mm). The cathode is positioned over the upper thigh, covering the motor point of rectus femoris and vastus lateralis. The anode is placed over the lower aspect of thigh, just above patella. Prior to each test, the electrodes are tested for suitable placement on the muscle by moving the electrode about the skin over the motor point, looking for the maximum muscular contraction using identical stimulation signals through the entire trials. A RehaStim Pro 8 channels (Hasomed GmbH, Germany) stimulator receives stimulation pulses generated in Matlab software through USB connection for application to the muscle. Figure 3.11 and Figure 3.12 show the surface electrodes and electrical stimulator used in this thesis.


**Figure 3.11: MultiStick™ gel surface electrodes**


**Figure 3.12: RehaStim Pro 8 channels stimulator**

More than 600 stimulation pulses with stimulation frequencies and pulse widths varying from 10Hz to 50Hz and 200μsec to 400μsec respectively are used to develop the muscle model. The frequency and pulse width range are selected based on suggested range that is suitable for paraplegic. There are 731 data obtained from the experiments, 500 data are used as training data set while 300 data, some of them are part of training data to balance from unused experiment data, are used as testing data set.

The network architecture for quadriceps muscle model consists of three inputs and one output. The parameters of choice as inputs must have an influence on the desired output. For this model, stimulation frequency, pulse width and stimulation time were selected as model inputs. These inputs and output are used to induce an ANFIS muscle model. The time is included since muscle torque has a significant influence on the stimulation time, and muscle fatigue occurs when the stimulation time increases.

### 3.5.2 Hamstrings Muscle Model

The same procedures as for quadriceps muscle model are applied for hamstrings muscle model. In this experiment, the cathode is positioned at the lower thigh, covering from the ischial tuberosity to the midpoint of the popliteal crease. The anode is placed between the tendons of the biceps femoris and the semimembranosus. There are 808 data obtained from the experiments, 588 data are used as training data set while 220 data are used as testing data set.

The network architecture for hamstrings muscle model also consists of three inputs and one output. It has the same input parameters as quadriceps muscle model and the output is hamstrings muscle torque. There are three membership functions of Gaussian types for each input is used to develop hamstrings muscle model. These parameters are generated automatically from the ANFIS Matlab toolbox with optimum model performance.

## 3.6 Results

### 3.6.1 Quadriceps Muscle Model

The performance of the ANFIS quadriceps muscle model obtained after training was evaluated by using the testing data set from one subject and validated with experimental results and 2 other quadriceps muscle models developed previously by other researchers. There were 500 data used for training and 300 data for testing purposes. Figure 3.13 shows the training data used in this work. Then, the quadriceps muscle model was validated with experiment data from same subject and with quadriceps muscle model developed by Reiner and Ferrarin. The quadriceps muscle model developed by Riener (1996, 1998) and Ferrarin (2001) was used considering all the parameters calculated based on the same subject.

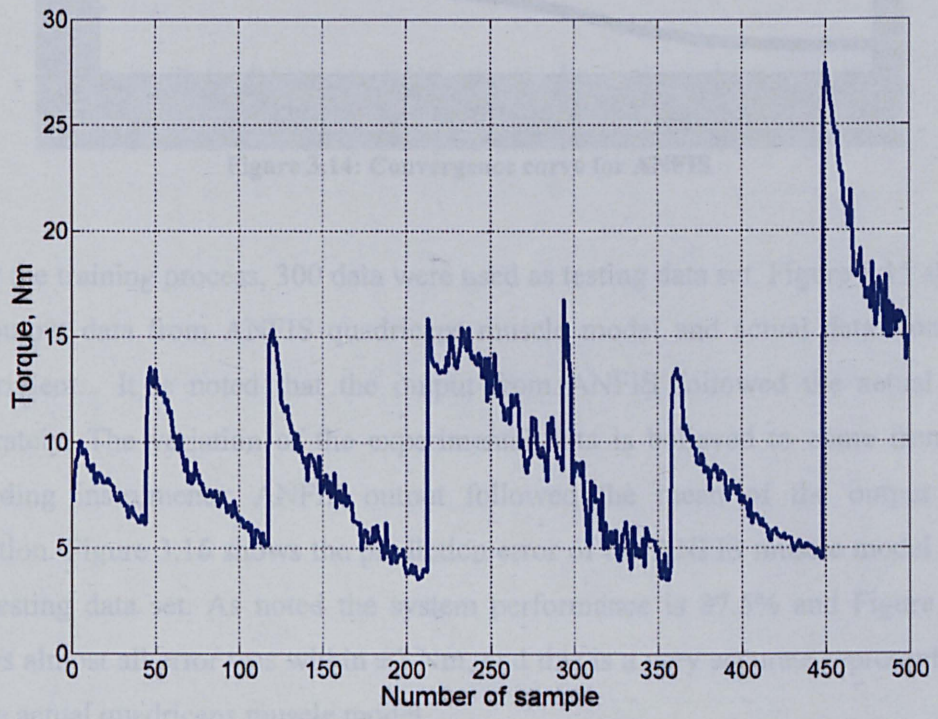


**Figure 3.13: Training data set**

There were 2500 epochs used to train the network. It was found that the network converged at around 220$^{th}$ iteration. Figure 3.14 shows the convergence curve during the training of the muscle model network. After 250$^{th}$ iteration, there was no further improvement on the training error and it was assumed that the network had already reached the global minimum.

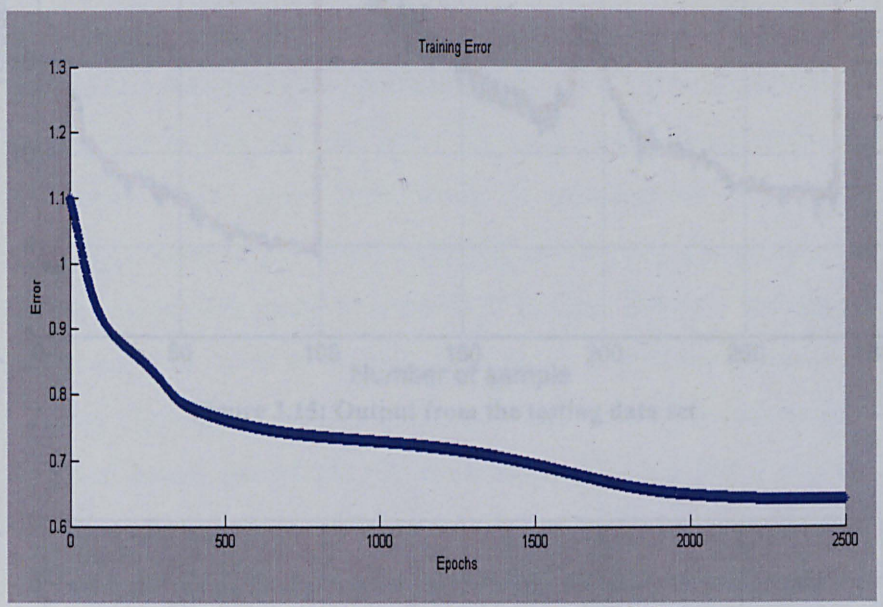


**Figure 3.14: Convergence curve for ANFIS**

After the training process, 300 data were used as testing data set. Figure 3.15 shows the output data from ANFIS quadriceps muscle model and actual data from the experiment. It is noted that the output from ANFIS followed the actual data accurately. The variation of the experimental data is believed to come from the recording instruments; ANFIS output followed the mean of the output data variation. Figure 3.16 shows the prediction error of the ANFIS muscle model from the testing data set. As noted the system performance is 87.5% and Figure 3.16 shows almost all error was within ±2 Nm, and this is a very accurate representation of the actual quadriceps muscle model.

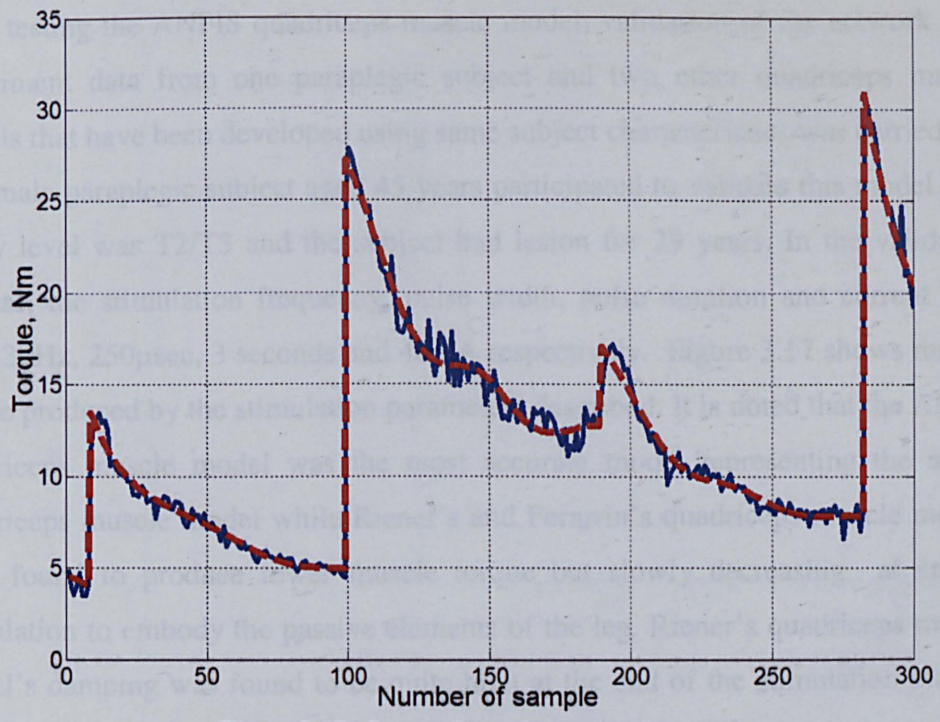


**Figure 3.15: Output from the testing data set**

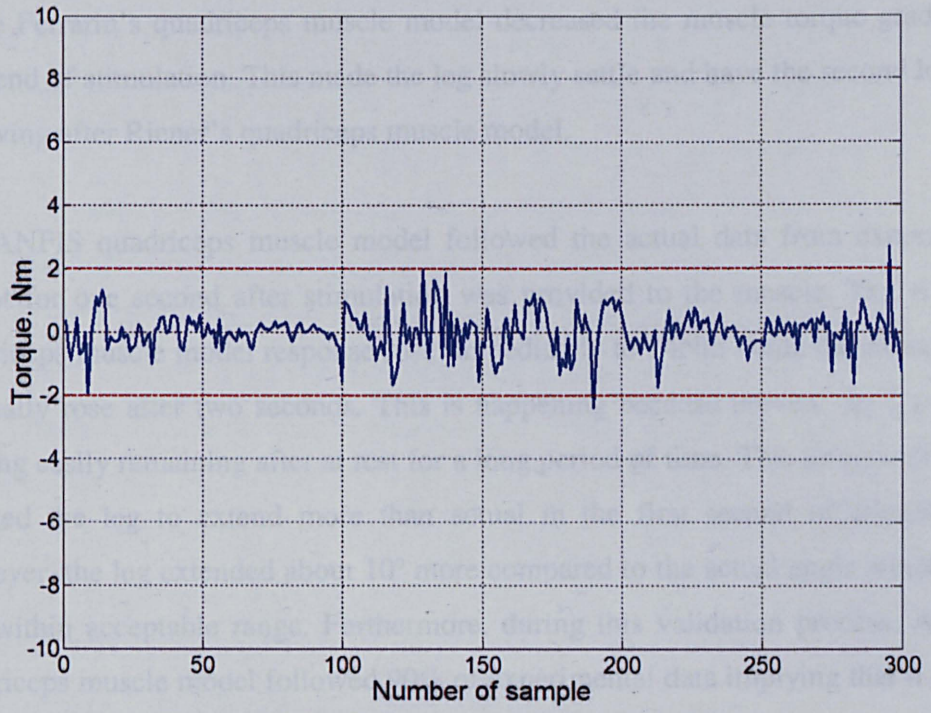


**Figure 3.16: Prediction error from the testing data set**

After testing the ANFIS quadriceps muscle model, validation of the network with experiment data from one paraplegic subject and two other quadriceps muscle models that have been developed using same subject characteristics was carried out. One male paraplegic subject aged 45 years participated to validate this model. The injury level was T2/T3 and the subject had lesion for 29 years. In the validation process, the stimulation frequency, pulse width, pulse duration and current used were 30Hz, 250μsec, 3 seconds and 40mA respectively. Figure 3.17 shows muscle torque produced by the stimulation parameters described. It is noted that the ANFIS quadriceps muscle model was the most accurate model representing the actual quadriceps muscle model while Riener's and Ferarrin's quadriceps muscle models were found to produce lower muscle torque but slowly decreasing at end of stimulation to embody the passive elements of the leg. Riener's quadriceps muscle model's damping was found to be quite high at the end of the stimulation making the leg swing higher and longer than expected and this behaviour was not representing the actual paraplegic leg since paraplegic leg has a shorter muscle. While Ferrarin's quadriceps muscle model decreased the muscle torque gradually after end of stimulation. This made the leg slowly settle and have the second longer leg swing after Riener's quadriceps muscle model.

The ANFIS quadriceps muscle model followed the actual data from experiment except for one second after stimulation was provided to the muscle. The ANFIS quadriceps muscle model response rose immediately to 14Nm while the actual data gradually rose after two seconds. This is happening because prevent the leg from moving easily remaining after at rest for a long period of time. This torque different resulted the leg to extend more than actual in the first second of stimulation. However, the leg extended about 10° more compared to the actual angle which was still within acceptable range. Furthermore, during this validation process, ANFIS quadriceps muscle model followed 90% of experimental data implying that it was a more accurate model compared to the other two quadriceps muscle models developed previously.

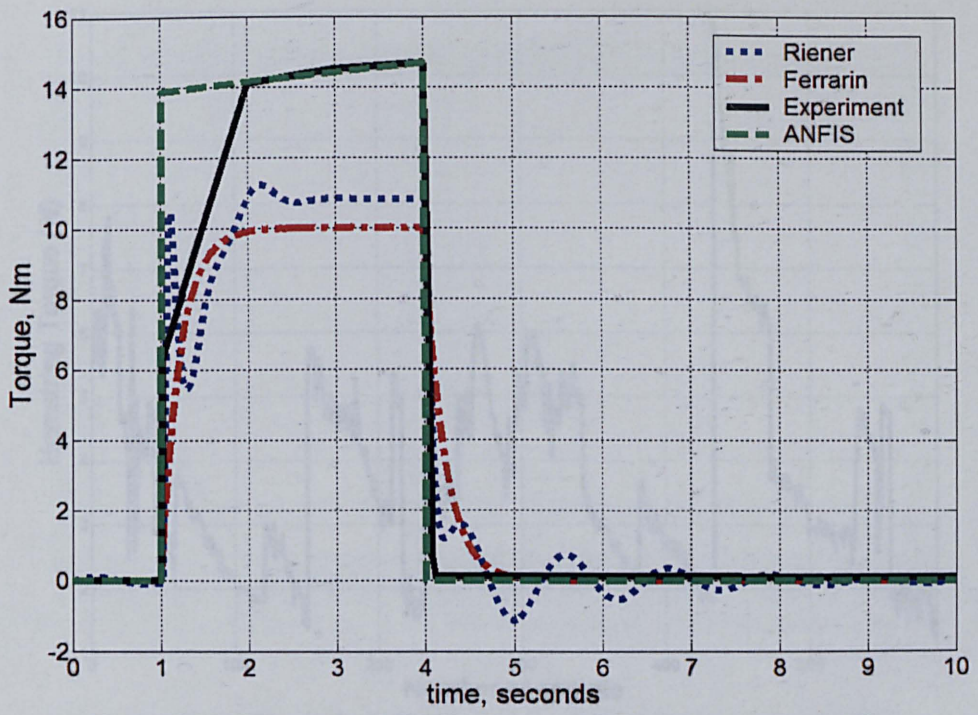


**Figure 3.17: Responses of ANFIS, Riener and Ferrarin muscle models**

### 3.6.2 Hamstrings Muscle Model

The performance of the ANFIS hamstrings muscle model obtained after training was evaluated using the testing data set and validated with experimental results. There were 588 data used for training and 220 data for testing purposes. Figure 3.18 shows the training data used in this work. Then, the hamstrings muscle model was validated with experimental data from the same subject as described in the previous section.

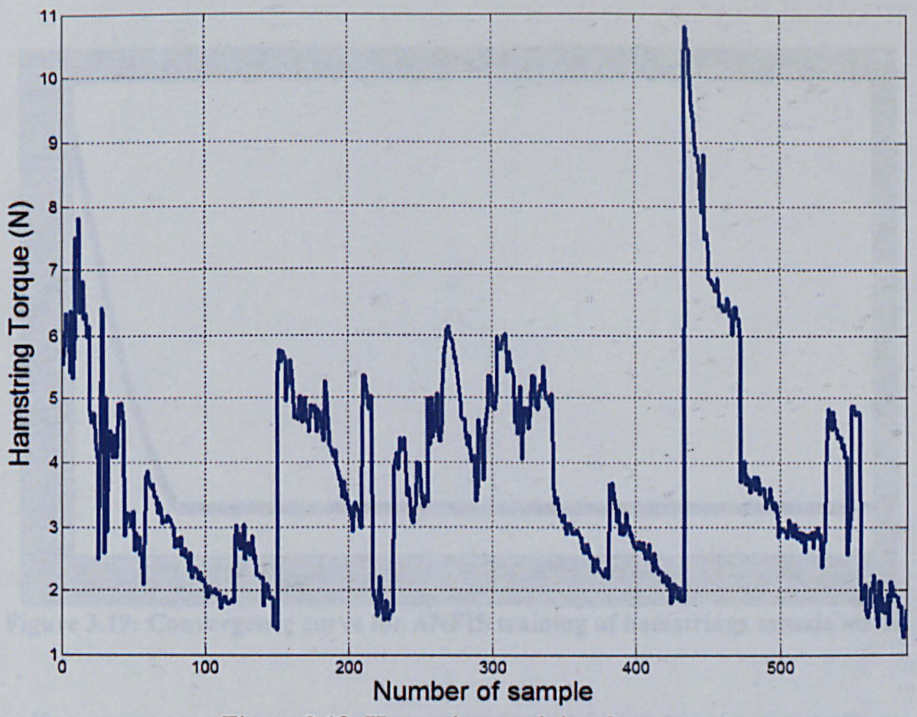


**Figure 3.18: Hamstrings training data set**

There were 1000 iterations used to train the network. It was found that the network converged at around 130$^{th}$ iteration. Figure 3.19 shows the convergence curve during the training of the hamstrings muscle model network. After 130$^{th}$ iteration, there was no further improvement on the training error and it was assumed that the network had already reached the global minimum.

After the training process, 220 data were used as testing data set. Figure 3.20 shows the output data from ANFIS hamstrings muscle model and actual data from the experiment. It is noted that the output from ANFIS followed the actual data accurately. The variation of the experimental data is believed to come from the recording instruments; ANFIS output followed the mean of the output data variation. Figure 3.21 shows the prediction error of the ANFIS muscle model from the testing data set. As noted 100% of the error was within ±1 Nm, and this very accurately represents the actual hamstrings muscle model. The accuracy of the testing data set was 96.46%.

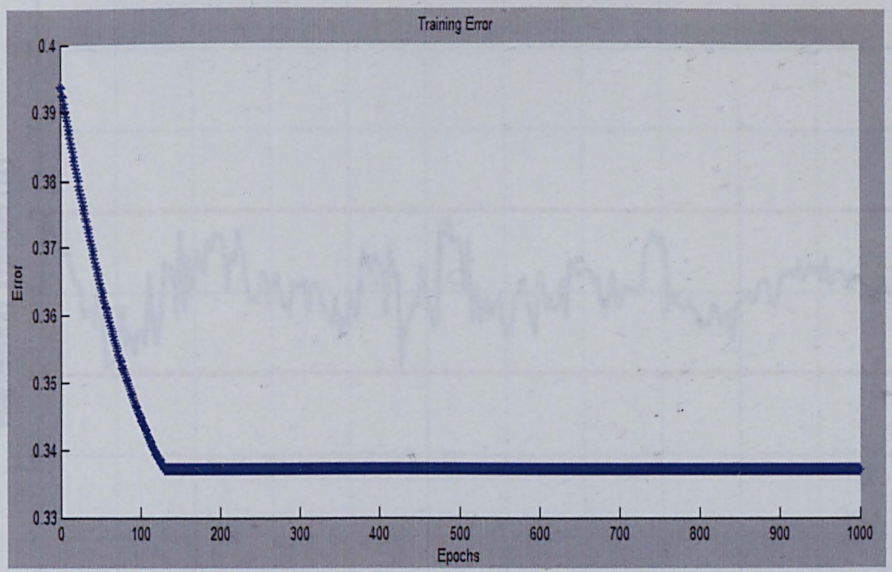


**Figure 3.19: Convergence curve for ANFIS training of hamstrings muscle model**

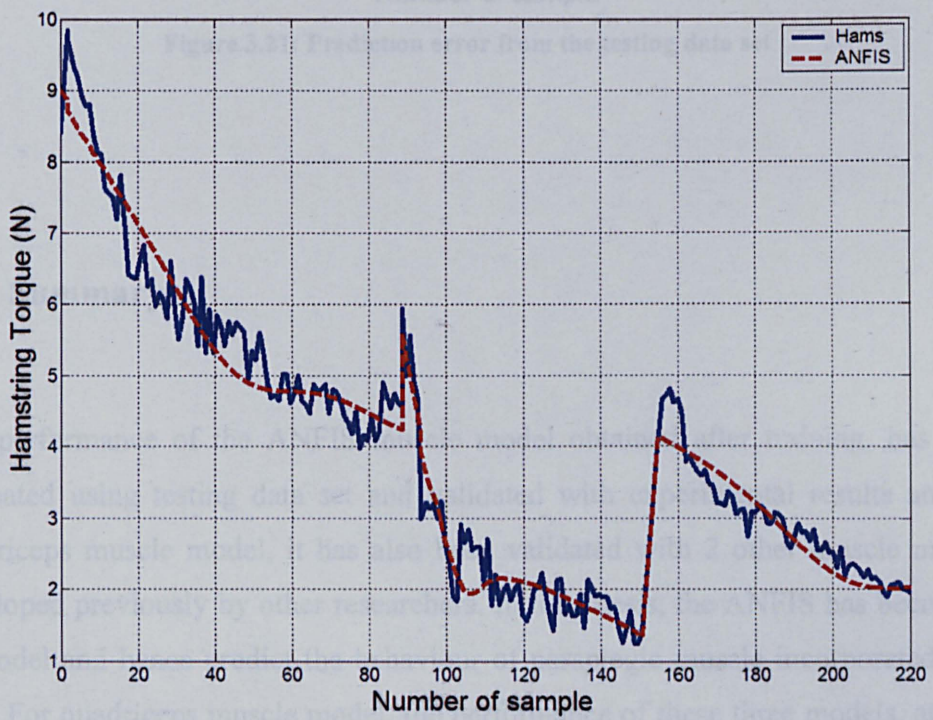


**Figure 3.20: Output from testing data set**

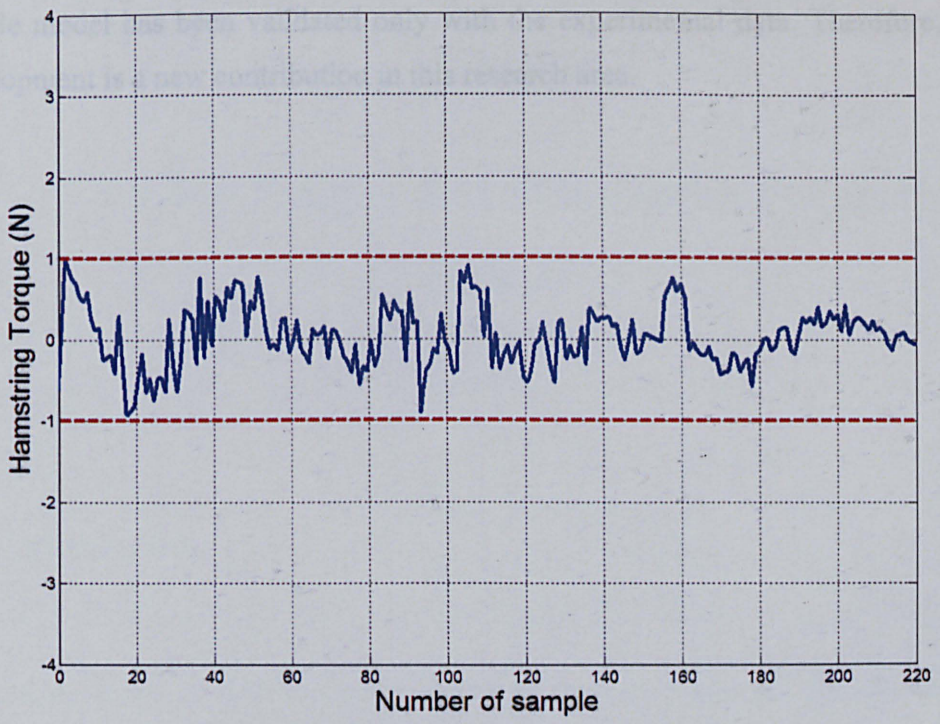


**Figure 3.21: Prediction error from the testing data set**

## 3.7 Summary

The performance of the ANFIS muscle model obtained after training, has been evaluated using testing data set and validated with experimental results and for quadriceps muscle model, it has also been validated with 2 other muscle models developed previously by other researchers. In this thesis, the ANFIS has been used to model and hence predict the behaviour of paraplegic muscle incorporated with FES. For quadriceps muscle model, the performance of these three models, at their respective most optimally tuned set of parameters, has been evaluated. Of these, the ANFIS quadriceps muscle model was found to be the most suitable model for use to determine the muscle torque while integrated with FES. The ANFIS hamstrings muscle model developed also showed outstanding performance. So far, there are almost no hamstrings muscle model developed, therefore the ANFIS hamstring

muscle model has been validated only with the experimental data. Therefore, this development is a new contribution in this research area.

# Chapter 4

# Muscle Fatigue and Stimulation Parameters Analysis

## 4.1 Introduction

Stimulation trains of different combination of frequency and pulse-width can be used to generate the muscle force required to perform a functional task during functional electrical stimulation (FES). However, with repetitive activation, the muscle will fatigue and an increase in either the frequency or the pulse-width of stimulation will be required to enable the targeted muscle force to be maintained. This study compares isometric performance and paraplegic muscle fatigue using two different protocols: protocol 1 uses 5 different stimulation frequencies varying from 10Hz to 50Hz with other parameters fixed; and protocol 2 uses 5 different stimulation pulse-widths varying from 200μs to 400μs with other parameters fixed. This range is selected based on a suitable frequency and a pulse width for paraplegic. Muscle performance is assessed by measuring percent decline in peak force and maximum muscle force for different stimulation frequencies and pulse-widths. A simple rule is introduced to avoid spasm or injury to the leg during FES application. The results from this study show that higher frequency gives faster muscle fatigue and the selection of force required to perform a functional task is important for obtaining the optimum stimulation parameters. Stimulation pulse-width has no significant effect on the muscle fatigue but highly affects the maximum muscle force. The rule proposed is important and is found to be useful to avoid leg injury, spasm or uncomfortable feeling during FES application. This rule also can be used to choose optimum stimulation parameters.

## 4.2 Muscle fatigue in human muscle

FES is widely used as substitute for the loss of voluntary motor control to enable people with spinal cord injury (SCI) to stand (Donalson and Chung-Huang, 1998; Veltink and Donaldson, 1998), walk (Popovic et al., 2001, 1999), grasp (Besio et al., 1997; Popovic et al., 2001) and do some lower limb exercises such as rowing (Hussain and Tokhi, 2008) and cycling (BeDell et al., 1996; Eser et al., 2003). However, one of the major drawbacks is that stimulated muscles are likely to fatigue very quickly because of the 'reversed recruitment order' of the artificially stimulated motoneurons, limiting the role of FES in certain applications (Rabischong and Guiraud, 1993). The absence of motor unit firing phenomena during FES application explained in Chapter 3 also makes the muscle fatigue appear more quickly. Therefore, increasing either the frequency or the pulse-width of stimulation will be necessary to permit the targeted muscle force to be maintained during a functional task.

Many studies have been conducted to investigate muscle fatigue from stimulated muscle and to arrive at solutions to overcome this problem. Binder-Macleod and Snyder-Mackler (1993) point out that stimulation parameters that have a supreme impact on muscle fatigue are stimulation frequency and pulse intensity. It was reported that muscle fatigue was greater at lower frequencies in intermittent stimulation (Binder-Macleod and Russ, 1999; Matsunaga et al., 1999) while opposite results have been obtained during continuous stimulation (Kesar and Binder-Macleod, 2006). However, all these studies have used healthy subjects in their investigations. These results may only represent those of normal human population. Furthermore, several studies have suggested different ways to overcome muscle fatigue during FES. These consist of FES using random modulation (Granham et al., 2006; Trasher et al., 2005), N-let pulse trains (Karu et al., 1995), variable frequency pulse trains (Mourselas and Granat, 1998) and many more.

Trasher et al. (2005) and Granham et al. (2006) concluded that random modulation of the stimulation frequency, amplitude and pulse-width did not have any effect on the muscle fatigue rate. However, if this technique gives opposite results, then having this kind of signal is not practically viable technique for muscle fatigue reduction. Moreover, this signal is difficult to control and apply in closed loop FES control applications.

Routh and Durfee (2003) and Bigland-Ritchie et al. (2000) proposed doublet stimulation signal to reduce muscle fatigue during FES. However, Routh and Durfee (2003) wrap up that doublet stimulation signal did worsen fatigue reduction and singlet stimulation signal led to 33 more cycles than doublet, with the same stimulation parameters. Moreover, doublet stimulation produces more than twice the amplitude of twitches force and tends to make the muscle fatigue quicker. Karu et al. (1995) reported that N-let pulse trains reduce 36% muscle fatigue rate compared to singlet stimulation signal. They used 1 to 6 pulse trains in their study and found the optimum stimulation train as doublet and triplet stimulation signal. This finding is conflicting with findings from Routh and Durfee (2003). This is possibly because of different protocols used in the studies. Yet, Bigland-Ritchie et al. (2000) proposed that using doublet stimulation signal for the first 2 minutes and then keeping on with singlet stimulation will cut muscle fatigue drastically as compared with constant rate trains. Again, this technique is difficult to implement practically in closed loop FES control applications.

Kesar et al. (2007) studied the effect of stimulation frequency and pulse-width on muscle fatigue and found that stimulation with frequency modulation gives less muscle fatigue rate compared with stimulation with pulse-width modulation. However, stimulation with frequency modulation is impossible with currently available off the shelf programmed stimulators since most of the stimulators allow pulse-width modulation with fixed frequency. Moreover, in their paper, they found that constant stimulation signal gives the least muscle fatigue compared to the others. Previously, Kesar and Binder-Macleod (2006) also concluded that using the lowest stimulation frequency and longest pulse duration could maximize muscle

performance if the stimulation frequency and intensity are kept constant. In both papers, they used healthy subjects in their experiments with very high pulse-width. Stimulation pulse-width more than 450μsec and stimulation frequency more than 50Hz are not suitable for paraplegic use (Riener, 1998), therefore these results are only valid for healthy subjects. Earlier, Mourselas and Granat (1998) performed the same experiment with five healthy subjects and one SCI subject with which the results of Kesar et al. (2006, 2008) agree and conclude that stimulation with frequency modulation increases muscle performance, but this effect is very small and almost non existent to many subjects. Therefore, the effect of stimulation with frequency modulation is not significant in improving muscle fatigue rate.

Up to now, the literature lacks publication on investigating the effect of stimulation frequency and pulse-width in intermittent stimulation with isometric measurement from paraplegic subjects. Furthermore, there are more studies to overcome muscle fatigue rather than to investigate the effect of stimulation frequency and pulse-width on muscle fatigue. Nevertheless, to know the effect of stimulation parameters on muscle fatigue is important before any suggestion can be made on reducing muscle fatigue.

## 4.3 Muscle fatigue test

Eight paraplegic subjects aged between 32 to 47 years participated in this study. The injury levels of the subjects were between T2 to T4. Throughout the experiments, a paraplegic subject was place in a semi-upright sitting position (45° to 60°) with the thigh hanging using thigh support at a frame to avoid any constraint on the leg movement. Velcro straps are used to stabilise the subject's upper trunk, waist and thigh. The isometric force output of the quadriceps muscle was recorded via a force transducer (PCE-FM200, PCE Group Company, Deutschland) placed aligned with the anterior aspect of the leg, about 5cm proximal to the lateral malleolus.

Fatigue of FES induced muscle contraction can be measured by 3 modes; isometric, isotonic or isokinetic. Isometric measurement was applied in this work because this mode of measurement allows easier control of testing parameters, thus minimizing problems associated with performance-based testing criteria (Mizrahi, 1997). The experiment consisted of 2 different protocols: protocol 1 used 5 different stimulation frequencies varying from 10Hz to 50Hz with step size of 10 Hz with other parameters fixed (current at 40mA, pulse-width at 250 μsec and pulse duration at 3 sec on and 7 sec off); and protocol 2 used 5 different stimulation pulse-widths varying from 200μs to 400μs with step size of 50 μs and with other parameters fixed (current at 40mA, frequency at 30Hz and pulse duration at 3 sec on and 7 sec off). The parameter values were chosen to be in the middle of selected range to make sure there were no biases in the measurement. Intermittent stimulation was chosen because the patterns are more realistic in practical use of FES, as actually happens during all functional tasks.

Electrical stimulation was delivered via two MultiStick™ gel surface electrodes (Pals platinum, Axelgaard Mfg. Comp, USA, 50mm x 90mm). The same position of the electrodes discussed in chapter 3 was used. A RehaStim Pro 8 channels (Hasomed GmbH, Germany) stimulator receives stimulation pulses generated in Matlab software through USB connection for application to the muscle.

## 4.4 Paraplegic ability test

One male paraplegic subject aged 45 years participated in this test. The injury level of the subject was T2/T3 and he has had the lesion for 29 years. Paraplegic ability test is to measure the maximum torque, force and angle that can be obtained from the subject's leg without any force applied to the leg. This is to avoid over stimulation of the subject's muscle, which will result in spasm and in turn will influence the output reading, which will not represent the actual output. It is also to prevent the subject from the uncomfortable feeling during the experiment resulting from over stimulation of muscle. A spasm is a sudden, involuntary contraction of a muscle or a group of muscles. It is sometimes accompanied by a sudden burst of pain, but is usually harmless and ceases after a few minutes. Ferrarin and Pedotti (2000) used similar test, but there is no detailed explanation given in their paper. It is very essential to discover the subject's ability so that the test can be done within it.

The maximum leg force, torque and angle were obtained by rising up the paraplegic's leg to maximum extension. The maximum leg extension angle was measured using a goniometer (SG150, Biometrics Ltd, United Kingdom) by placing it in the middle of the outer side and parallel with standing knee position. The position of the leg was recorded instantaneously using Matlab software through analog to digital converter (ADC) card and serial connection. The force and torque were also recorded simultaneously.

## 4.5 Results

### 4.5.1 Muscle Fatigue Test

Muscle performance was assessed by measuring percent decline in peak force and maximum force for different stimulation frequencies and pulse-widths. From the results, it was found that higher frequency gave faster fatigue and the percentage decline of peak force linearly increased with stimulation frequency. It is noted in Figure 4.1 that the force at higher frequencies started at higher peak value at the beginning of stimulation and gave minimum peak value at after 75 stimulations.

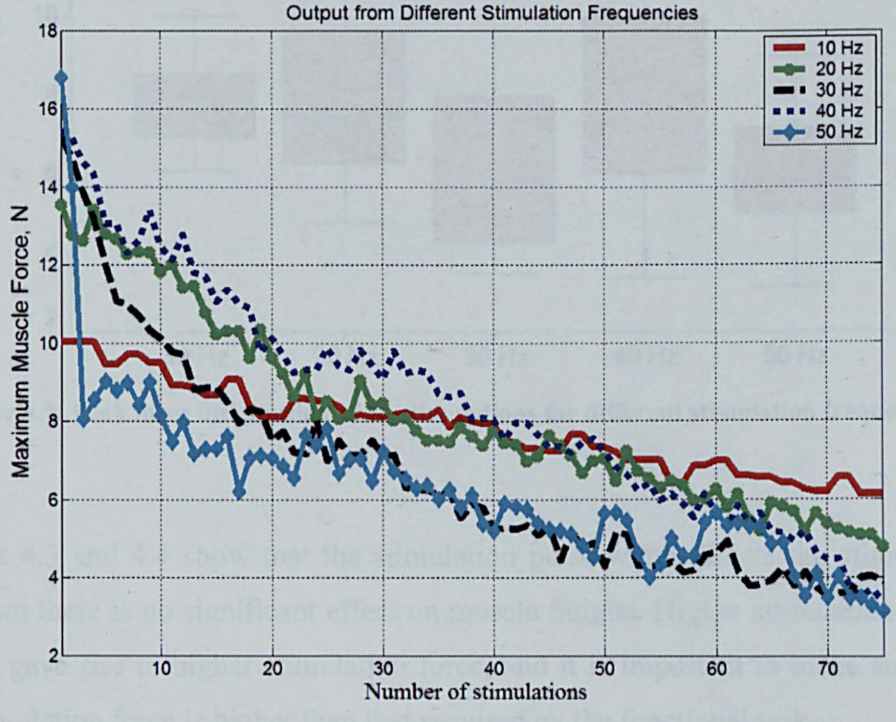


**Figure 4.1: Peak force for 75 stimulations with different stimulation frequencies.**

Figure 4.2 shows the range of peak force for stimulation frequencies from 10Hz to 50Hz. A stimulation frequency at 10Hz gave rise to minimum muscle fatigue and minimum peak force about 10N. Therefore, this frequency is only suitable to be used for stimulation of free swing leg since this task requires minimum torque. It is

not advisable to use a stimulation frequency of 50Hz because it gives rise to the fastest muscle fatigue and can only maintain high force in the first 2 stimulations. Stimulation frequencies between 20Hz to 30Hz are suitable for use in most functional tasks since they will provide high force during the stimulation and can compensate for muscle fatigue.

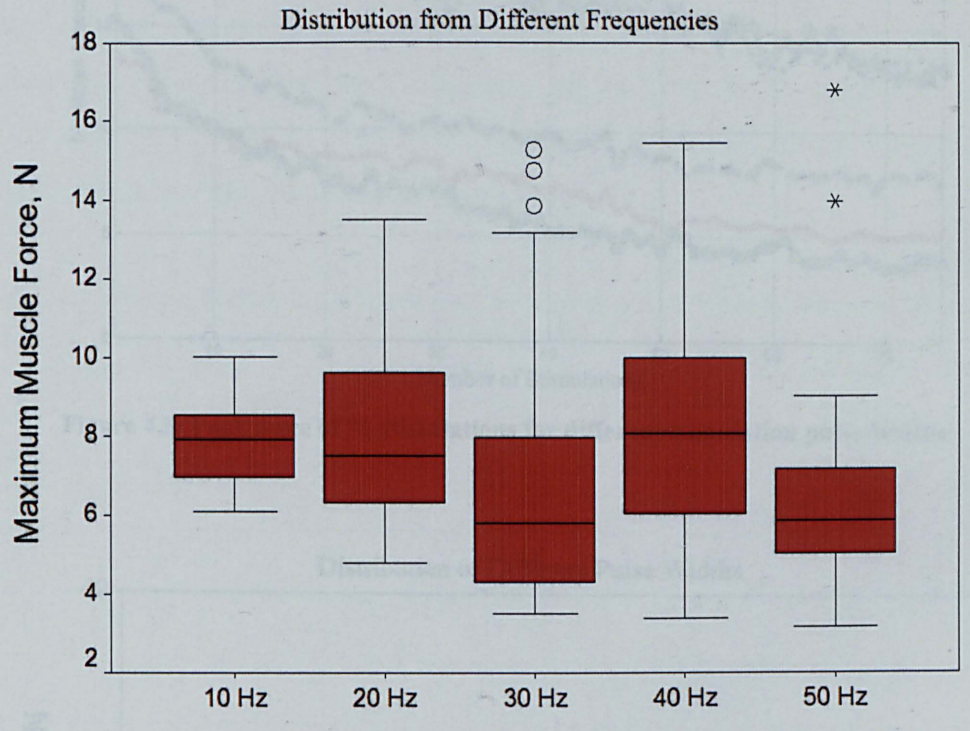


**Figure 4.2: Peak force distribution of 75 stimulations for different stimulation frequencies**

Figures 4.3 and 4.4 show that the stimulation pulse-width affects the stimulation force but there is no significant effect on muscle fatigue. Higher stimulation pulse-widths gave rise to higher stimulation force, and it is important to make sure that the stimulation force is higher than that required by the functional task.

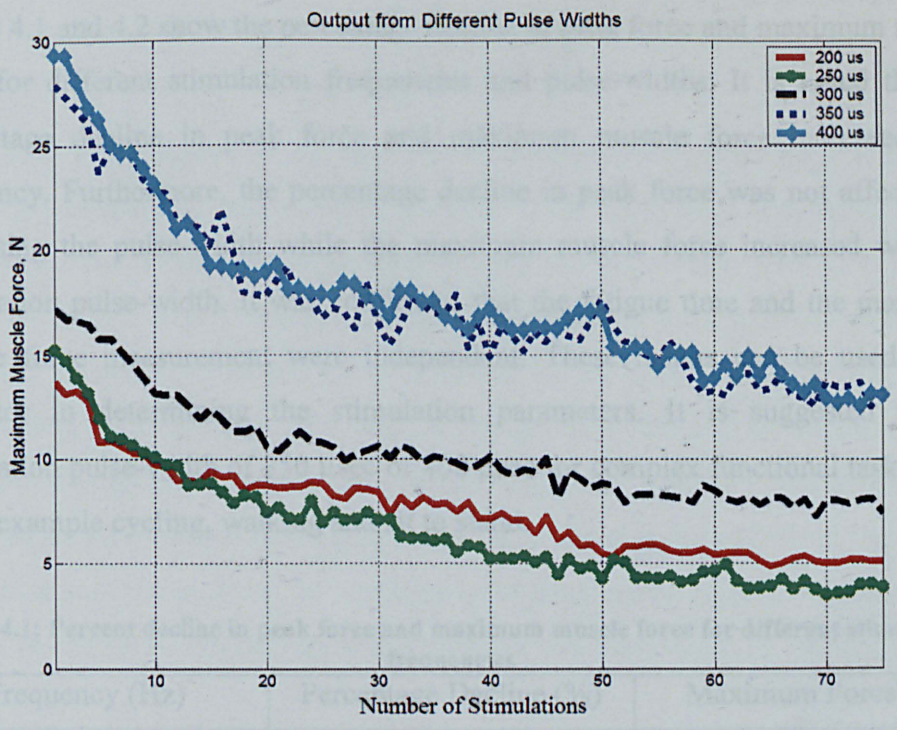


**Figure 4.3: Peak force of 75 stimulations for different stimulation pulse-widths**

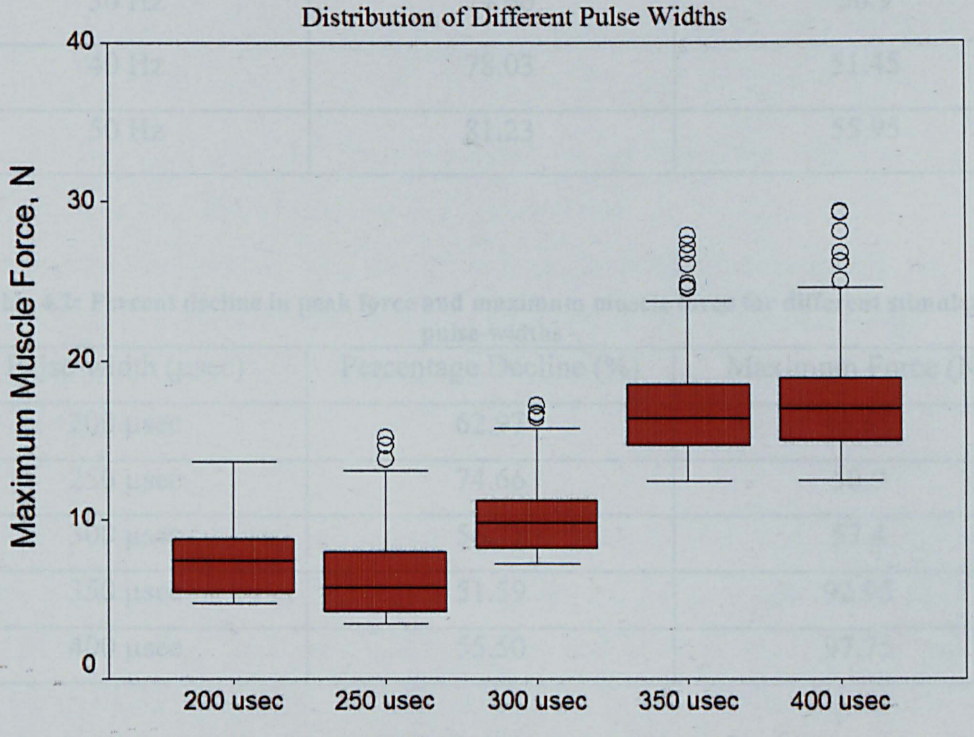


**Figure 4.4: Peak force distribution of 75 stimulations for different stimulation pulse-widths**

Tables 4.1 and 4.2 show the percentage decline in peak force and maximum muscle force for different stimulation frequencies and pulse-widths. It is noted that the percentage decline in peak force and maximum muscle force increased with frequency. Furthermore, the percentage decline in peak force was not affected by increasing the pulse-width while the maximum muscle force increased with the stimulation pulse-width. It was confirmed that the fatigue time and the maximum muscle force measurement were independent. These results can be used as an indicator in determining the stimulation parameters. It is suggested to use stimulation pulse-width of 350 μsec or 400 μsec for complex functional tasks, such as for example cycling, walking and sit to stand.

**Table 4.1: Percent decline in peak force and maximum muscle force for different stimulation frequencies**

| Frequency (Hz) | Percentage Decline (%) | Maximum Force (N) |
|---|---|---|
| 10 Hz | 39.01 | 33.45 |
| 20 Hz | 64.52 | 37.65 |
| 30 Hz | 74.66 | 50.9 |
| 40 Hz | 78.03 | 51.45 |
| 50 Hz | 81.23 | 55.95 |

**Table 4.2: Percent decline in peak force and maximum muscle force for different stimulation pulse-widths**

| Pulse-width (μsec) | Percentage Decline (%) | Maximum Force (N) |
|---|---|---|
| 200 μsec | 62.97 | 45.65 |
| 250 μsec | 74.66 | 50.9 |
| 300 μsec | 56.71 | 57.4 |
| 350 μsec | 51.59 | 92.95 |
| 400 μsec | 55.50 | 97.75 |

### 4.5.2 Paraplegic Ability Test

In order to avoid spasm during and after the experiment, paraplegic's leg ability was tested. In this test, one selected paraplegic subject was used to demonstrate this assessment. The maximum torque, force and leg extension angle were 15 Nm, 47 N and 139° respectively. Therefore, these values represent the maximum leg torque, force and extension angle that can be given to the leg in the condition that the leg swings freely without any force attached or given to the leg. In addition, if the stimulation is given to the leg for specific functional task, the stimulation force produced by the stimulation is equal to the task force plus the additional force. This is to make sure the task can be performed and there are no large amounts of force wasted. A simple rule to overcome this problem was introduced, as follows;

$$Force_{Stimulation} = Force_{Task} + Force_{additional} \tag{4.1}$$

therefore,

$$Force_{Additional} < Force_{Test} \tag{4.2}$$

where $Force_{Stimulation}$ is the force produced by leg from the stimulation given, $Force_{Task}$ is a total force to perform a functional task, $Force_{Additional}$ is the additional force to be added to make sure that the task can be performed accurately; the range of this force is proposed between 5 N to 10 N which can lift around 50kg to 100kg load. $Force_{Test}$ is the force produced from the ability test. This force value varies with subject.

The additional force proposed is in the range of 5 N to 10 N and less than the test force to make sure the functional task given can be performed accurately, not wasted on the extra force produced by the leg and to avoid any injury or spasm to the leg during FES application. Results from the muscle fatigue tests can be used together with simple rules introduced from this work to find the optimum stimulation parameters for a given functional task. For example, if the total force required for performing rowing exercise is 35N and the additional force is 5N, then

$$Force_{Stimulation} = 35 + 5 = 40N$$

and

$$Force_{Additional} < Force_{Test}$$

where the test force for this subject is found as 47N. Thus, with reference to Figure 4.1 to Figure 4.4 an optimum combination of stimulation parameters to produce optimum leg force with low muscle fatigue will be; frequency at 20Hz and pulse-width at 350μsec.

## 4.6 Summary

The results from this study showed that high frequencies give rise to faster muscle fatigue and the selection of force required to perform a functional task is important for obtaining the optimum stimulation parameters. Stimulation pulse-width has no significant effect on the muscle fatigue but highly affects the maximum muscle force. Contradictory results found in some of the previous studies are influenced by dissimilarity in experimental protocols. The results from this work can serve as a guidance to determine the optimum stimulation parameters such as frequency and pulse-width to reduce muscle fatigue during FES application. In order to determine the stimulation parameters, paraplegic ability test has to be conducted on the paraplegic to determine their maximum leg force to avoid spasm or leg injury during and after stimulating paraplegic leg. As a result, frequency of 30Hz to 40Hz and control of stimulation pulse-widths up to maximum 400 μsec are the best stimulation parameters to be used for the FES application. This is because from the analysis conducted in this chapter, these values adequate to produce enough muscle torque during FES functional task.

# Chapter 5

# Control of FES-Assisted Walking with Wheel Walker

## 5.1 Introduction

This chapter presents simulation of bipedal locomotion through regulation of stimulation pulses for activating muscles for paraplegic walking with wheel walker using functional electrical stimulation (FES). The study is carried out with a model of humanoid with wheel walker using the Visual Nastran (vN4D) dynamic simulation software. The developed muscle models of quadriceps and hamstrings discussed in Chapter 3 are used for knee extension and flexion. Proportional-integral-derivative (PID) and fuzzy logic control (FLC) are designed in Matlab/Simulink to regulate the muscle stimulation pulse-width required to drive FES-assisted walking gait and the computed motion is visualised in graphic animation from vN4D. The performance of FLC and PID control are assessed and the best controller that can be used to reduce electrical stimulation is obtained. Firstly, the analysis is carried out without the muscle model to analyse the optimum stimulation parameters to be used for this purpose. Then, the controls are applied to regulate muscle stimulation pulse-width required with the optimum stimulation parameters setting. In this study, pre-defined knee trajectory is used as a reference for FES walking with wheel walker. Later, the body weight transfer (BWT) technique is introduced to improve the paraplegic walking performance by reducing the electrical stimulation required. The effectiveness of this technique is discussed and highlighted.

## 5.2 Control of FES for Paraplegic

FES has been shown to improve impaired function and muscle deterioration in paralyzed limb of SCI patients. However, one of the major limitations is that the stimulated muscles tend to fatigue very rapidly, and this limits the role of FES (Gharooni et al., 2007). Similar to other hybrid FES activities, the performance of FES-assisted walking gait can be enhanced through the implementation of an efficient control strategy. Suitable electrical stimulation to the muscle is required to achieve smooth and well coordinated walking gait.

Many researchers have investigated various control strategies to address the variability and nonlinearities of the musculoskeletal system, muscle conditioning and fatigue in many different FES-activities (Chizeck, 1988, 1992). Control has been a great challenge in paraplegic mobility research due to the highly non-linear and time-varying nature of the system involved. Conventional control has been used, but knowledge based control such as neural networks (Chen et al., 2004; Graupe and Kordylewski, 1994), fuzzy logic (Chen et al., 2004; Feng and Andrews, 1994; Davoodi and Andrews, 2004; Sau Kuen and Chizeck, 1994) and genetic algorithm (Davoodi and Andrews, 1999) is still the practical choice in most current mobility control systems. Feng and Andrews (1994) used adaptive fuzzy logic control (FLC) to control FES for swinging leg. They found that the controller can customize a general rule based controller and adapt to the time-varying parameters due to muscle while Yu-Luen et al. (2004) found that fuzzy control solves the non-linear problem by compensating for the motion trace errors between neural network control and actual system. One of the possible methods is the use of closed-loop adaptive control technique that measures the output and alters the muscle stimulation for better control.

This chapter presents the effectiveness of two main approaches; body weight transfer and control strategy to enhance the performance of walking gait and reduce stimulation pulses required to drive FES-walking manoeuvre.

## 5.3 Walking Gait and Predefined Reference Trajectories

Walking gait is the medical term to describe human locomotion. Interestingly, every individual has a unique gait pattern. A person's gait can be greatly affected by injury or disease. The gait cycle is used to describe the complex activity of walking, or a gait pattern. This cycle describes the motions from initial placement of the supporting heel on the ground to when the same heel contacts the ground for a second time.

The gait cycle is divided into two phases, stance and swing. Stance is defined as the interval in which the foot is on the ground, and this constitutes approximately 60% of the gait cycle. It is divided into four phases; heel strike (HS), foot flat (FF), mid stance, heel off (HO) and toe off (TO). On the other hand, swing is defined as the interval which the foot is not in contact with the ground, and this constitutes approximately the remaining 40% of the gait cycle. Swing is divided into two phases; acceleration to mid-swing and deceleration from mid swing to complete one full gait cycle. Figure 5.1 illustrates the stance and swing phases for one complete normal human gait cycle (Anonymous, 2011).

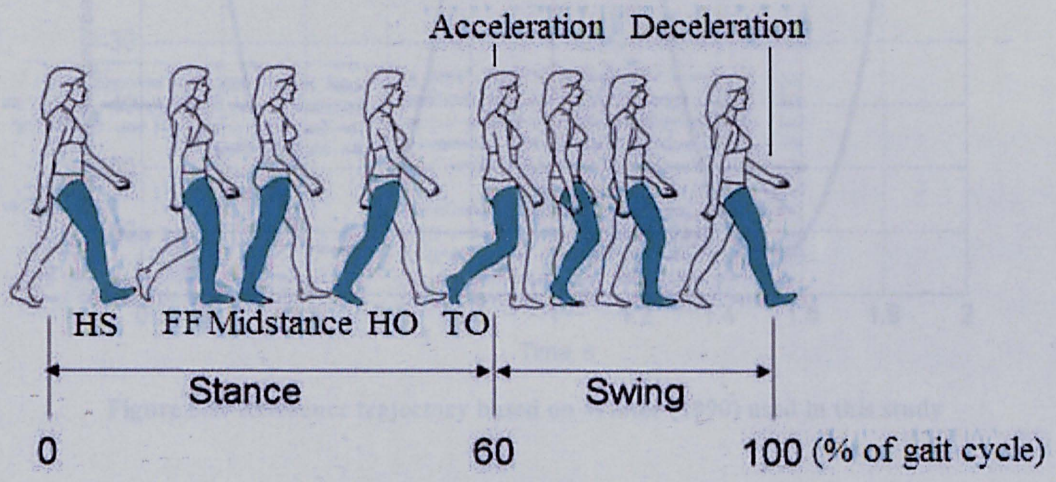


**Figure 5.1: Gait cycle (Anonymous, 2011)**

Currently, physical therapist evaluates each individual phase of the gait cycle to obtain clues into specific muscular weaknesses and shortening. Addressing these issues in a rehabilitation program will lead to a more efficient gait pattern, resulting in decreased risk of injury, less energy expenditure, greater functional independence, and improved muscular balance. However, here one reference trajectory obtained from Winter (1990) referring to the normal human gait based on anthropometric data of one paraplegic subject is used for this study. Figure 5.2 shows the reference trajectory for FES walking used in this work. Electrical stimulation used is limited to the hamstrings and quadriceps muscles. Hip movement will follow the hip flexion kinetics theory that will be explained later in section 6.3.3. Therefore, in this study the reference trajectory considered is represented by walking knee angle only. The same reference trajectory will be used throughout the thesis so that comparative assessments can be made. In addition, all experiments and simulations are based on the same subject so that results from this study can be further validated by experimental work applied to the particular subject.

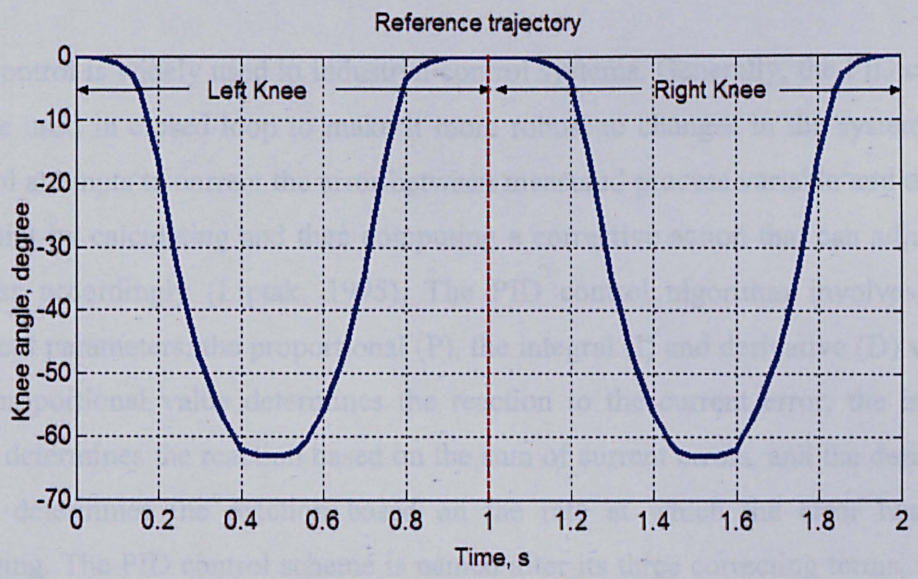


**Figure 5.2: Reference trajectory based on Winter (1990) used in this study**

## 5.4 Control of FES-Assisted Walking with Wheel Walker

This chapter aim is to gain an insight into control strategies which subsequently served as a basis for the synthesis of a life-like control scheme suitable for restoration of functional FES-assisted control of paraplegic walking with wheel walker. Two different type of controllers used in this thesis; there are proportional-intergral-derivatives (PID) linear controller and fuzzy logic nonlinear controller. In this chapter, the controllers are applied to investigate the torque required and to control stimulation pulse-width for walking with and without body weight transfer. The approach was an engineering attempt, based on biomechanical analysis of single and double inverted pendulum stabilization requirements, addressing several crucial questions related to integration of the actions of the intact physiological system (upper body) with the actions of the FES system supporting the paralyzed physiological system (lower extremities).

### 5.4.1 PID control

PID control is widely used in industrial control systems. Generally, the PID control can be used in closed-loop to make it more robust to changes in the system. PID control attempts to correct the error between measured process variable and desired set point by calculating and then computing a corrective action that can adjust the process accordingly (Liptak, 1995). The PID control algorithm involves three different parameters; the proportional (P), the integral (I) and derivative (D) values. The proportional value determines the reaction to the current error, the integral value determines the reaction based on the sum of current errors, and the derivative value determines the reaction based on the rate at which the error has been changing. The PID control scheme is named after its three correcting terms, whose sum constitutes the output. Hence the output is given as:

$$Output(t) = P_{out} + I_{out} + D_{out} \tag{5.1}$$

where $P_{out}$, $I_{out}$ and $D_{out}$ are the contributions to the output from the PID controller. The proportional term makes a change to the output that is proportional to the current error value. The proportional response can be adjusted by multiplying the error, $e(t)$ by a constant $K_p$, called the proportional gain. The magnitude of the contribution of the integral term to the overall control action is determined by the integral gain, $K_i$. The magnitude of the contribution of the derivative term or rate to the overall control action is determined by the derivative gain, $K_d$. The PID controller output that is the final form of PID algorithm is combination of these three terms and is given as:

$$u(t) = K_p e(t) + K_i \int_0^t e(\tau)d\tau + K_d \frac{de}{dt} \tag{5.2}$$

### 5.4.2 Fuzzy Logic control

An FLC system is a control system that analyzes analog input values in terms of logical variables and takes on continuous values between 0 and 1. FLC was first proposed by Lotfi A. Zadeh of the University of California at Berkeley in 1965 (Zadeh, 1965). The ideas of fuzzy logic were elaborated in 1973 that introduced the concept of "linguistic variables", which equates to a variable defined as a fuzzy set. A fuzzy logic is described as computing with words rather than numbers and a fuzzy control can be described as control with sentences rather than equations (Jantzen, 1998).

FLCs are used to control consumer products, such as washing machines, video cameras and rice cookers, as well as industrial processes, such as cement kilns, underground trains and robots. One of the first industrial applications of the FLC was the cement kiln built in Denmark. Mamdani implemented FLC on steam engine in 1974 (Mamdani, 1974). Many practical applications of fuzzy logic were invented including the subway Sendai Transportation control system in Japan, automated aircraft vehicle landing and the first fuzzy TV set by Sony in 1990.

Today the number of fuzzy logic interventions and projects are enormous and fuzzy logic systems have been employed as powerful tools in many control techniques in different areas such as robotics, medicine instrumentation and industry.

A typical fuzzy system consists of a rule-base, membership functions (MFs), and an inference procedure. Figure 5.3 shows the basic control architecture of FLC. A brief description of the fuzzy logic paradigm is provided in this section.

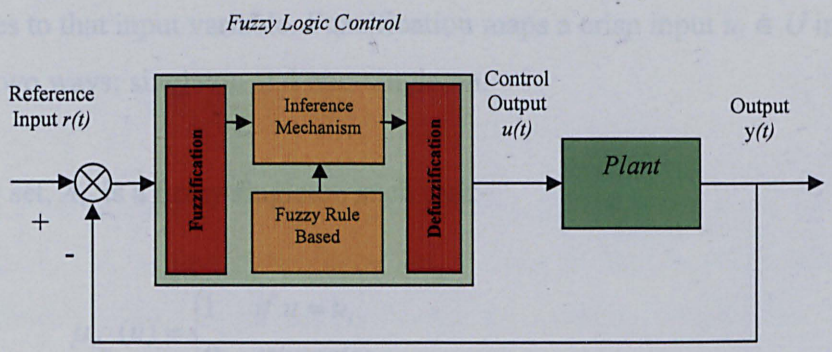


**Figure 5.3: Basic fuzzy logic control architecture**

### 5.4.2.1 Fuzzy sets

The input variables in a fuzzy control system are in general mapped into membership functions and are known as fuzzy sets. A fuzzy set that is represented by a membership function is defined in the universe of discourse, which is the space where the fuzzy variables are defined. The membership function gives the grade or degree of the membership within the set of any element of the universe of discourse. The membership function is quantifies with the certainty of the variable that belongs to the fuzzy set. Each of the membership functions will have a boundary that starts from one point and ends at another point. This boundary might fall into a triangle, trapezium or Gaussian shape. The numbers that are mapped by the membership functions are said to be its members. The membership function of a fuzzy set is a continuous function in the range of 0 to 1 (Passino and Yurkovich, 1998).

5.4.2.2 Fuzzification

The first block inside the FLC architecture is fuzzification, which converts each piece of numeric input data to fuzzy input in degree of memberships by a lookup in one or several membership functions. Figure 5.4 shows example of a triangular membership function. The fuzzification block thus matches the input data with the condition of the rules to determine how well the condition of each rule matches that particular input instance. There is a degree of membership for each linguistic term that applies to that input variable. Fuzzification maps a crisp input $u_i \in U$ into fuzzy set $A_{u_i}$ in two ways; singleton and non-singleton.

The fuzzy set, $A_{u_i}$ is a fuzzy singleton such that:-

$$\mu_{A_{u_i}}(u) = \begin{cases} 1 & if\ u = u_i \\ 0 & otherwise \end{cases} \tag{5.3}$$

The fuzzy set, $A_{u_i}$ is a fuzzy non-singleton or fuzzy set (triangular, trapezoidal or Gaussian MF) such that:-

$$\mu_{A_{u_i}}(u) = \begin{cases} 1 & if\ u = u_i \\ 0 & decreases\ from\ 1\ as\ u\ moves\ from\ u_i \end{cases} \tag{5.4}$$

where $\mu_{A_{u_i}}(u)$ is the MF and $U$ is the universe of discourse. Note that the singleton fuzzification is generally used in the implementations where there is no noise.

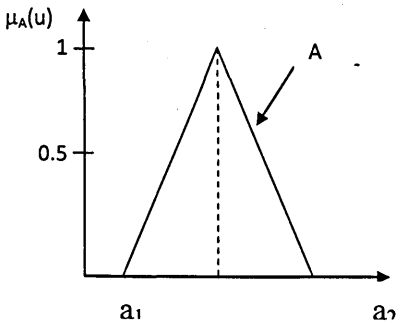


**Figure 5.4: Triangular membership functions**

5.4.2.3 Fuzzy inference mechanism

Inference is the process of formulating a mapping from a given input space to the output space. The mapping then provides a basis of the decisions that can be accomplished. The process of fuzzy inference involves the membership functions, fuzzy logical operations and fuzzy if-then rules base. There is more than one type of fuzzy rules processing that have been widely employed in various control applications and the most popular ones are the Mamdani-type fuzzy rules processing and Sugeno-type fuzzy rules processing. The differences between these fuzzy inference processes are the consequents of the fuzzy rules, aggregations and defuzzification procedures.

Mamdani's fuzzy inference method is the most commonly seen fuzzy methodology. Mamdani's method was among the first control systems built using fuzzy set theory. Mamdani's effort was based on Zadeh's work on fuzzy algorithms for complex systems and decision processes. Mamdani-type inference expects the output membership functions to be fuzzy sets. After the aggregation process, there is a fuzzy set for each output variable that needs defuzzification. The Sugeno-type inference process replaced the Mamdani's consequent part of the fuzzy rules by a function.

5.4.2.4 Fuzzy rule base

A fuzzy system is characterized by a set of linguistic statements based on expert knowledge. The expert knowledge is usually in the form of *if-then* rules which are easily implemented by fuzzy condition statements in fuzzy logic. The rules may use several variables both in the condition and the conclusion of the rules. The controllers can therefore be applied to both multi-input-multi-output (MIMO) problems and single-input-single-output (SISO) problems. The typical SISO problem is to regulate a control signal based on an error signal. The controller may actually need both the error, the change of error and the accumulated error as inputs but in principle all three are formed from the error measurement.

Basically a linguistic controller contains rules in the *if-then* format but can be presented in different formats. In many systems, the rules are presented to the end-user in a format similar to the following:-

i) Standard fuzzy system: This fuzzy system uses linguistic fuzzy rules (Mamdani-type fuzzy rules) which are formed solely from linguistic variables and values. They are simply abstract ideas about how to achieve good control. The general form of Mamdani rules is
**IF** <*premise*> **OPERATOR** <*premise*> **THEN** <*consequent*>

This type of fuzzy system is used as the FLC strategy throughout this study. For example:

**IF** $e(t)$ is *NB* **AND** $\Delta e(t)$ is *Z* **THEN** $u(t)$ is *NS*
**IF** $e(t)$ is *PB* **AND** $\Delta e(t)$ is *Z* **THEN** $u(t)$ is *PS*

where variables $e(t)$, $\Delta e(t)$ and $u(t)$ are the system error, change of error and output whereas the NB, NS, Z, PS and PB are the linguistic values that are the linguistic qualifier determined for a proper

variable and refers to as *negative big*, *negative small*, *zero*, *positive small* and *positive big* respectively.

ii) Functional fuzzy system: This is known as Takagi-Sugeno-Kang (TSK) fuzzy system, proposed as an alternative to the standard fuzzy systems. The TSK rules can be described as follows:

$IF\ x_1\ is\ C_1^l\ and \cdots and\ x_n\ is\ C_n^l,\ THEN\ \ y^l = c_0^l + c_1^l x_1 + \cdots + c_n^l x_n$

where $C_i^l$ are fuzzy sets, $c_i^l$ are constants, and $l$=1,2,... n is the rule number. The IF parts of the rules are the same as in the ordinary fuzzy IF-THEN rules, but the THEN parts are linear combinations of the input variables $x = (x_1,...,x_n) \in U$ (Wang, 1997).

#### 5.4.2.5 Defuzzification

After fuzzy reasoning, the linguistic output variable needs to be translated back into crisp value. The objective of the translation is to derive a single crisp numeric value that best represents the inferred fuzzy value of the linguistic output variable. Defuzzification is such inverse transformation that maps the output from the fuzzy value back into crisp value. Some defuzzification methods tend to produce an integral output considering all the elements of the resulting fuzzy set with the corresponding weights. Other methods take into account just the element corresponding to the maximum points of the resulting membership functions (Shaw, 1998). There are several defuzzification methods described as follows:

i) Centroid of Area (CoA): This method is often referred to as Centroid of Gravity (CoG) method that computes the centriod of the composite representing the output fuzzy term. Figure 5.5 shows the CoG defuzzification method on a fuzzy output, where $u_c$ is chosen to represents the centre of gravity of the shaded area.

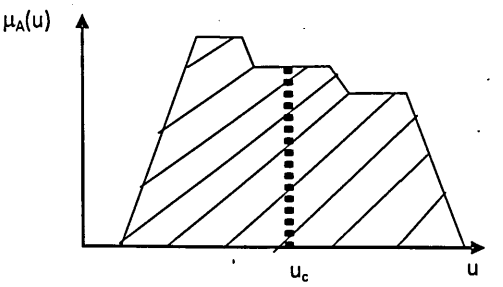


**Figure 5.5: CoG defuzzification methods on a fuzzy output**

$$u_c = \begin{cases} \dfrac{\int \mu_A(u).u.du}{\int \mu_A(u).du} & \textit{in the continous case} \\ \dfrac{\sum \mu_A(u).u}{\sum \mu_A(u)} & \textit{in the discrete case} \end{cases} \tag{5.5}$$

This method is used throughout this study.

ii) Centroid of Maximum (CoM): This method uses the peak values of membership functions. The defuzzified crisp compromise value is determined by finding the place where the weights are balanced. The crisp output is computed as a weighted mean of the term membership maxima, weighted by the inference results.

iii) Middle of Maxima (MoM): This method consists of taking the mean level of all maxima within the fuzzy membership shape. This method is normally used in some cases when the CoM approach does not work. This occurs whenever the maxima of the membership functions are not unique.

Figure 5.6 demonstrates an example of the max-min inferencing and centroid defuzzification for a system with input variables "*e(t)*", "*Δe(t)*", and "*MS*" and an

output variable "*u(t)*". Note that "*mu*" is standard fuzzy-logic nomenclature for "truth value". Each rule provides a result as a truth value of a particular membership function for the output variable. In centroid defuzzification the values are OR'd, that is, the maximum value is used and values are not added, and the results are then combined using a centroid calculation.

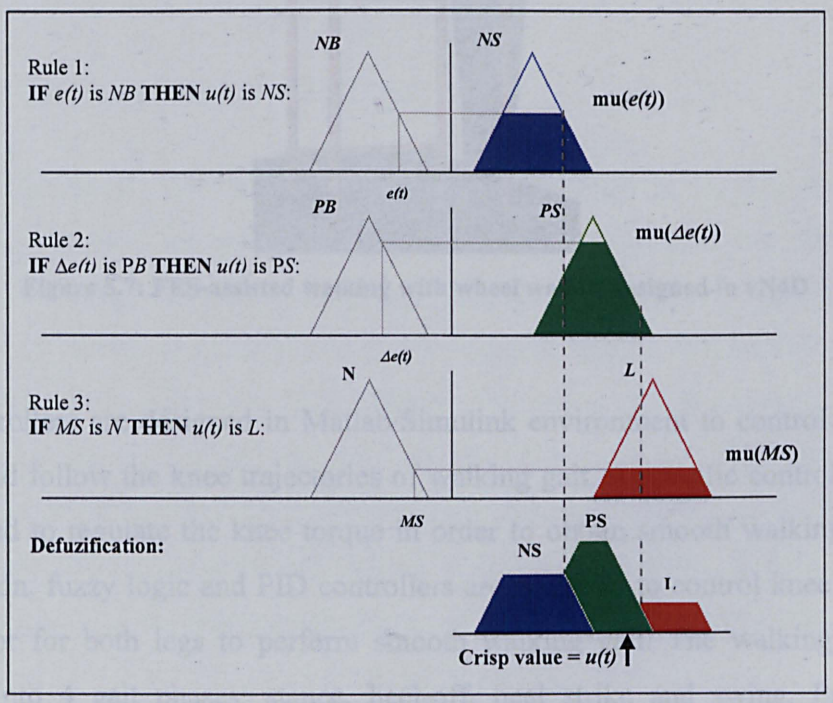


**Figure 5.6: Max-min inferencing and CoG defuzzification method**

## 5.5 Control of Output Torque for FES-Assisted Walking

The FES-assisted walking with wheel walker developed using vN4D is shown in Figure 5.7. It is controlled to follow the predefined reference trajectory discussed in section 5.3 by controlling the torque amount of right and left knee to coordinate the body movement for a smooth walking gait. In this section, the knee output torque

for walking manoeuvre is analysed so that the stimulation parameters can be obtained. Therefore, the muscle model is not included in this section.

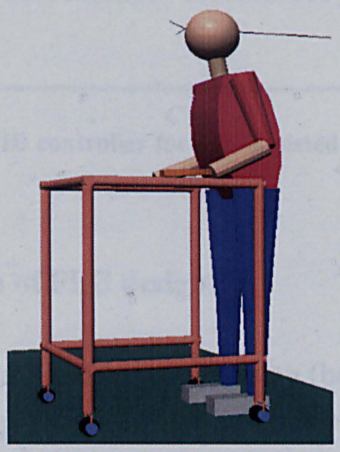

**Figure 5.7: FES-assisted walking with wheel walker designed in vN4D**

The controllers are designed in Matlab/Simulink environment to control the knee torque and follow the knee trajectories of walking gait. A specific control strategy is required to regulate the knee torque in order to obtain smooth walking gait. In this section, fuzzy logic and PID controllers are designed to control knee extensor and flexor for both legs to perform smooth walking gait. The walking cycle is divided into 4 gait phases; stance, heel-off, heel strike and swing. Predefined walking trajectory is used as a reference trajectory for both controllers.

### 5.5.1 Implementation of PID control design

In this section, two PID controllers are used, one for each leg. For left knee PID controller, the parameter values used were 3.6, 0.02 and 0.05 while for right knee PID controller parameter values were 3, 0.01 and 0.025 for P, I and D respectively. These controller parameters were tuned by trial and error to obtain the best trajectories that tracked the predefined reference trajectories. Figure 5.8 shows a block diagram of the PID controller applied to evaluate the knee torques of the paraplegic walking system. The PID controller input is an error between the system output and the reference while the output is stimulation knee torques.

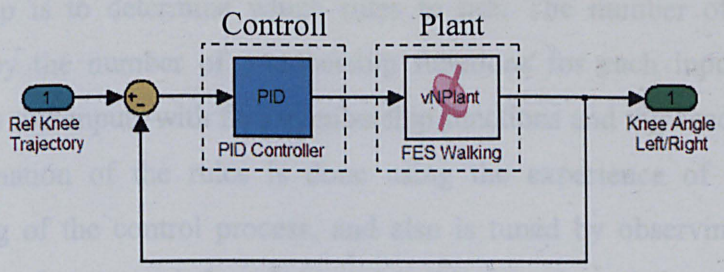


**Figure 5.8: Block diagram of PID controller for FES-assisted walking without muscle model**

### 5.5.2 Implementation of FLC design

For the FLC design, five equal distributed Gaussian (bell-shaped) type membership functions were used for each input and output. The FLC inputs and outputs were fuzzified by using a fuzzy set of five variables defined by Gaussian shaped membership functions: negative big (NB), negative small (NS), zero (Z), positive small (PS) and positive big (PB). Figure 5.9 shows the distribution of fuzzy membership functions used in this section. Moreover, in this study, equal distribution of the membership functions gives sufficient satisfaction for the control process, because changing the distribution will change the results significantly. The Gaussian shape for the membership functions is recommended when smoothness is needed.

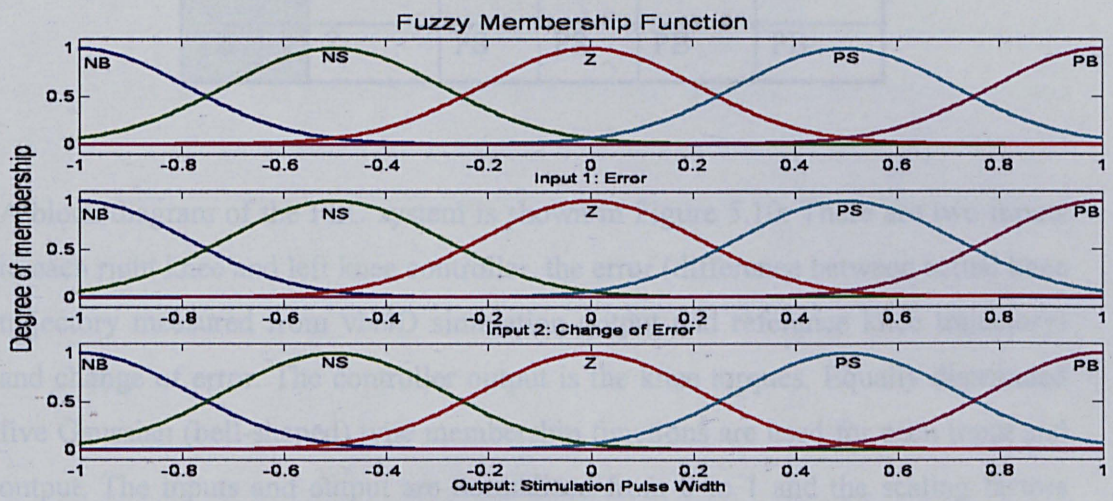


**Figure 5.9: Fuzzy membership functions**

The next step is to determine which rules to use. The number of the rules is determined by the number of membership functions for each input. The fuzzy controller has two inputs with five membership functions and this leads to 25 rules. The determination of the rules is done using the experience of the designer, understanding of the control process, and also is tuned by observing the control process, taking important information and building up knowledge of the system. Any combination of two linguistic variables fires at least one rule. They are consistent, with no contradictions and are continuous. Table 5.1 shows the fuzzy rules for torque of both. The fuzzy output is generated by using the standard five by five fuzzy rules table as shown. The final step of the design process is the defuzzification method which converts the linguistic values into crisp values by using several defuzzification methods. The centroid of gravity method is used here because it is commonly used in feedback control due to its smooth output.

**Table 5.1: Fuzzy rules for leg extension**

| e \ Δe | NB | NS | Z | PS | PB |
|---|---|---|---|---|---|
| NB | NB | NB | NS | NS | Z |
| NS | NB | NS | NS | Z | PS |
| Z | NS | NS | Z | PS | PS |
| PS | NS | Z | PS | PS | PB |
| PB | Z | PS | PS | PB | PB |

A block diagram of the FLC system is shown in Figure 5.10. There are two inputs to each right knee and left knee controller, the error (difference between actual knee trajectory measured from vN4D simulation output and reference knee trajectory) and change of error. The controller output is the knee torques. Equally distributed five Gaussian (bell-shaped) type membership functions are used for each input and output. The inputs and output are normalised from 0 to 1 and the scaling factors used in left leg FLC were 0.1, 0.0025 and 70 while in the right leg FLC these were 0.055, 0.0025 and 70 for error, change of error and output respectively. The knee

torques from fuzzy controller are used to drives the vN4D model to follow the walking gait. Then the error and change of error are fed back to the fuzzy controller to adjust knee torques required to the optimum level.

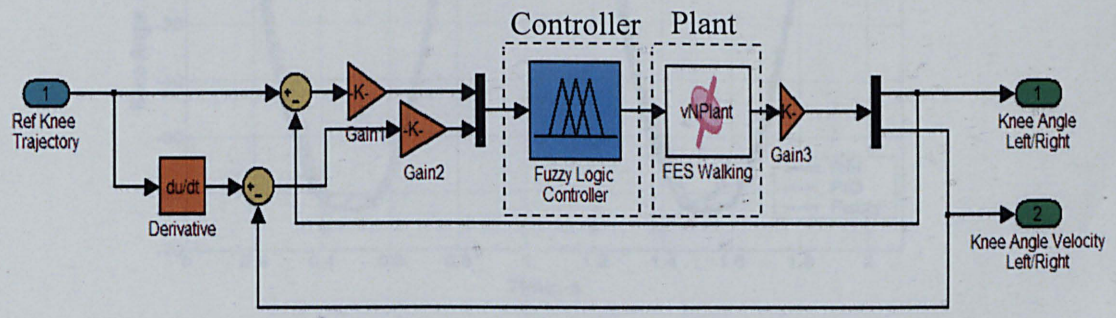


**Figure 5.10: Block diagram of FLC for FES-assisted walking without muscle model**

### 5.5.3 Results and Discussion

The control strategy was implemented in Matlab/Simulink with incorporation of humanoid with wheel walker model in vN4D to investigate the knee torques required for FES-assisted walking manoeuvre with wheel walker. The control objective is to regulate the level of knee torques to perform smooth walking gait by following the reference trajectory. The knee trajectories for walking gait from PID and FLC are shown in Figure 5.11. Due to various perturbations and limited strength of the hip and knee flexor and extensor muscles, the shank and thigh may not perfectly track the reference trajectory but one walking cycle was completed steadily. The performance of FES walking manoeuvre in this chapter was assessed by evaluating the walking trajectories and visually observing the walking progress and system stability from the vN4D.

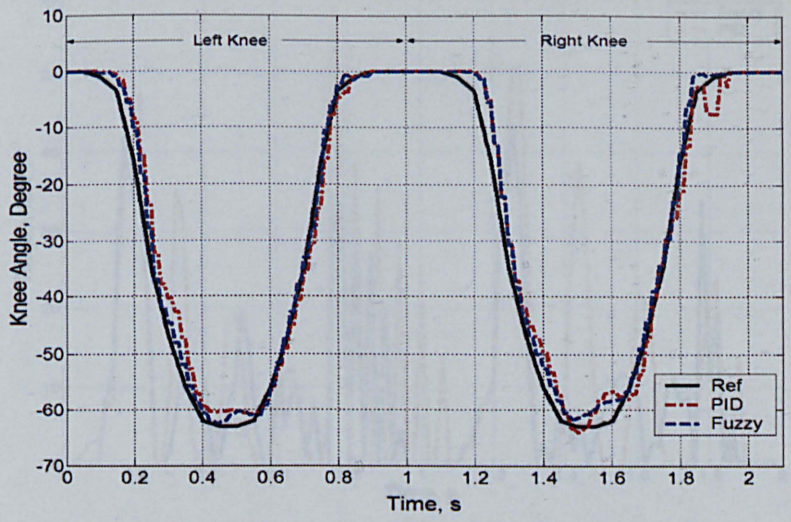


**Figure 5.11: Reference and actual trajectories from PID and FLC**

The accuracies of these two techniques in terms of walking gait were similar but for FLC, the total torque required was slightly less. Figure 5.12 and Figure 5.13 show the quadriceps and hamstrings torques respectively for one complete walking cycle from PID and FLC. It is noted that the maximum torque required for one complete walking cycle was not more than 60Nm for both control techniques. According to the analysis in chapter 4, suitable stimulation frequency to be used for walking in this thesis is between 30Hz to 40Hz. In this frequency range, muscle fatigue can be minimised and the paraplegic can possibly have more than 10 complete walking cycles before the knee torque reaching below 60Nm because of muscle fatigue. Therefore, 35Hz has been selected as a stimulation frequency from this point and throughout the thesis. It is to minimise muscle fatigue while having an enough torque power to drive FES for paraplegic walking with wheel walker.

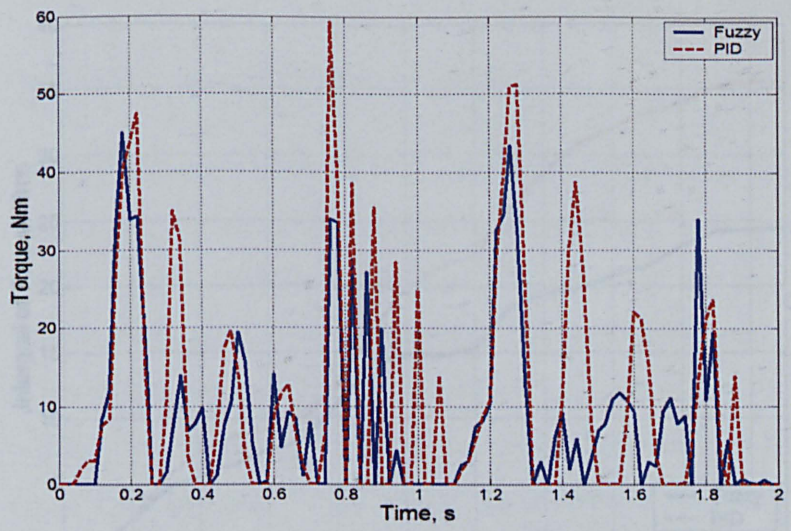


**Figure 5.12: Quadriceps torque required from PID and FLC**

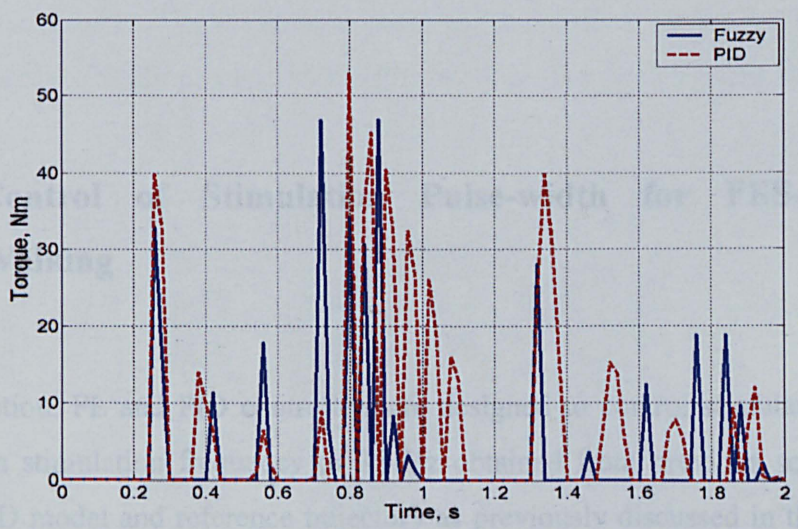


**Figure 5.13: Hamstrings torque required from PID and FLC**

Figure 5.14 shows the integral of knee torques for both controllers. It is noted that the torque required for one complete gait using PID was 33.33% more than the total torque required using FLC. The percentage of reduction or increment was calculate by taking the difference between integral of both techniques over the initial value, in this case maximum integral value from PID was the initial value.

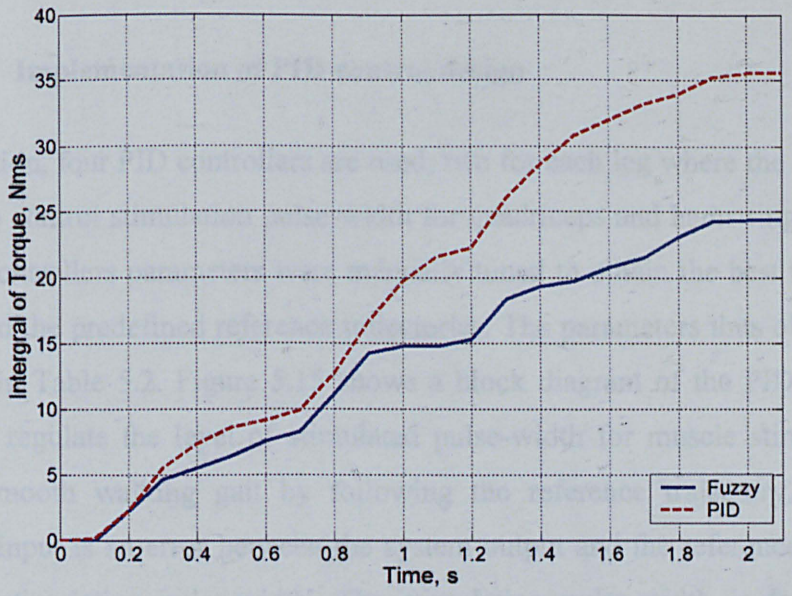


**Figure 5.14: Integral of knee torque of PID and FLC**

## 5.6 Control of Stimulation Pulse-width for FES-Assisted Walking

In this section, FL and PID controllers are designed to control stimulation pulse-width with stimulation frequency of 35 Hz obtained from previous section. The same vN4D model and reference trajectory as previously discussed in this chapter are used. In addition to the system, quadriceps and hamstrings muscle models developed in Chapter 3 ares used in this section. The controllers are used to control the stimulation pulse-width and feed to the muscle models. Then, the output knee torque produced form the muscle models are used to drive the knee to follow the trajectories of walking gait. The same predefined walking trajectory is used as a reference trajectory for the controllers.

### 5.6.1 Implementation of PID control design

In this section, four PID controllers are used; two for each leg where the controllers are used to control stimulation pulse-width for quadriceps and hamstrings muscles. The PID controllers parameters were manually tuned to obtain the best trajectories that tracked the predefined reference trajectories. The parameters thus obtained are as shown in Table 5.2. Figure 5.15 shows a block diagram of the PID controller applied to regulate the level of stimulated pulse-width for muscle stimulation to perform smooth walking gait by following the reference trajectory. The PID controller input is an error between the system output and the reference while the output is stimulation pulse-width. The stimulation pulse-width is fed into the quadriceps and hamstrings muscle models to produce an accurate knee torque for the particular subject. The stimulation pulse-width produced by the controllers will be the same stimulation pulse-width produced in the FES system for walking purpose.

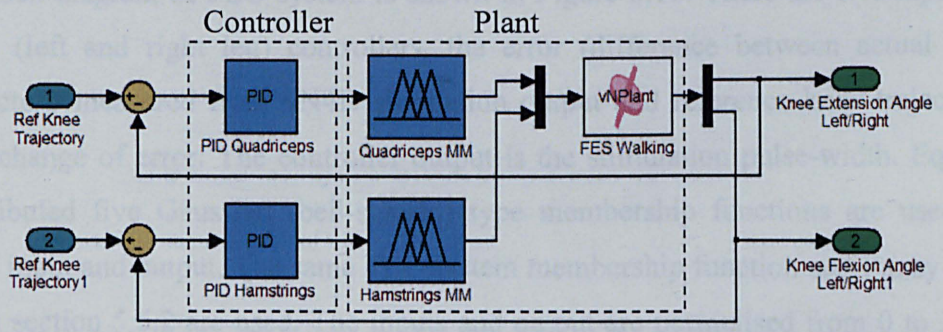


**Figure 5.15: Block diagram of PID controller for FES-assisted walking with muscle model**

**Table 5.2: PID controller parameters for FES walking with muscle model**

| Control | | Proportional gain, $K_p$ | Integral gain, $K_i$ | Derivative gain, $K_d$ |
|---|---|---|---|---|
| Right Leg | PID controller for quadriceps muscles | 6.4 | 2.19 | 0.13 |
| | PID controller for hamstrings muscles | 12.4 | 2.97 | 0.16 |
| Left Leg | PID controller for quadriceps muscles | 6.21 | 2.13 | 0.11 |
| | PID controller for hamstrings muscles | 12.18 | 2.85 | 0.14 |

### 5.6.2 Implementation of FLC design

A block diagram of FLC system is shown in Figure 5.16. There are two inputs to each (left and right leg) controllers, the error (difference between actual knee trajectory measured from vN4D simulation output and reference knee trajectory) and change of error. The controller output is the stimulation pulse-width. Equally distributed five Gaussian (bell-shaped) type membership functions are used for each input and output. The same FLC system membership function and Fuzzy rules as in section 5.5.2 are used. The inputs and output are normalised from 0 to 1 and the scaling factors used are shown in Table 5.3. The input and output scaling factors were manually obtained by trial and error technique to attain the best trajectories. The stimulation pulse-width from fuzzy controller is used as input for the quadriceps and hamstring muscle models. The muscle models will produce suitable knee torques to drive the vN4D model to follow the walking gait. Then the error and change of error are fed back to the fuzzy controller to adjust the knee torques to the required optimum level.

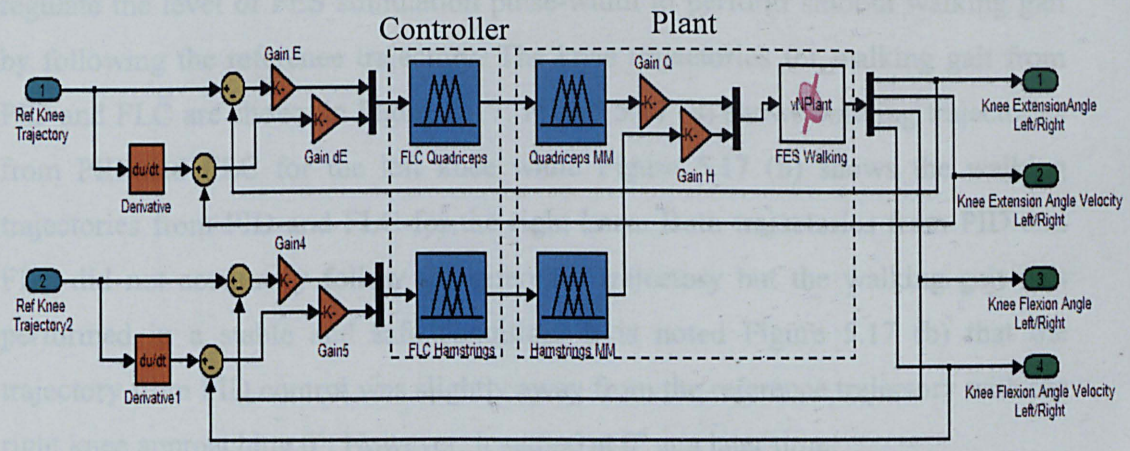


**Figure 5.16: Block diagram of FLC for FES-assisted walking with muscle model**

**Table 5.3: FLC scaling factors for FES walking with muscle model**

| Control | | Input scaling factor, $G_E$ | Input scaling factor, $G_{\Delta E}$ | Output scaling factor, $G_O$ |
|---|---|---|---|---|
| Right Leg | FL controller for quadriceps muscles | 0.12 | 0.025 | 551 |
| | FL controller for hamstrings muscles | 0.15 | 0.027 | 528 |
| Left Leg | FL controller for quadriceps muscles | 0.08 | 0.025 | 551 |
| | FL controller for hamstrings muscles | 0.13 | 0.027 | 528 |

### 5.6.3 Results and Discussion

The same control strategy as in the previous section was implemented with incorporation of humanoid with wheel walker model in vN4D and quadriceps and hamstrings muscle model to control the FES stimulation pulse-width required for

FES-assisted walking manoeuvre with wheel walker. The control objective is to regulate the level of FES stimulation pulse-width to perform smooth walking gait by following the reference trajectory. The knee trajectories for walking gait from PID and FLC are shown in Figure 5.17. Figure 5.17 (a) shows walking trajectories from PID and FLC for the left knee while Figure 5.17 (b) shows the walking trajectories from PID and FLC for the right knee. Both trajectories from PID and FLC did not accurately follow the reference trajectory but the walking gait was performed in a stable and safe condition. It is noted Figure 5.17 (b) that the trajectory from PID control was slightly away from the reference trajectory with the right knee approaching 0°. However, it settled at 0° at a later time.

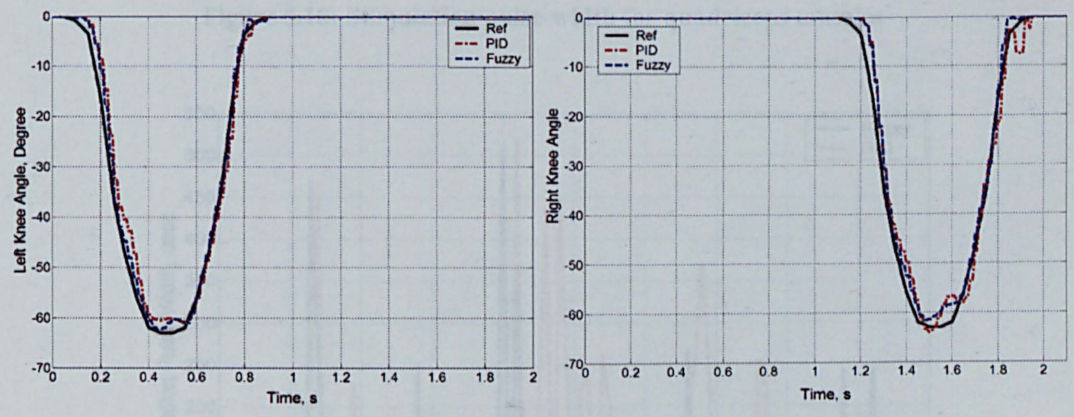


**(a) Left Knee** **(b) Right Knee**

**Figure 5.17: Reference and actual trajectories from PID and FLC**

The accuracies of the two controllers in terms of walking gait were similar but for FLC, the total stimulation pulse-width required was less, leading to reduced and muscle fatigue. Figure 5.18 shows the stimulation pulse-width for the quadriceps muscle model from the PID and FL controllers while Figure 5.19 shows the stimulation pulse-width for the hamstring muscle model from the PID and FL controllers. This stimulation pulse-width was generated from PID and FL controllers. It is clearly noted that the stimulation pulse-width for hamstring muscle model from FLC was less than PID control but stimulation pulse-width for the quadriceps muscle model could not be easily observed. Therefore, Figure 5.20 shows the integral of stimulation pulse-width for both controllers and both muscle models so that the stimulation pulse-width reduction can be compared.

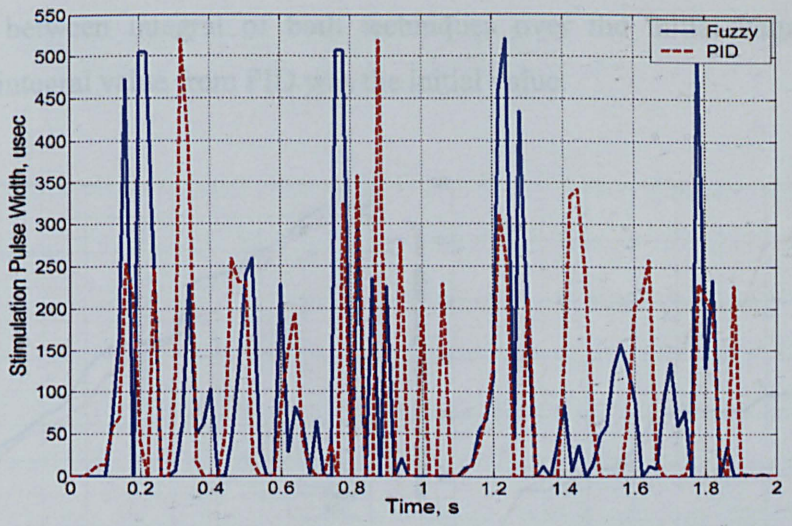


**Figure 5.18: Stimulation pulse-width for quadriceps muscles**

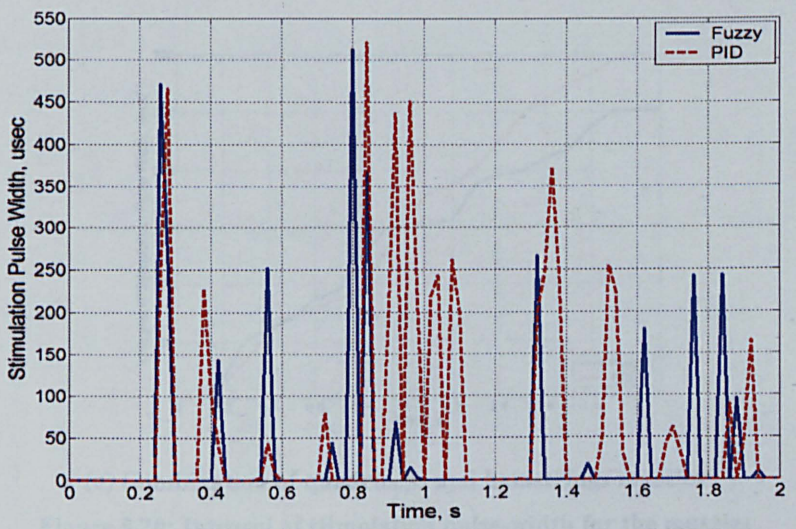


**Figure 5.19: Stimulation pulse-width for hamstring muscles**

Figure 5.20 shows the integral of stimulation pulse-width for quadriceps, hamstrings and combination of both muscle models for PID and FL controllers. It is noted that the stimulation pulse-width required for quadriceps muscles from FLC was 1.96% higher than PID while stimulation pulse-width required for hamstrings muscles from FLC was reduced by 18.02% compared to the FLC. This means that for one complete gait using FLC the overall stimulation pulse-width was 16.06% less than total stimulation pulse-width required using PID control. As same as

before, the percentage of reduction or increment was calculate by taking the difference between integral of both techniques over the initial value and the maximum integral value from PID was the initial value.

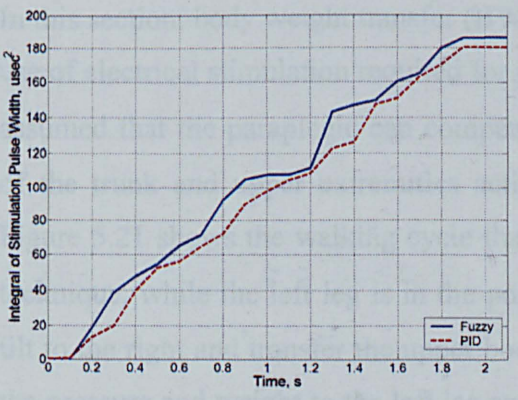


(a) Quadriceps muscles

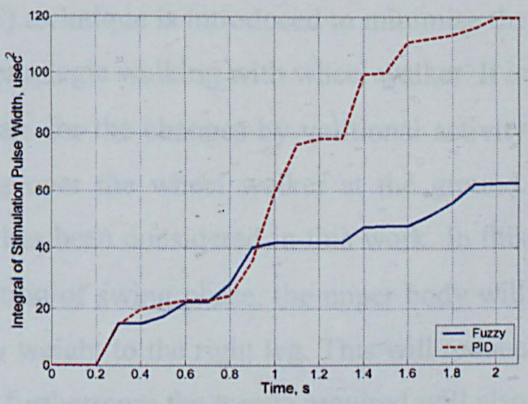


(b) Hamstrings muscles

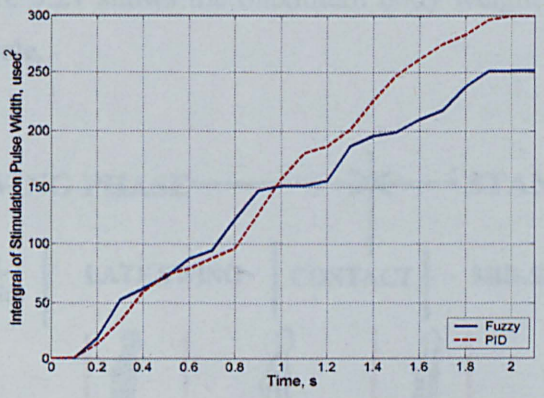


(c) Combination of quadriceps and hamstrings muscles

**Figure 5.20: Integral of stimulation pulse-width for the muscles**

## 5.7 Control of Stimulation Pulse-width for FES-Assisted Walking with Body Weight Transfer

In this section, body weight transfer (BWT) technique is introduced to minimise the use of electrical stimulation required for paraplegic walking with wheel walker. It is assumed that the paraplegic can compensate for the changes by volitional activity of the trunk and upper extremities acting over the wheel walker at the ground. Figure 5.21 shows the walking cycle that has been considered in this work. In this technique, while the left leg is in the position of swing phase, the upper body will tilt to the right and transfer the upper body weight to the right leg. This will reduce the pressure and weight to the left leg and furthermore the torque required will also decrease. The same procedure is used with the left leg in the stance phase. The shaded area in Figure 5.21 shows the maximum body weight position during one complete walking cycle.

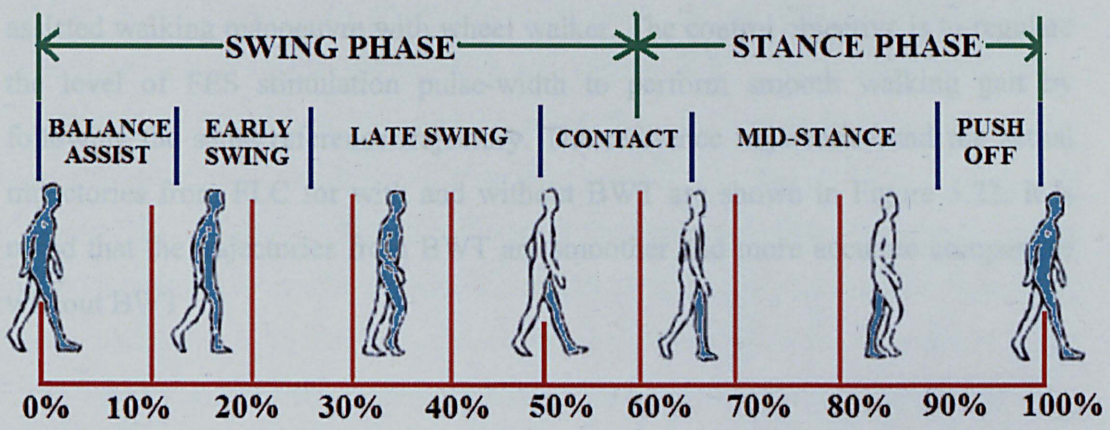


**Figure 5.21: Body weight transfer in walking cycle**

### 5.7.1 Implementation of FLC design

In this section, FLC is selected to investigate the effectiveness of BWT to reduce the stimulation pulse-width. This is because in the previous study, FLC was found to give the minimum stimulation pulse-width compared to PID control for the same

task. The same FLC system with quadriceps and hamstrings muscle models in section 5.6.2 is used as in Figure 5.16. In this section, the only difference is on the body weight transfer where the position of the body is considered in the model in vN4D. The model is developed to follow the body weight transfer theory so that it will reduce the pressure and weight on the stimulated leg. The same scaling factors used in section 5.5.3 were found to be suitable for this propose. Therefore, all the FLC values were set as before and no changes were made to the control part.

### 5.7.2 Results and Discussion

The BWT is introduced to reduce the stimulation pulse-width. This section investigates the effectiveness of BWT by analysing the output of the controller. The same FLC system is adopted with the modified humanoid with wheel walker model in vN4D that integrates the BWT theory and both quadriceps and hamstrings muscle models to control the FES stimulation pulse-width required for FES-assisted walking manoeuvre with wheel walker. The control objective is to regulate the level of FES stimulation pulse-width to perform smooth walking gait by following the same reference trajectory. The reference trajectories and the actual trajectories from FLC for with and without BWT are shown in Figure 5.22. It is noted that the trajectories from BWT are smoother and more accurate compare to without BWT.

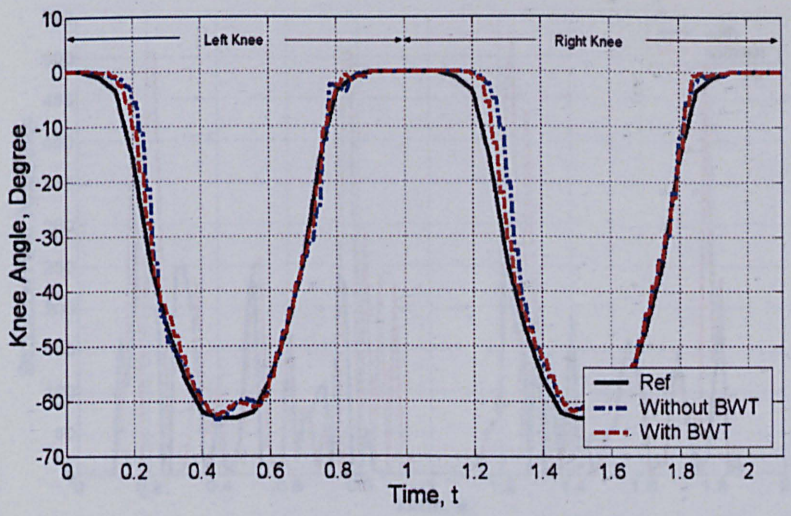


**Figure 5.22: Reference and actual trajectories from with and without BWT**

Although the accuracy of the system with BWT in terms of walking gait was better compared to the system without BWT, the most important feature is to have less stimulation pulse-width so that the muscle fatigue can be minimised to the optimum level. Figure 5.23 shows the stimulation pulse-width for the quadriceps muscle models while Figure 5.24 shows the stimulation pulse-width for the hamstring muscle models from the system with and without BWT. This stimulation pulse-width was generated from the same FL controllers. It is noted in these figures that the stimulation pulse-width for the system with BWT was less than the system without BWT. Therefore Figure 5.25 shows the integral of stimulation pulse-width for both controllers so that the stimulation pulse-width reduction can be compared. It is noted that for the hamstrings muscles, stimulation pulse-width more than 500 μsec was require for the system without BWT while the system with BWT only required less than 250 μsec. This reduction is half with the system with BWT. Especially for hamstrings muscles which tend to fatigue very quickly compared to the quadriceps muscles.

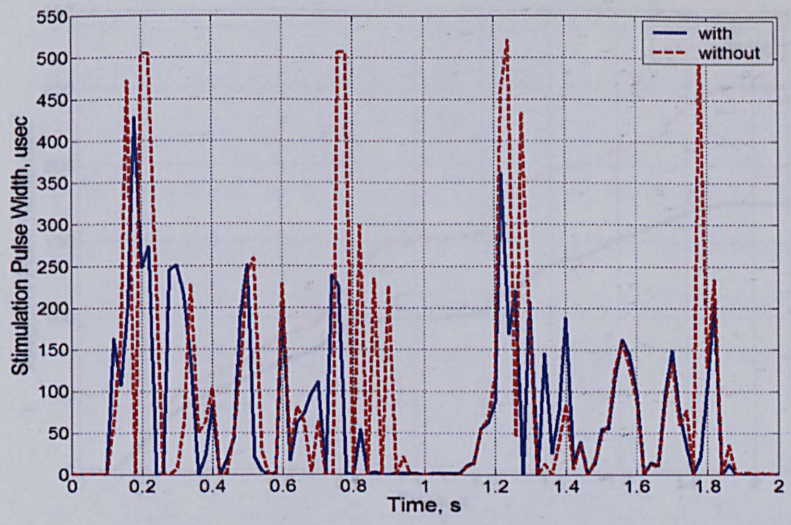


**Figure 5.23: Stimulation pulse-width from quadriceps muscle**

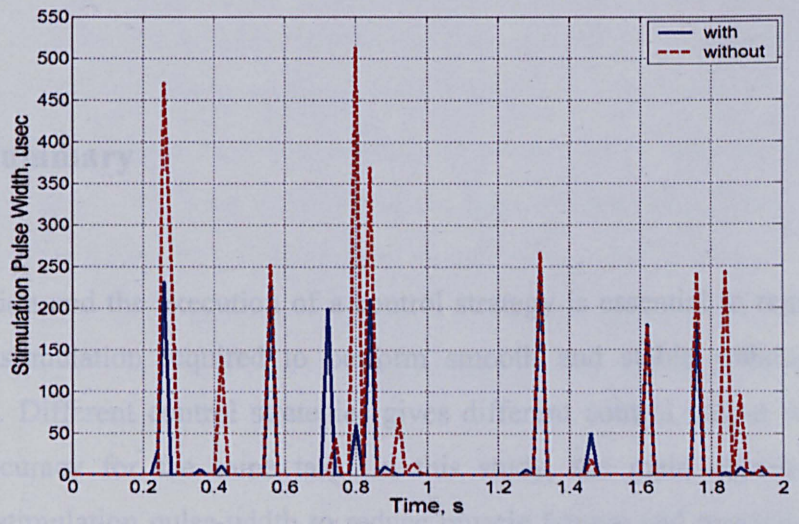


**Figure 5.24: Stimulation pulse-width from hamstring muscles**

Figure 5.25 shows the total integral of stimulation pulse-width for system with and without BWT. It is noted that the stimulation pulse-width required for system with BWT was 30.58% less than the system without BWT. This means that the system with BWT greatly reduces stimulation pulse-width required for walking with wheel walker. This technique is also a practical solution as it does not require any addition instrument to be attached to the paraplegic. It only requires training to be given to the paraplegic so that the upper body movement is used well to transfer body weight to the correct leg at the correct time.

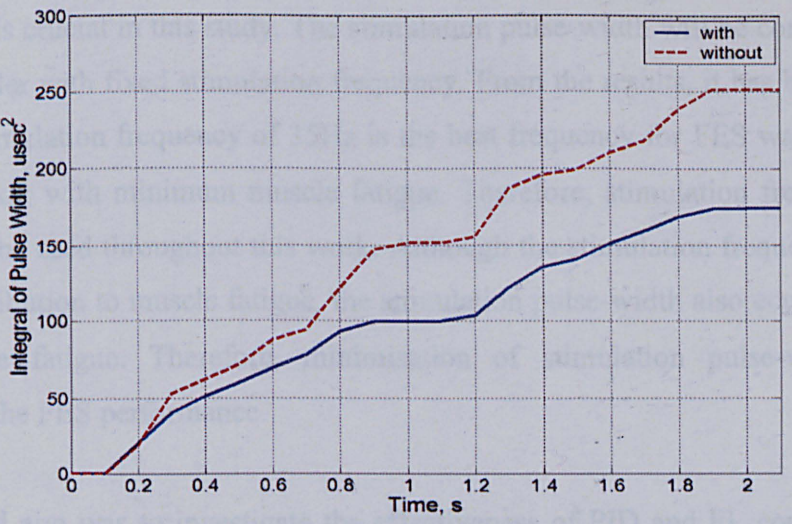


**Figure 5.25: Integral of stimulation pulse-width for combination of quadriceps and hamstrings muscles**

## 5.8 Summary

The selection and the execution of a control strategy is essential in regulating the electrical stimulation required to perform smooth and stable walking gait for paraplegic. Different control strategies gives different control output with almost similar accuracy for the same task. In this study, the main objective was to minimise stimulation pulse-width to reduce muscle fatigue and maximise the FES performance. This chapter discussed the strategies to control the stimulation pulse-width required for both quadriceps and hamstrings muscles for FES walking with wheel walker. Two control strategies used in this chapter were PID and FLC and their performances were evaluated.

The first aim of this chapter was to investigate the torque required for FES walking with wheel walker. The torque required has been compare with the results from Chapter 4 and then used to decide on suitable stimulation pulse-width to be used in this study. It is explained in the previous chapter that only stimulation frequency will greatly affect the muscle fatigue. Therefore the selection of stimulation

frequency is crucial in this study. The stimulation pulse-width will be controlled by the controller with fixed stimulation frequency. From the results, it has been found that the stimulation frequency of 35Hz is the best frequency for FES walking with wheel walker with minimum muscle fatigue. Therefore, stimulation frequency of 35Hz will be used throughout this work. Although the stimulation frequency is the main contribution to muscle fatigue, the stimulation pulse-width also contributes to the muscle fatigue. Therefore, minimisation of stimulation pulse-width will maximise the FES performance.

The second aim was to investigate the effectiveness of PID and FL controllers in minimising the stimulation pulse-width required. The results have shown that in one complete walking cycle, there has been more than 15% reduction in stimulation pulse-width and more than 18% reduction in torque required for walking with FLC as compared with the torque required for walking with PID. It is also concluded that PID and FLC have been successfully implemented to regulate the level of stimulation pulse-width used to stimulate the knee extensor and flexor muscle for FES-assisted walking with wheel walker. Based on the control strategy developed, a stable walking gait has been achieved. The advantage of FLC to minimise stimulation pulse-width and torque required in FES-assisted walking with wheel walker has been demonstrated.

The third and last aim in this chapter was to demonstrate the advantage of body weight transfer to minimise stimulation pulse-width and torque required in FES-assisted walking with wheel walker. The results have shown that in one complete walking cycle, there has been more than 30% reduction in stimulation pulse-width required for walking with body weight transfer compared with walking without body weight transfer. It is also concluded that FLC has been successfully implemented to regulate the level of stimulation pulse-width used to stimulate the knee extensor and flexor muscles for FES-assisted walking with wheel walker with minimum muscle fatigue.

# Chapter 6

# Spring Break Orthosis

## 6.1 Introduction

This chapter presents the simulation of a bipedal locomotion through regulation of stimulation pulses for activating muscles for paraplegic walking with wheel walker using FES with spring break orthosis (SBO). A new methodology for paraplegic gait, based on exploiting natural dynamics of human gait, is introduced. The work is a first effort towards restoring natural like swing phase in paraplegic gait through a hybrid orthosis, referred to as SBO. This mechanism simplifies the control task and results in smooth motion and more-natural like trajectory produced by the flexion reflex for gait in spinal cord injured subjects. The study is carried out with a model of humanoid with wheel walker using the Visual Nastran (vN4D) dynamic simulation software. Stimulated muscle model of quadriceps is developed for knee extension. FLC and PID control are developed in Matlab/Simulink to regulate the muscle stimulation pulse-width required to drive FES-assisted walking gait and the computed motion is visualised in graphic animation from vN4D. A comparative assessment of the FLC and PID control is carried out and the associated results are presented and discussed.

## 6.2 Hybrid Orthosis

Restoring gait in individuals with SCI is a research challenge. Researchers have investigated various electrical, mechanical and combined techniques, also called hybrid orthosis, to restore functional movement in the lower limbs (Ferguson et al., 1999; Isakov et al., 1992; Nene, 1989; 1990; Philips and Hendershot, 1991; Popovic et al., 1989; Solomonow et al, 1997; Tinazzi, 1997). Among the gait phases, the swing phase is important in advancing the leg in order to contribute to movement of the body in the direction of gait progress. Hip flexion is an essential part of pick-up in the swing phase of reciprocal gait, whilst passive hip extension is important during the trunk glide in stance. Researchers have attempted to provide hip flexion to improve walking by FES. FES was first introduced in 1967, is a technique that uses a low level of electrical current to stimulate the physical or bodily functions lost through nervous system impairment, that is affected by paralysis resulting from SCI, head injury, stroke or other neurological disorders, restoring function in people with disabilities (Cooper et al., 2005). Nowadays, the applications of FES include standing, walking, cycling, rowing, ambulation, grasping, male sexual assistance, bowel-and-bladder function control and respiratory control. To support walking support, FES-assisted paraplegic walking needs parallel bars, walker or crutches. Moreover, paraplegic walking with only FES has significant drawbacks in function restoration. Firstly, due to stimulated muscle contractions, muscle fatigue will quickly occur because of the reversed recruitment order of the artificially stimulated motoneurons. As a result, there are limitations in standing time and walking distance. Another disadvantage is erratic stepping trajectories because of poor control of joint torque (Hausdorff and Durfee, 1991).

Hybrid systems can overcome these limitations by combining FES with the use of a lower limb orthotic brace. Orthoses can guide the limb and reduce the number of degrees of freedom in order to simplify the control problem. The use of active muscle can also be reduced by locking orthosis joints (Goldfarb et al., 2003). Moreover, the approach is useful to support body weight, protect the joint and ligament (Huq, 2009). Furthermore, its rigidity improves walking efficiency and reduces overall energy cost (Stallard and Major, 1995). Several hybrid systems have been developed. The first hybrid orthosis system combining powered orthosis with FES called hybrid assistive system (HAS) has been introduced by Tomovic (1972), and then the work on HAS has continued by Popovic and Schwirtlich (Popovic, 1987,1990; Schwirtlich, 1984). Afterward HAS has been changed to powered orthosis because of the use of direct current (DC) motor in the orthosis. Another type of hybrid system is called powered orthosis which provides more function than purely passive hybrid orthosis. A small DC electric motor is installed at one or more joints with or without electrical stimulation support. A functional movement mimics the swing phase of gait closer than the flexion reflex (Popovic et al., 1987;1989;1990). However, this type of hybrid system is not used in practice because of the size and weight of motor and batteries. Figure 6.2 shows the power orthosis.

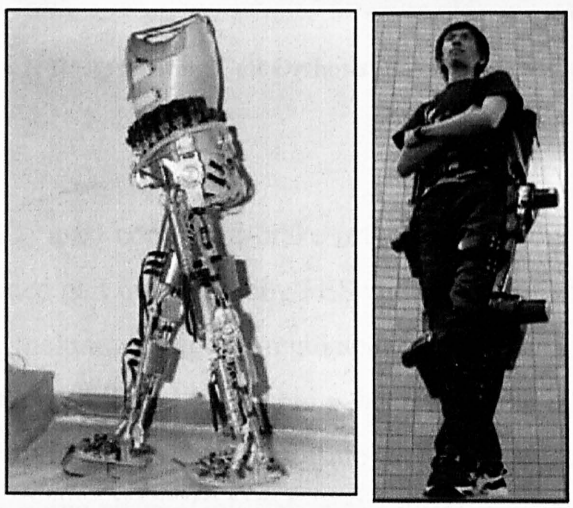

**Figure 6.1: Power orthosis (Ferris et al., 2005)**

The most widely tested orthosis, named reciprocating gait orthosis (RGO) (Hendershot, 1991; Isakov et al., 1992; Philips and Solomonow et al, 1997), has been designed to meet the needs of the spina bifida patient. This mechanism moves the contralateral limb forward by using surface stimulation of hip extension. Then, by alternating stimulation of the hip extensors, the walking can be achieved with less energy consumption. However, during the leg-swing phase the body requires to be lifted by the arm with the help of crutches, making it difficult to produce foot clearance. Consequently, muscle fatigue will quickly occur (Solomonow et al., 1997). Figure 6.2 shows the RGO in the market.

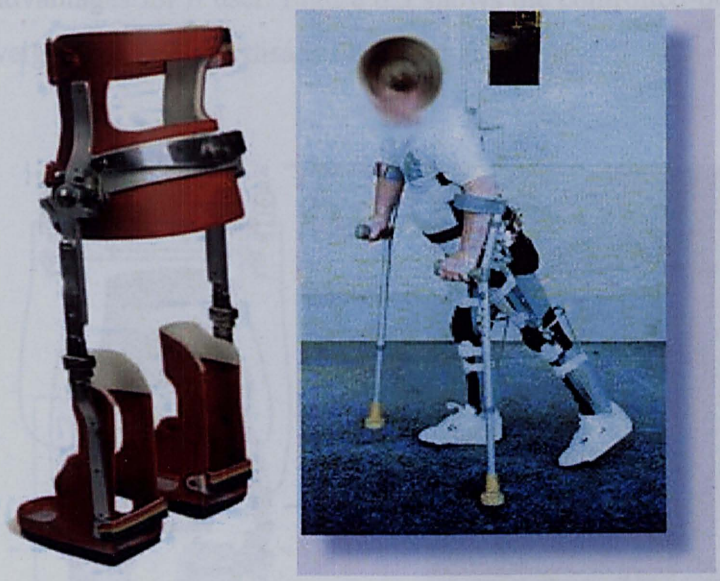

**Figure 6.1: Reciprocating Gait Orthosis (Solomonow et al., 1997)**

Goldfarb et al. (2003) used controlled-brake orthosis, which is able to address the constraint of FES-aided gait by combining FES with a controllable passive orthosis. This hybrid system includes computer-regulated friction brake at the hip and the knee. Muscle fatigue is reduced by locking the brakes during stance phase and turning off stimulation to the quadriceps muscle. In addition, leg movement repeats smoothly during the swing phase (Goldfarb et al., 2003).

Kobetic et. al (2009) introduced their hybrid orthosis called hybrid neuroprosthesis (HNP). The system uses 16 channels of FES stimulation delivered via chronically indwelling intramuscular electrodes to activate 8 different muscles for the knee, hip and ankle flexion and extension. Electrodes are connected to an external control unit (ECU) temporarily or permanently to an implanted generator powered and controlled via radio frequency by ECU. The variable constraint hip mechanism (VCHM) consisting of hydraulic system with double acting cylinders linked to each hip joint and controlled by energizing specific solenoid valves has been designed to maintain hip posture (Kobetic et. al, 2009). The result obtained from the clinical test with one paraplegic subject is promising. However the system size and weight outweigh the advantages for it user. Figure 6.3 shows the controlled-brake orthosis. The size and weight also become disadvantageous for it user.

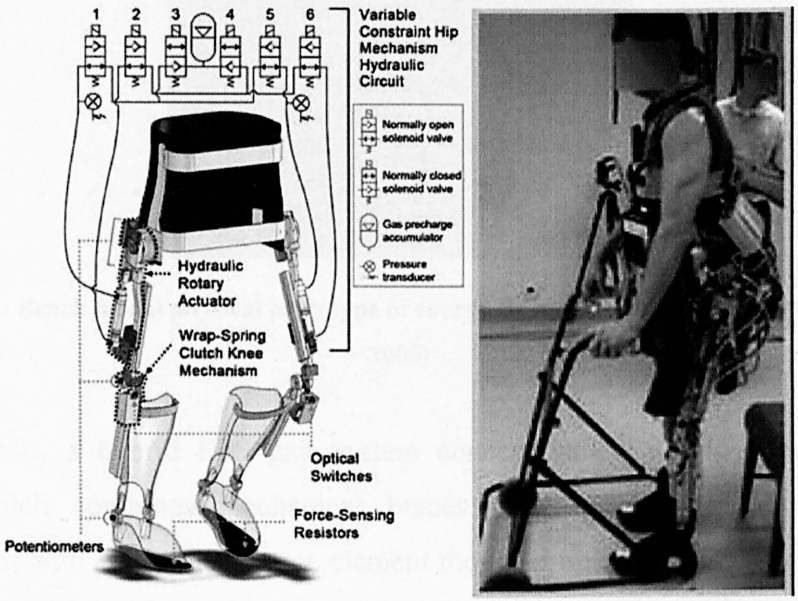


**Figure 6.3: Controlled-Brake Orthosis (Kobetic et al., 2009)**

Durfee and Rivard (2005) introduced energy storage orthosis (ESO) which can be driven through a complete gait cycle. This mechanism uses stimulated muscle power to move the limb and also to drive the orthosis structure, storing energy in the process. Gas springs crossing the hip and knee joints are flexed equilibrium energy-storage elements. The energy store and transfer systems comprise a pneumatic fluid power system connected between knee and hip joints. This can

capture the excess energy during the quadriceps stimulation in order to transfer to the hip and release at appropriate instant to achieve hip extension (Durfee and Rivard, 2005). Figure 6.4 shows the bench model of energy storage orthosis developed by Durfee and Rivard which consists of gas spring on the back side.

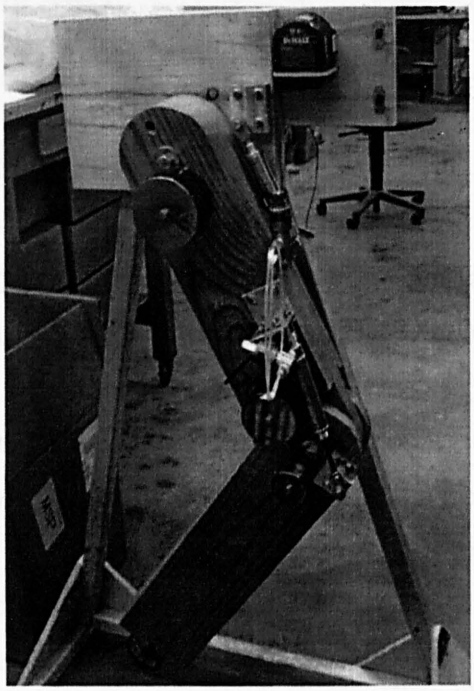

**Figure 6.4: Bench model physical prototype of energy storage orthosis (Durfee and Rivard, 2005)**

In this thesis, a hybrid FES gait system concept called Spring-Brake-Orthosis (SBO) which combines mechanical braces (with coordinated joint locking mechanism) with an energy storage element mounted on it and FES to generate the swing phase of paraplegic gait is presented (Gharooni, 2001). This approach also substantially simplifies and reduces the problem of control tasks in a hybrid orthosis while offering more benefits on quality of a swinging leg. Previous work, (Gharooni, 2001) has developed and validated SBO for leg swing phase while Huq (2009) used SBO in body weight supported treadmill locomotion in simulation environment. In this thesis, the application of SBO is widened where it is used for paraplegic walking with wheel walker. The new concept in hybrid orthotics provides solutions to the problems that affect current hybrid orthosis, including

knee and hip flexion without relying on the withdrawal reflex or a powered actuator and foot-ground clearance without extra upper body effort.

## 6.3 Walking Gait in SBO

There are two major forces that act during walking particularly the swing phase; gravity and segment interaction forces. Gravity acts on all masses comprising the body, and for the purpose of analysis, they can all be replaced with a single resultant force acting at the point of centre of mass (CoM). The projection of the centre of mass on the ground is called centre of gravity (CoG). In the SBO the spring acts as an external force on the knee joint and causes the knee to flex and potential energy is stored in the lower leg (by raising the CoM). Consequently, this causes firstly the shank to accelerate and secondly change in relative angle between the shank and thigh, with the lower extremity taking a new configuration. Both of these produce moments about the hip joint as will be illustrated in the following sections.

### 6.3.1 Segment Interaction

In the movement of a multiple link mechanical structure such as the arm/forearm system, the torques at the joints arise not only from muscles acting on the joints but also from interactions due to movement of other links. These interaction torques are not present during movement at only a single joint and represent a significantly complicated function in the dynamic analysis of movement (Hollerbach and Flash, 1982).

### 6.3.2 Hip Flexion Kinetics

During normal gait, flexion and extension of the hip and knee are linked by bi-articular muscles such as the rectus femoris and the hamstrings group, as well as kinematically and kinetically. Normal gait is initiated by hip flexion with little muscular action around the knee; the inertial properties of the shank cause the knee to flex in response to the accelerating thigh, producing ground clearance (Inman et al., 1981). Additionally, as the hip flexes the shank remains in the lowest potential energy position and this leads to additional knee flexion.

These inter-segment linkages also apply when knee flexion occurs without muscular activity at the hip. If the knee is flexed the action of the accelerating shank will cause the hip to flex; additionally, the new orientation of the knee will cause the leg to adopt a new minimum energy configuration with a flexed hip as illustrated in Figure 6.5 and Figure 6.6. The static relationship between the knee angle ($\alpha$) and hip angle ($\theta$) (Winter, 1990) based on anthropometric data used in this thesis is given as:

$$\tan\theta = \sin\alpha/(2.426+\cos\alpha) \qquad (6.1)$$

This relationship is plotted in Figure 6.6, which represents an ideal situation and assumes no spasticity or muscle contracture. Additional hip flexion is produced by the dynamic inter segment coupling and is dependent on the angular acceleration of the knee. Thus, it can be seen that if the knee can be made to flex by any means then this will also lead to hip flexion. The amount of hip flexion produced by the dynamic inter segment coupling is dependent on the angular acceleration of the knee. Figure 6.7 shows the natural hip flexion produced during knee flexion in SBO. These situations agree with the theory presented in this section.

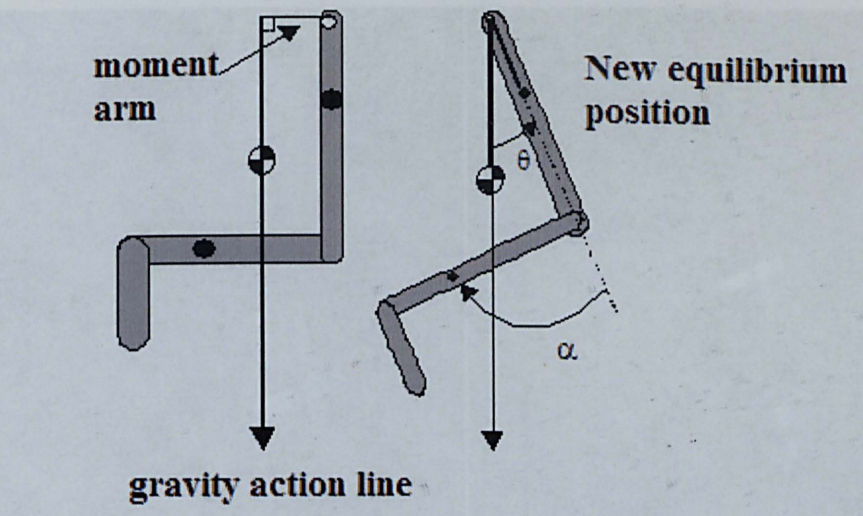


**Figure 6.5: Hip flexion resulting from flexed knee**

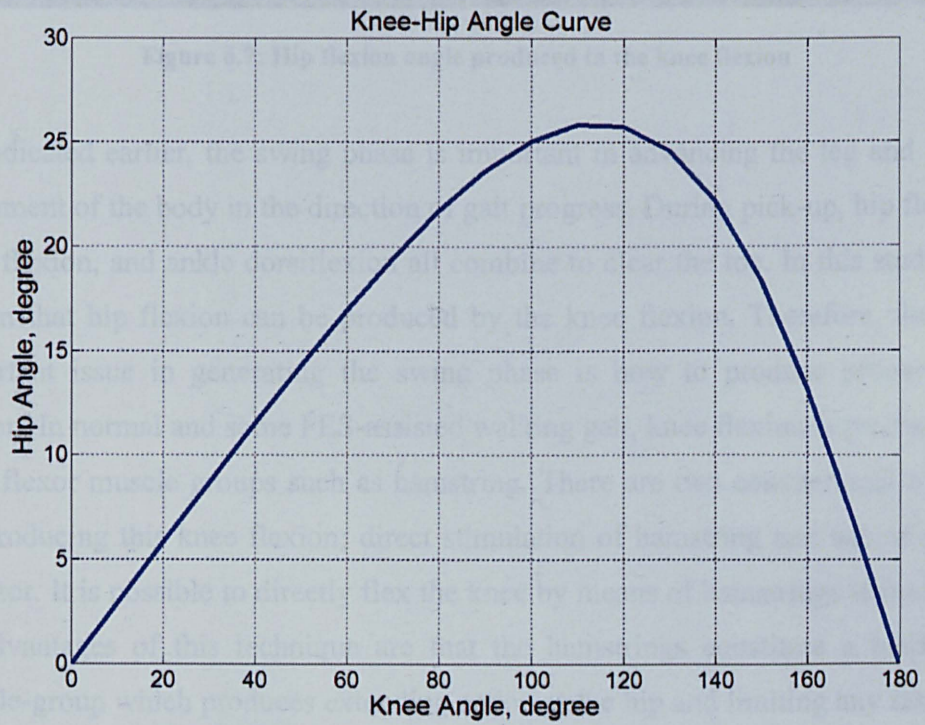


**Figure 6.6: Static relation between knee and hip flexion angle**

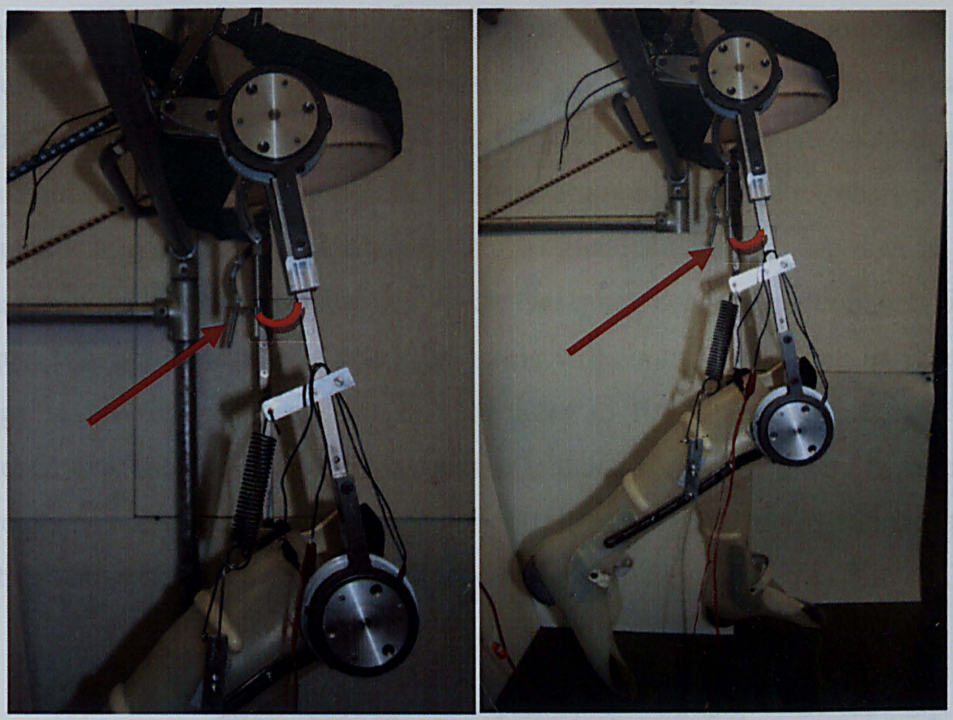

**Figure 6.7: Hip flexion angle produced in the knee flexion**

As indicated earlier, the swing phase is important in advancing the leg and hence movement of the body in the direction of gait progress. During pick-up, hip flexion, knee flexion, and ankle dorsiflexion all combine to clear the toe. In this study it is shown that hip flexion can be produced by the knee flexion. Therefore, the only important issue in generating the swing phase is how to produce proper knee flexion. In normal and some FES-assisted walking gait, knee flexion is produced by knee flexor muscle groups such as hamstring. There are two conventional options for producing this knee flexion; direct stimulation of hamstring and use of power actuator. It is possible to directly flex the knee by means of hamstrings stimulation. Disadvantages of this technique are that the hamstrings constitute a biarticular muscle-group which produces extending action at the hip and limiting any resulting hip flexion, hamstrings muscle is also a weak muscle which easily tends to fatigue. The knee may also be flexed through the use of a powered-actuator such as a DC motor. To minimise inertial properties, it should be mounted away from the knee, as proximal as possible. The previously mentioned disadvantages of size and weight apply.

In this chapter, the combination of spring and brake at the knee is introduced. The stimulated quadriceps muscles group can usually produce much more torque than is required to extend the leg, even with the thigh horizontal. A spring acts to resist knee extension, then the additional quadriceps torque can be used to 'charge' (store potential energy in) the spring when the leg is extended. A brake can then be used to maintain the knee in extension without further quadriceps contraction, preventing fatigue. When the brake is released the spring will contract, releasing its potential energy as kinetic energy and causing the knee to flex. The advantage of this approach over the use of a powered actuator is that a spring has a very high torque to weight and size ratio, efficient, robust and does not require any control signals or electrical power. Figure 6.8 shows the spring for knee flexion used in SBO.

**Figure 6.8: Spring for knee flexion in SBO**

In order to prevent the dynamic hip flexion produced by the accelerating knee from being lost, a means of 'catching' the hip at its maximum flexion angle is required. This can be achieved by using a ratchet/brake at the hip. This leads to an orthosis combining a ratchet at the hip with a brake and spring at the knee and electrical stimulation of the quadriceps.

### 6.3.3 The Swing Phase of SBO

Figure 6.9 demonstrates the swinging leg in the SBO. To synthesise the swing phase of gait using the SBO, the following procedure is required.

1) At the beginning the knee brake is on to provide isometric torque against the spring to keep the leg in stance phase (Figure 6.9 (a)).

2) The brake at the knee is released, and the spring causes the knee to begin to flex (Figure 6.9(b)). It should be noticed that in practice the toe will interfere with the ground at the initiation of swing, and may prevent knee flexion. This problem can be overcome by allowing the unloaded foot to dorsiflex, thus allowing the toe to slide along the ground.

3) Following toe-off, the spring torque will continue to accelerate the shank backwards, producing a reaction at the knee, which accelerates the thigh forwards.

4) The combination of the reaction and the moment due to the weight of the flexed shank cause the hip to continue to flex, the flexed knee allows the toe to clear the ground (Figure 6.9(b)).

5) While the hip reaches its maximum flexion angle, the hip ratchet keeps it in peak angle (Figure 6.9(b)).

6) The quadriceps muscle is then stimulated to extend the knee against the spring torque (Figure 6.9(c)).

7) When the knee is fully extended the brake at the knee is applied and quadriceps stimulation is turned off (Figure 6.9(d)).

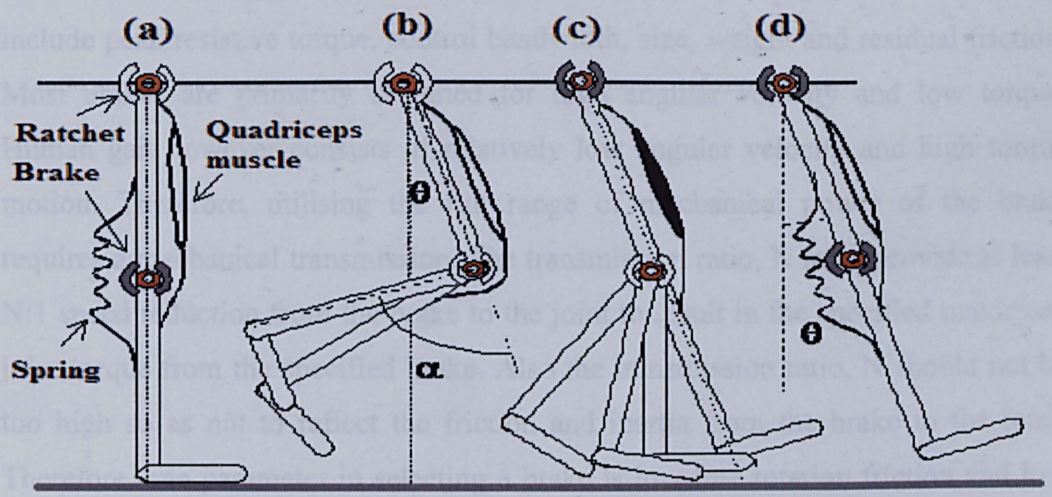


**Figure 6.9: SBO swing phase synthesis**

It can be seen that it is possible to obtain knee flexion, knee extension and hip flexion using only a single channel of stimulation per leg.

## 6.4 The Development of SBO

### 6.4.1 Brakes

The controlled brake is the main part in those types of hybrid orthoses which use the brake as a dissipative element. Considerations for selecting a brake technology include peak resistive torque, control bandwidth, size, weight and residual friction. Most brakes are primarily designed for high angular velocity and low torque. Human gait however consists of relatively low angular velocity and high torque motion. Therefore, utilising the full range of mechanical power of the brake requires a mechanical transmission. The transmission ratio, N must provide at least N:1 speed reduction from the brake to the joint to result in the specified maximum joint torque from the specified brake. Also the transmission ratio, N should not be too high so as not to reflect the friction and inertia from the brake to the joint. Therefore, one parameter in selecting a brake is low free rotation friction and low inertia.

There are varieties of technologies for controlled brakes in hybrid orthoses. Among these two different types of brakes, namely, wrap-spring clutch and magnetic particle brake have been reported by some researchers in hybrid orthosis design. Irby et al. (1999) have suggested using a wrap-spring clutch within a knee-ankle foot arthosis (KAFO) system. The wrap-spring clutch is a principle that is proven in transmission of rotational movement. The effects of friction when a flexible body is surrounding a non-movable body are amplified in an exponential manner; thus, a small force at one end can hold a large force at the other end. This design allows device minimisation and overall reduction in energy consumption when compared with other brake systems used in orthotics. Durfee and Hausdorff (1990) reported the use of magnetic particle brake in the CBO. It was shown in their report that magnetic particle brake as a controllable mechanical damping element at the joint with combined stimulation provides good control of limb motion despite variations in muscle properties.

Fortunately, the kinematics of the SBO reduces the complexity of brake dynamics. In the SBO, brake torque is applied to oppose the isometric torque of the spring. As described in the previous section, the brake should be on when the knee joint reaches its maximum extension. In this case the angular velocity is zero, therefore the brake only needs to provide a *static* torque equal and opposite to the spring torque. This point simplifies the issues related to the selection and design of a brake further, as the *dynamic* characteristics of the brake do not need to be accounted for.

#### 6.4.1.1 Maximum brake torque

Since power flow is from the joint to the brake, the brake in any circumstance should be capable of producing the maximum resistive torque required on the joint flexion and extension range of motion. Maximum joint torque specification of the orthosis joint depends upon three desired capabilities;

1) The orthosis should be able to provide the dissipative torque observed in normal gait. Maximum dissipative torque for knee and hip are approximately 0.4 Nm/kg for knee and 0.3 Nm/kg for hip (Winter, 1991). For a body of 80 kg, the maximum dissipative knee and hip torques are 32 Nm and 24 Nm.

2) The orthosis must be capable of locking a joint against a stimulated muscle contraction. The strength of electrically stimulated knee extensors (quadriceps muscle) was studied by Baid and Kralj (1995) in some groups of paraplegic subjects. According to their experience knee joint torque over 50 Nm permits the performance of FES activities, such as standing up and reciprocal walking.

3) The orthosis should be able to perform controlled stand-to-sit manoeuvre without the help of muscle stimulation.

Based on the above, Goldfarb and Durfee (1996) selected maximal braking loads of 50 Nm for the knee and 30 Nm for the hip joint. However, in the case of SBO as the knee brake is resisting the spring torque and not the muscle torque, the minimum braking load is reduced to 10 Nm, which is the spring torque exerted on the knee joint.

It is also important in selecting the brake to consider those types of brakes which provide high torque with minimum input power for minimum size and weight. The wrapped spring clutches among other types of brakes offer high torque in a small package size and low power consumption for their torque capability when compared with typical friction clutches and brakes. Figure 6.10 shows the brake that has been chosen in this thesis for SBO development. In this SBO, as the knee reaches full extension position the brake is turned on at the knee joint by push button switch.

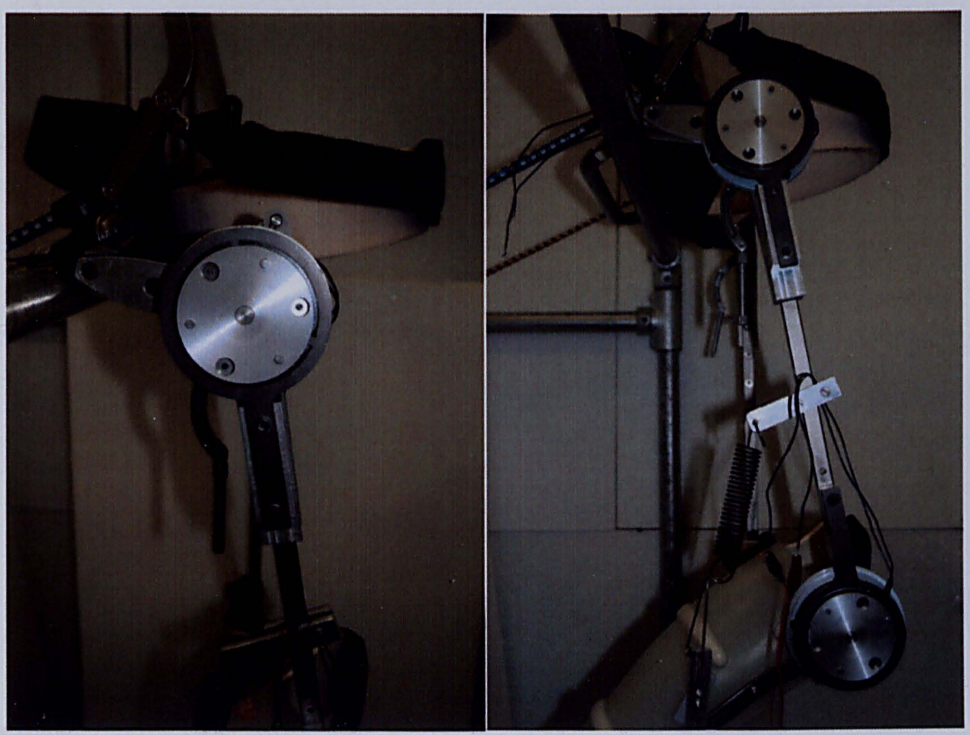

(a) (b)

**Figure 6.10: (a) Brake used in SBO (b) Brake for knee and hip in SBO**

### 6.4.2 Spring

This section will discuss selection of spring parameters in SBO development. In the SBO, spring torque will act as an external elastic element to generate knee and hip flexion. In this section, test is performed to find the optimum spring parameters that produce the minimum quadriceps torque required for knee extension in SBO. In this test, the same knee flexion trajectory is used for all spring parameters. Fifteen different spring parameters consisting of three different spring lengths and five different spring constants were considered to find the minimum quadriceps torque required for knee extension. In this simulation test, spring length from 0.1m to 0.3m and spring constant from 200N/m to 400N/m were used. Figure 6.11 shows the results from the simulation test. The minimum quadriceps torque required was calculated by taking the integral of total quadriceps torque for the knee extension in SBO at the respective spring parameters. It is noted that the spring constant of 250N/m and spring length of 0.3m produced the minimum quadriceps torque required for the knee extension in SBO. Using this value the knee flexion also flexed according to predefined knee flexion trajectory, hence the test objective was successfully achieved. Therefore, this value is used throughout this chapter.

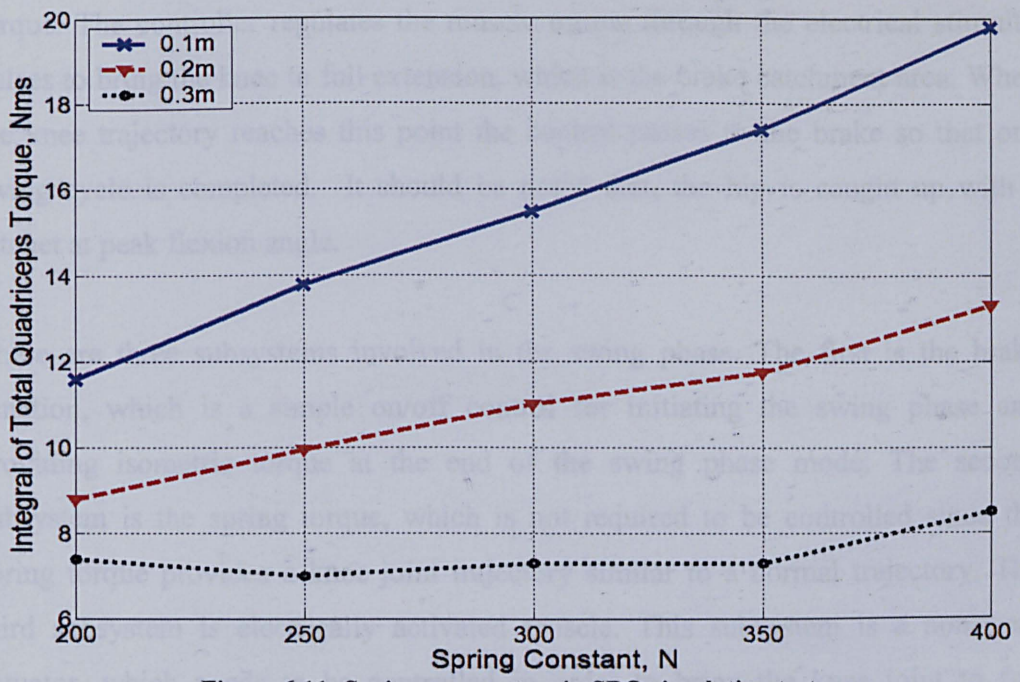


**Figure 6.11: Spring parameters in SBO simulation test**

## 6.5 Control of Knee Extension

The incorporation of feedback into human movement control system is expected to provide several significant improvements. Feedback correction for internal disturbances may also reduce the need for frequent retuning, but only if the closed-loop system's performance itself is robust, or relatively insensitive to internal disturbances.

As discussed earlier, the swing phase kinematics consist of some states such as hip and knee flexion, mid swing, forward swing and knee extension at late swing. In the SBO, three elements namely, spring, brake, and muscle are involved in synthesising the leg swing function. The swing function is initiated by the schedule controller command to release the brake. Then the spring torque rotates the knee towards mid swing. At the knee flexion peak angle the control task passes muscle

torque. The controller regulates the muscle torque through the electrical stimulus pulses to bring the knee to full extension, which is the brake catchment area. When the knee trajectory reaches this point the control passes to the brake so that one swing cycle is completed. It should be noted that, the hip is caught up with a ratchet at peak flexion angle.

There are three subsystems involved in the swing phase. The first is the brake function, which is a simple on/off control for initiating the swing phase and providing isometric torque at the end of the swing phase mode. The second subsystem is the spring torque, which is not required to be controlled since the spring torque provides a knee joint trajectory similar to a normal trajectory. The third subsystem is electrically activated muscle. This subsystem is a nonlinear actuator, which needs to be controlled in order to bring the knee joint to full extension position and after that the brake isometric torque keeps the knee in position without muscle activity. Therefore this section will discuss the control for knee extension in SBO. There are two control systems used in this chapter; PID and FLC are used for knee extension in SBO and performances of both techniques are evaluated and discussed.

### 6.5.1 Fuzzy logic control for knee extension

The essential aim of the fuzzy controller in this chapter is to make the knee extension follow a pre-defined trajectory by applying a suitable torque to it. There are two inputs selected for the controller. These are the error (difference between actual knee trajectory measured from vN4D simulation output and reference knee trajectory) and change of error which is the same as the difference between the reference and actual angular velocities. The controller output is the stimulated pulse-width which then is fed into the muscle model to produce muscle torque. The details of FLC were discussed in Chapter 5.

In this chapter, five equal distributed Gaussian (bell-shaped) type membership functions are used for each input and output (Figure 6.12). In this chapter, equal distribution of the membership functions same as FLC in the previous chapter is used. The Gaussian shape for the membership functions is selected because this is likely to produce a smooth output.

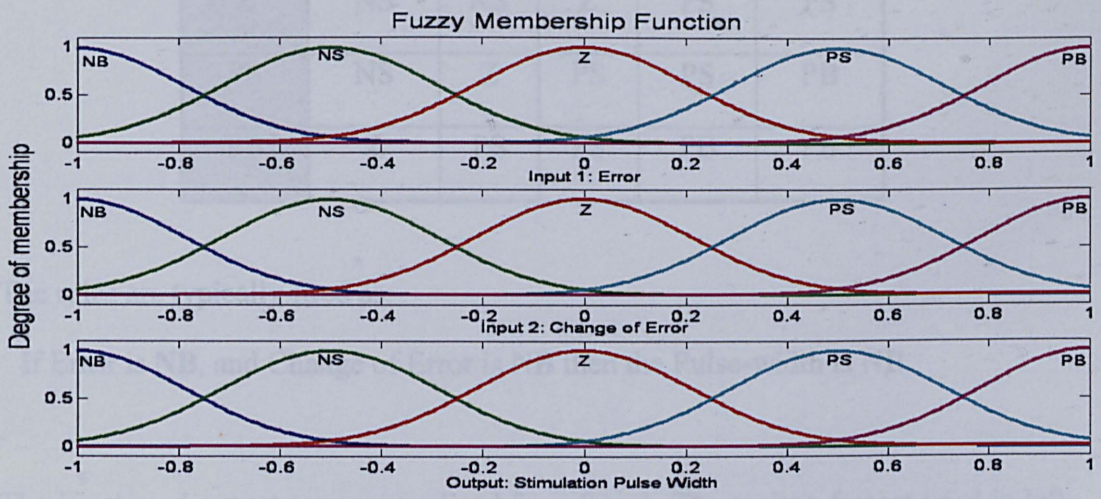


**Figure 6.12: Fuzzy membership functions**

The next step is to determine which rules to use. The number of rules is determined by the number of membership functions for each input. The fuzzy controller has two inputs with five membership functions and this leads to 25 rules. Table 6.1 shows the fuzzy rules for stimulated pulse-width for quadriceps muscle. Fuzzy set of five variables, defined by Gaussian shaped membership functions: negative big (NB), negative small (NS), zero (Z), positive small (PS) and positive big (PB) is considered in this chapter. The centroid of gravity methods is used as a defuzzification method because it is commonly used in feedback control due to its smooth output.

**Table 6.1: Fuzzy rules for leg extension**

| e \ Δe | NB | NS | Z | PS | PB |
|---|---|---|---|---|---|
| NB | NB | NB | NS | NS | Z |
| NS | NB | NS | NS | Z | PS |
| Z | NS | NS | Z | PS | PS |
| PS | NS | Z | PS | PS | PB |
| PB | Z | PS | PS | PB | PB |

The rules are typically fired as:

If Error is **NB**, and Change of Error is **NB** then the Pulse-width is **NB**.

The inputs and output were normalised from 0 to 1. The scaling factors used in left leg FLC were 0.1, 0.0025 and 322 while in the right leg FLC were 0.058, 0.0025 and 322 for error, change of error and output respectively. The input and output scaling factors were manually obtained by trial and error technique to attain the best trajectories. Figure 6.13 shows a block diagram of the control system. The stimulation pulse-width from the fuzzy controller is fed into the muscle model to produce muscle torque to drive the vN4D model to follow the walking gait. Then the error and change of error are fed back to the fuzzy controller to adjust stimulation pulse-width to the optimum level. In order to apply muscle torque at the correct time, which is the peak time of knee flexion, a block was designed to detect the peak angle of the knee joint. This block sensed the peak time and sent a strobe signal to the controller to initiate controlling the plant.

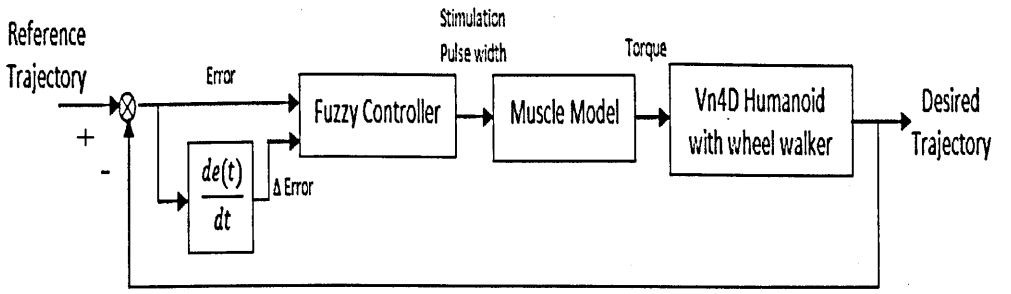


**Figure 6.13: Block diagram of the FLC system**

### 6.5.2 PID control for knee extension

In this chapter, two PID controllers are used, one for each leg. For left knee PID controller, the parameter values used were 6.5, 0.02 and 0.04 while for right knee PID controller parameter values were 6.5, 0.05 and 0.035 for P, I and D respectively. Figure 6.14 shows a block diagram of the PID control applied to the walking system. The PID controller input is an error between the system output and the reference while the output is stimulation pulse-width. Details of PID controller were discussed in chapter 5.

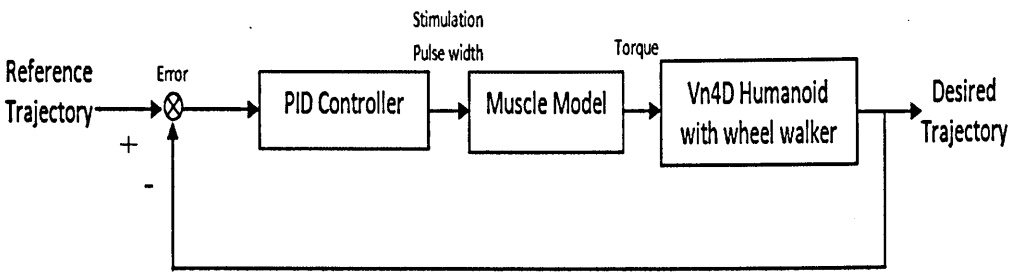


**Figure 6.14: Block diagram of the PID control system**

## 6.6 Simulation Results

Simulations were carried out using Matlab/Simulink with incorporation of humanoid with wheel walker model in vN4D to illustrate the effectiveness of SBO in FES-assisted walking with wheel walker. The same humanoid model with wheel walker discussed in Chapter 2 was used. The control objective was to regulate the level of stimulated pulse-width for muscle stimulation in knee extension by following the reference trajectory. Due to various perturbations and limited strength of the hip and knee flexor and extensor muscles, the shank and thigh may not perfectly track the reference trajectory.

The tasks of swing phase in view of its functional characteristics can be divided into two modes, namely passive and active. In passive mode, combination of functions of passive elements (brake and spring) initiates a swing phase by flexing the knee joint. A large range of knee flexion picks up the foot to make enough ground clearance. The inertia and pendular effects of the lower extremity advance the leg forward. In this study a spring constant and spring length of 250 N/m and 0.3m respectively were used after a trial and error process. This spring constant value gives the best flexion trajectory referring to the predefined trajectory. In active mode, electrically stimulated knee extensor muscles group provides the leg extension so that the heel reaches the ground. The timing block schedules and adjusts two passive and active modes by sending a strobe signal at appropriate times. It should be noted that the passive mode is double pendulum driven by only the spring torque in the knee joint and the active mode is a simple pendulum in which the joint trajectory is tracked by the electrically activated muscle torque. This is because the hip brake catches the hip at the maximum flexion angle, and does not allow the hip to move until the end of swing phase.

### 6.6.1 Fuzzy logic control

Figure 6.15 shows the stimulation pulse-width, knee and hip trajectory for both legs. In the left knee, the stimulation starts at 0.48 second and at the time that knee is in full flexion. The same situation takes place with the right knee where the stimulation starts at 1.58 seconds. The results show that the controller designed worked as expected. The results show that the left hip brake caught the maximum hip angle at 25° while the right hip brake caught the maximum hip angle at 27°. This is because the left leg begins to provoke the start of periodic gait cycle and the right leg is where all body parts are in the movement condition where the centre of body is gravity and inertia driven in the direction of progression.

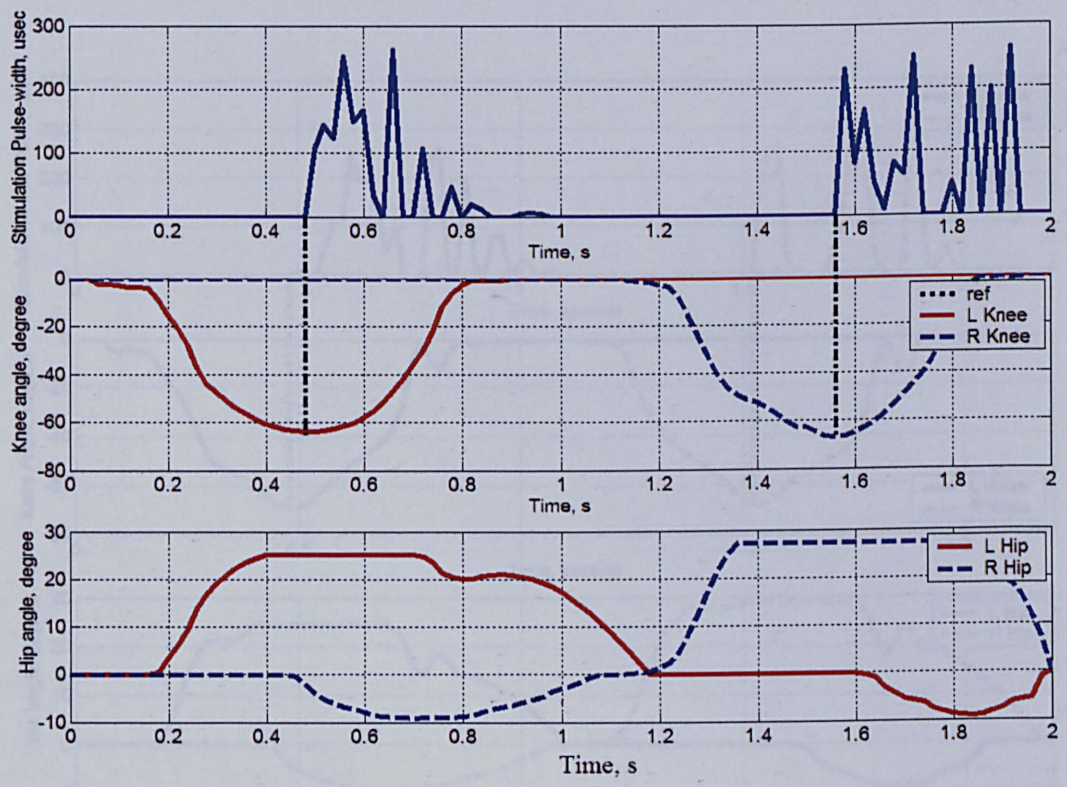


**Figure 6.15: Stimulation pulse-width, knee and hip trajectory of FLC for complete walking gait**

### 6.6.2 PID control

Figure 6.16 shows the stimulation pulse-width, knee and hip trajectory for both legs produced using PID control. In the left knee, the stimulation started at 0.48 second and at the time that knee was in full flexion. The same situation took place with the right knee where the stimulation started at 1.58 seconds. The simulation time was set to be the same as with FLC so that fair evaluation can be made between these two techniques. The results show that the PID controller designed also worked as expected. In PID control, the left hip brake caught the maximum hip angle at 25° while the right hip brake caught the maximum hip angle at 28°. This was 1° higher compare with right hip brake angle from FLC. The trajectory of knee and hip found with FLC was smoother compared to that with PID control.

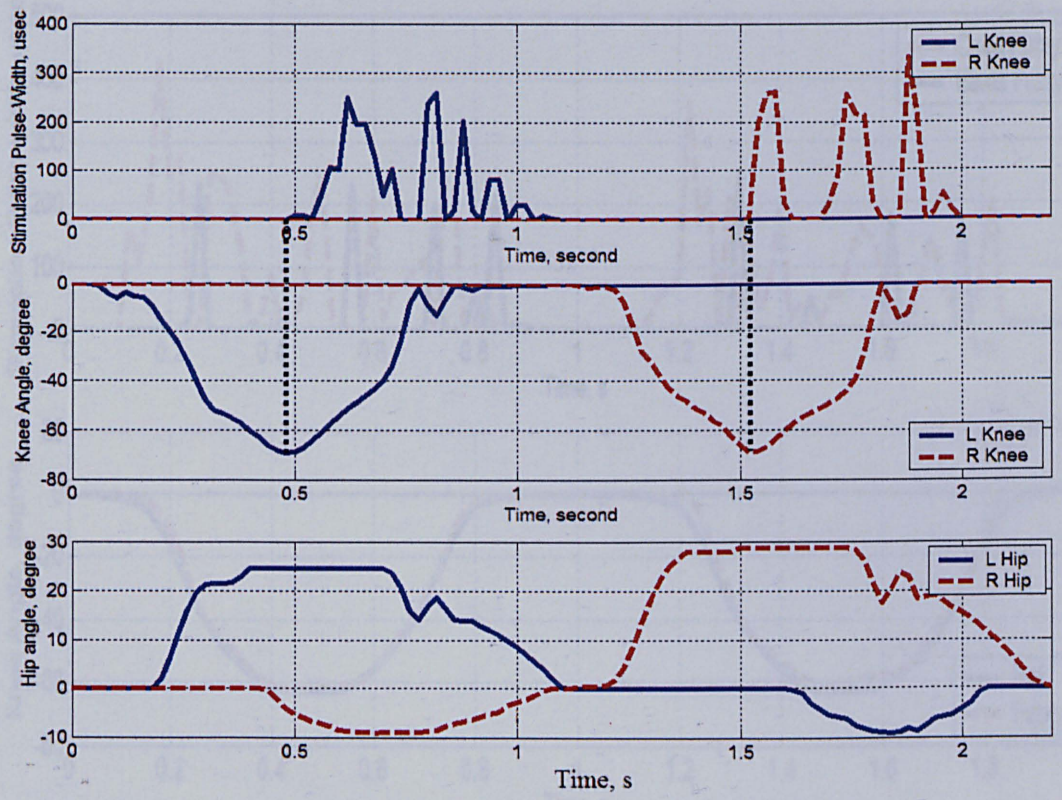


**Figure 6.16: Stimulation pulse-width, knee and hip trajectory of PID control for complete walking gait**

### 6.6.3 Comparison with and without SBO

Figure 6.17 shows the stimulation pulse-width and knee trajectory from walking without SBO simulation. The stimulation pulses were controlled by FLC at both quadriceps and hamstring muscles. The results clearly show that the stimulation pulses from this technique were more than walking with SBO. The torque required in walking with SBO in FLC was reduced by 11.49% and 100% for quadriceps and hamstrings muscles respectively as compared with the torque required for quadriceps and hamstring muscles in walking without SBO. As explained above, there is no torque required for hamstring muscle in walking with SBO as spring is used for knee flexion. The percentage of reduction or increment was calculated by taking the difference between integral of both techniques over the initial value; in this case integral value from walking without SBO was the initial value.

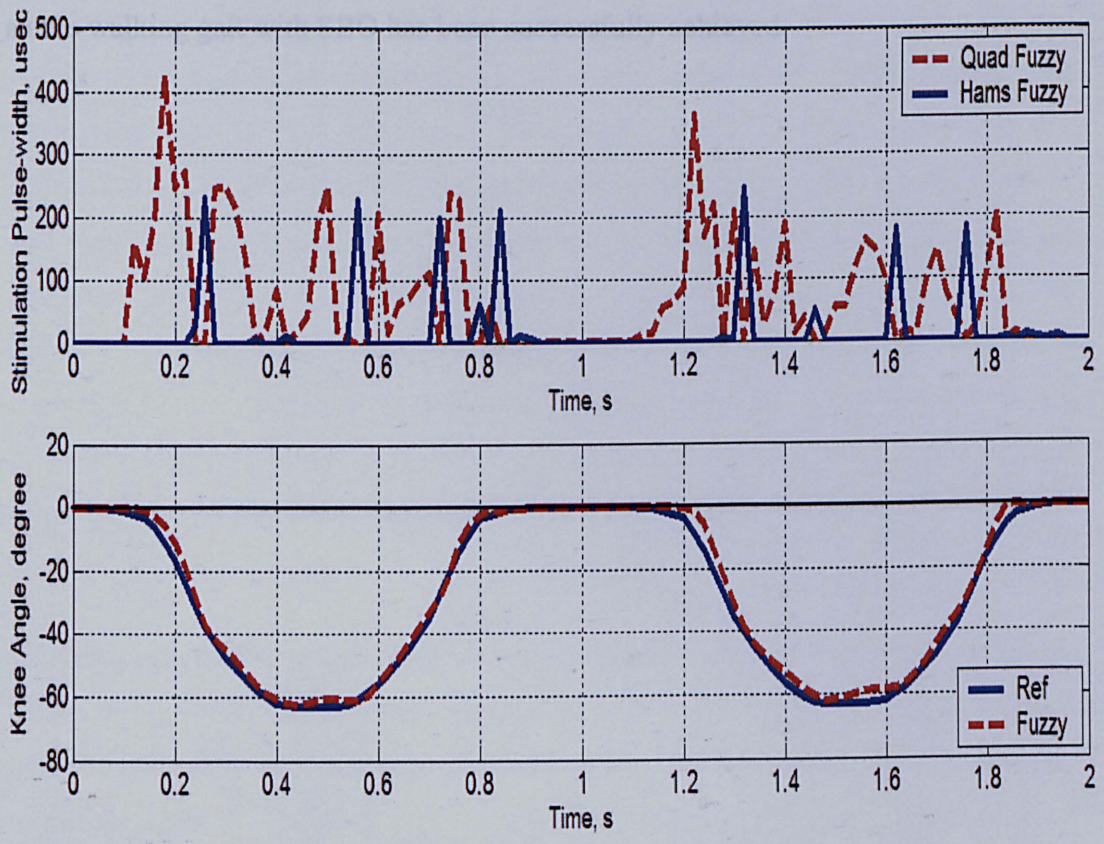


**Figure 6.17: Stimulation pulse-width and knee trajectory for complete walking gait without SBO**

## 6.7 Summary

The objective of the SBO approach is to eliminate reliance on the withdrawal reflex and the associated problems of habituation and poor controllability. Instead, a simple switchable brake with a spring elastic element with well-defined properties provides the necessary function and trajectory. The technique seems promising in producing functional hip flexion. The results of the SBO typical behaviour with the model simulation confirm the effectiveness of the SBO for FES-assisted walking with wheel walker. It is also concluded that FLC and PID control can be successfully implemented to regulate the level of stimulation pulse-width used to stimulate the knee extensor muscle for FES-assisted walking with wheel walker in SBO. The FLC has been found to be more suitable compared with PID control for its smoothness in knee and hip trajectories. Based on the simulation developed, a stable walking gait with SBO has been successfully achieved.

# Chapter 7

# Finite State Control for FES Walking with SBO

## 7.1 Introduction

In the proposed FES walking with SBO, the application of FES for knee extension, the spring for knee flexion and the brake at knee and hip from the SBO are synchronised with the incidence of specific events in the walking gait, such as knee extension, knee flexion, hip brake, knee brake, etc. However, timing and co-ordination of the FES and SBO parameters applied in the system can be difficult and may lead to instability in the system due to incorrect detection of gait event from the sensor signals or muscle fatigue. The use of finite state control can overcome this drawback since gait sensor values are interpreted by a finite state controller in the situation of the subject's current system state. Therefore, switching of FES, spring and brake in the SBO are applied to the subject when the correct sequence of state transition takes place.

This chapter presents a finite state control (FSC) of paraplegic walking with wheel walker using functional electrical stimulation (FES) with SBO. The study is carried out with the same FES walking with SBO system discussed in Chapter 6 with the implementation of FSC to control the transition between different states in the FES walking with SBO. This is to improve the previous system so that in case of any failures during the walking cycle, the next walking state can be terminated. It is also to increase the paraplegic's safety and system stability during the FES walking. At

the end of this chapter, the results from this technique are compared with results from the previous chapter and conclusion is made on the performance of both techniques.

## 7.2 Finite State Control in FES

A finite state controller or finite state machine is a conceptual machine comprising a set of states which are represented in a data structure, a set of input events, a set of output events and functions which determine changes of state resulting from input and trigger consequent output (Bavel, 1983). Each state represents an aspect of the system's behaviour and the complete range of the system behaviour is characterised by the set of all possible system states. It is a behaviour model composed of a finite number of states, transitions between those states, and actions. Finite state machines switch between states according to the system input and the current system state, similar to a flow graph in which one can inspect the way logic runs when certain conditions are met, as illustrated in Figure 7.1. Finite state machines can be represented graphically, using the notation where states are represented by circles and transitions are written above arrows signifying the state transition, inputs causing the respective state transitions are indicated above the arrows (Bavel, 1983).

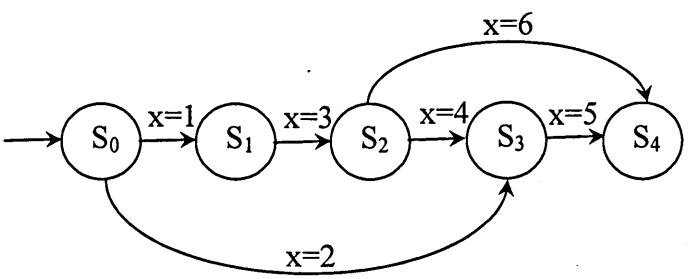


**Figure 7.1: Finite state operation**

Finite-state machines can solve a large number of problems and has been used in a wide range of applications. In biology and biomedical research, state machines are used to describe neurological systems while in FES, it was first proposed by Liberson et al. (1961) for the correction of foot drop and at the same time, FSC of human gait was proposed by Tomovic and Karplus (1961) to control the human gait. Since this first report, Tomovic and McGhee (1966) initiated the concept of finite state controlled neural prosthesis. They consider the human gait as composed of a sequential pattern of movements. Later McGhee (1968) investigated the finite state element in the leg locomotion. In these two papers, the concept introduced was to relate the control of robot walking machines to the artificial control of human locomotion. It was conclude that the human and animal locomotion were the most suitable application to be controlled using FSC as the walking gait can be represented as different states in FSC. Later, the combination of FES and human locomotion in FSC motivated other researchers (Andrews et al., 1992; Franken et al., 1994; Popovic et al., 1989) to use FSC with FES for paraplegic gait restoration.

Many researchers investigated the effectiveness of FSC in various FES-activities. Mulder et al. (1991,1992) used low level FSC of knee joint in paraplegic standing. In this paper, low level FSC consisted of locked and unlocked states to control the electrical stimulation given to the quadriceps muscles in FES standing. The locked state was detected by knee angular velocity while unlocked state was switch on when there is zero velocity detection from the goniometer used. In these papers, FSC is found to have higher duration of standing and less quadriceps torque required compared to open loop control for all of the subjects.

Davoodi et al. (2002) developed an automatic FSC to replace the voluntary decision making procedure of pressing and releasing control buttons by fingers to be used with the modified rowing machine of FES rowing exercise for paraplegic. To provide sensory feedback to the FSC, two optical encoder sensors were used to measure the positions of the seat and handle during rowing. In this paper, FES rowing with FSC was found to be more convenient and easy to use but required

more electrical stimulation compared to manual voluntary FES control. This is because in the manual voluntary FES control, the subject can switch off the electrical stimulation whenever they believe it was not necessary.

Henry et al. (1993) used finite state to model paraplegic walking gait. They investigated performances of two different types of sensory strategies. Nine walking states were set in FSC to represent paraplegic walking gait. The first sensory feedbacks were two goniometers and eight footswitch while the second sensory feedbacks are two goniometers and two piezo electric placed inside the crutches to be used to detect nine walking states in FSC. They used FSC to control nine pre-defined walking states and FSC was found as a promising technique to represent paraplegic walking gait.

The clinical results over last forty years on FSC for FES application in neural prosthesis has shown that FSC is an effective and efficient control method to be used in FES application. In this chapter, FSC is used as a switching from one walking gait to other. It is used to improve the robustness of FES walking with spring brake orthosis discussed in the previous chapter where FSC is used to control the transition between the states.

## 7.3 FSC in FES Walking with SBO

Finite state control is principally an event triggered approach, where transition from one state to another one takes place if and only if a predefined event occurs. In this chapter, the decisions regarding the number and definition of states as well as the events that will provoke the transitions are based on the FES walking with SBO sequence described in the previous chapter. The FSC design and implementation is developed in Matlab Simulink and interaction with vN4D model is made for the

output analysis. According to the FSC concept, each state focuses on a specific behaviour of the system that happens under certain circumstances and the whole states represent an overview of the system for complete period of time. Referring to the FES walking with SBO in the previous chapter, walking states are identified for used in FSC development as double stance (initial), knee flexion, knee extension, knee full extension, heel strike and mid stance. These states are applied to both right and left legs and these are not a usual walking states used by other researchers as these walking states are based on FES walking with SBO in this thesis. The states are selected according to the switching period in spring, hip brake, knee brake and FES to the quadriceps muscles in the FES walking with SBO.

In general, there are two types of transition; normal transition and default transition. In the normal transition, a predefined event acts as a trigger to switch from one state to another and if the event does not occur, the current state will continue to execute the current action. Table 7.1 shows the list of states obtained to represent the FSC of FES walking with SBO. The same set of states is used for both right and left leg with different starting state. Right and left leg states are active at the same start time with double pendulum where both legs are in the stance position with hip and knee brakes on. Figure 7.2 shows the implementation of the FSC states, listed in Table 7.1 in a state flow diagram.

**Table 7.1: State description of the FSC of FES walking with SBO**

| | State | Action | Transition's input/ event |
|---|---|---|---|
| 0 | Double Stance (initial) | Hip Brake = 1<br>Knee Brake = 1<br>FES = 0<br>Spring = 0 | Initial, t=0 |
| 1 | Knee Flexion | Hip Brake = 0<br>Knee Brake = 0<br>FES = 0<br>Spring = 1 | For left knee, first start at t=0.1<br>For the right knee: Left Knee = 0°, Left Hip = 0° |
| 2 | Knee Extension | Hip Brake = 0<br>Knee Brake = 0<br>FES = 1<br>Spring = 0 | Hip = 27° |
| 3 | Full Knee Extension | Hip Brake = 0<br>Knee Brake = 1<br>FES = 0<br>Spring = 0 | Hip = 27°<br>Knee = 0° |
| 4 | Mid Stance | Hip Brake = 1<br>Knee Brake = 1<br>FES = 0<br>Spring = 0 | Hip = 0° |

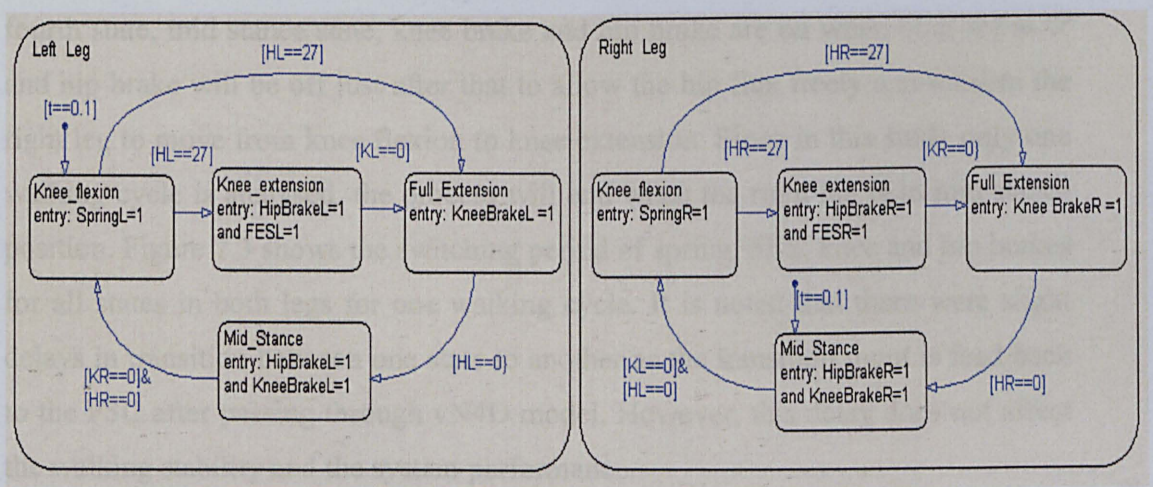


**Figure 7.2: FSC state flow diagram**

In this study, there are three switches to be controlled by FSC. The switches are hip brake, knee brake and FES stimulation. In FES walking with SBO, spring is a potential energy storage device where it will automatically flex the knee when the knee brake is off. Therefore, in this case there is no control applied to the spring and the spring is put in the state flow only for observation purposes.

In the FES walking with SBO, four main states are considered. The first state is knee flexion where it is a transition from the stance position and first applied to the left leg when time is at 0.1 second while the right leg will remain at foot flat and mid stance position until the left leg complete the leg swing. In this state, the hip and knee brakes are off and allow the spring to flex the knee and at the same time produce the hip extension. The hip extension theory was explained in detail in the previous chapter. After the hip extends until 27°, the second state (knee extension) is switched on. To get this state, FES is applied to the quadriceps muscles and hip brake is on when the hip reaches 27 ° extension angle.

The third state is full leg extension where the main aim is to make the leg fully extend and leg swing completed. At the end of this state, the knee brake is on when the knee angle reaches 0°, the upper body is moved forward and hip brake is off immediately to allow the heel strike and mid stance position take over. During the fourth state, mid stance state, knee brake and hip brake are on when both are at 0° and hip brake will be off just after that to allow the hip flex freely and tolerate the right leg to move from knee flexion to knee extension. Since in this study only one walking cycle is analysed, the process will end when the right leg is in mid stance position. Figure 7.3 shows the switching period of spring, FES, knee and hip brakes for all states in both legs for one walking cycle. It is noted that there were slight delays in transition between one state to another as the transition input is feed back to the FSC after passing through vN4D model. However, this delay does not affect the walking stability and the system performance.

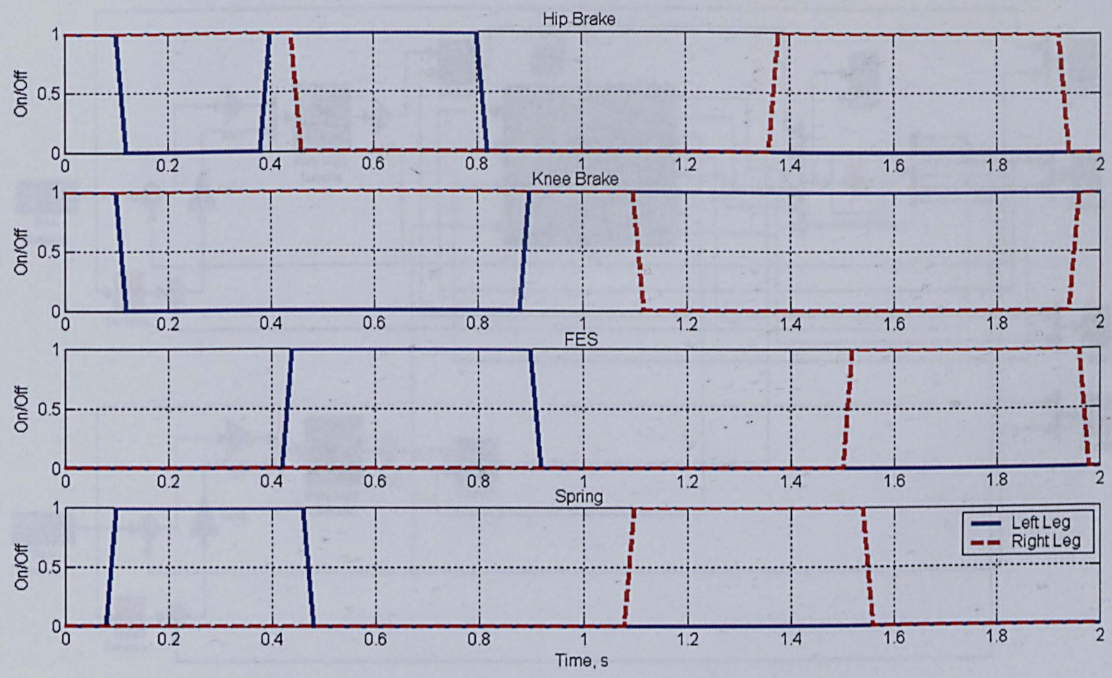


**Figure 7.3: The switching period for the FES, spring, hip and knee brake for both legs**

In this study, FSC is used together with FLC for knee extension. Figure 7.4 shows a block diagram of the complete FSC of FES walking with SBO used in this chapter. The same FL controller's parameters and settings in the previous chapter were found to be suitable to be used in this chapter. The comparative function is used for the FLC and the FSC outputs so that FES for knee extension will be fed to the vN4D model if only FES switch at FSC is on. Hip and knee brake switches are set in the vN4D model to activate or deactivate the brakes. In a practical situation, these switches can be directly attached to the SBO brake switch as the brakes used in the SBO development are activated by putting a voltage to them. The spring switch from the FSC is used for the monitoring purposes as the spring is an energy storage device and in this study it will activate immediately if the knee brake is released.

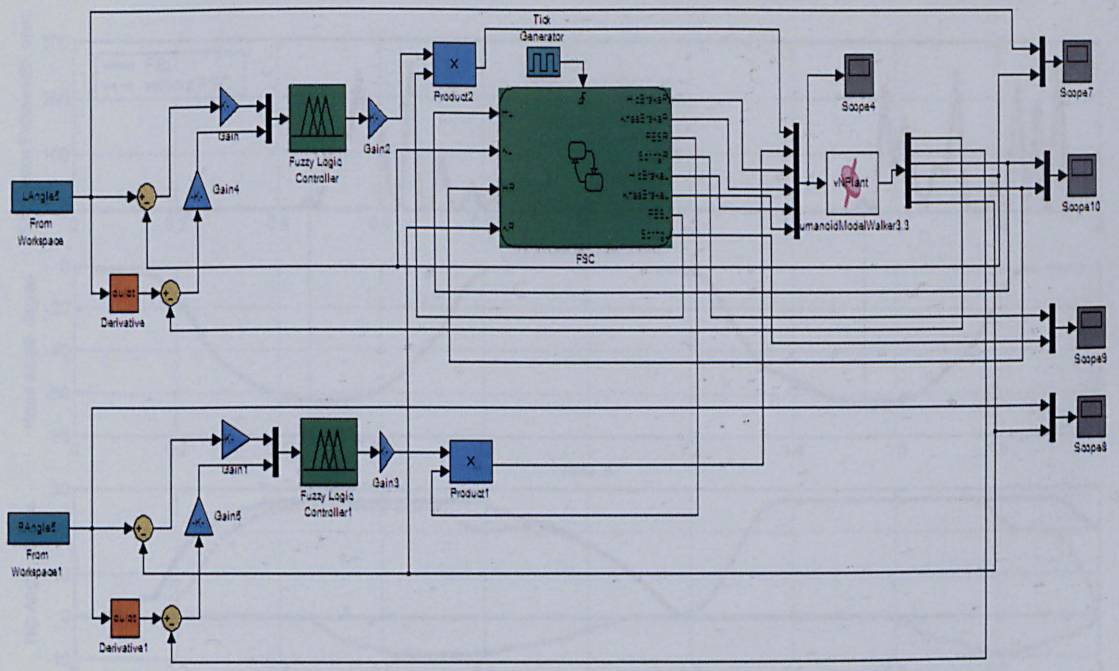


**Figure 7.4: Block diagram of FSC of FES walking with SBO**

## 7.4 Results

In this chapter, FSC is used to enhance the switching states in the FES walking with SBO developed in the previous chapter. Figure 7.5 shows the knee trajectories, stimulation pulse-width and hip trajectories from with and without FSC of FES walking with SBO. In the previous chapter, the switching of FES, knee and hip brakes was set manually according to the pre-defined reference trajectory and the principle of SBO. Therefore, the knee and hip brakes were switched on and off even though the time was not right. In Figure 7.5, the left hip angle was locked before it reached 27° in the without FSC system as the hip brake switch was set manually.

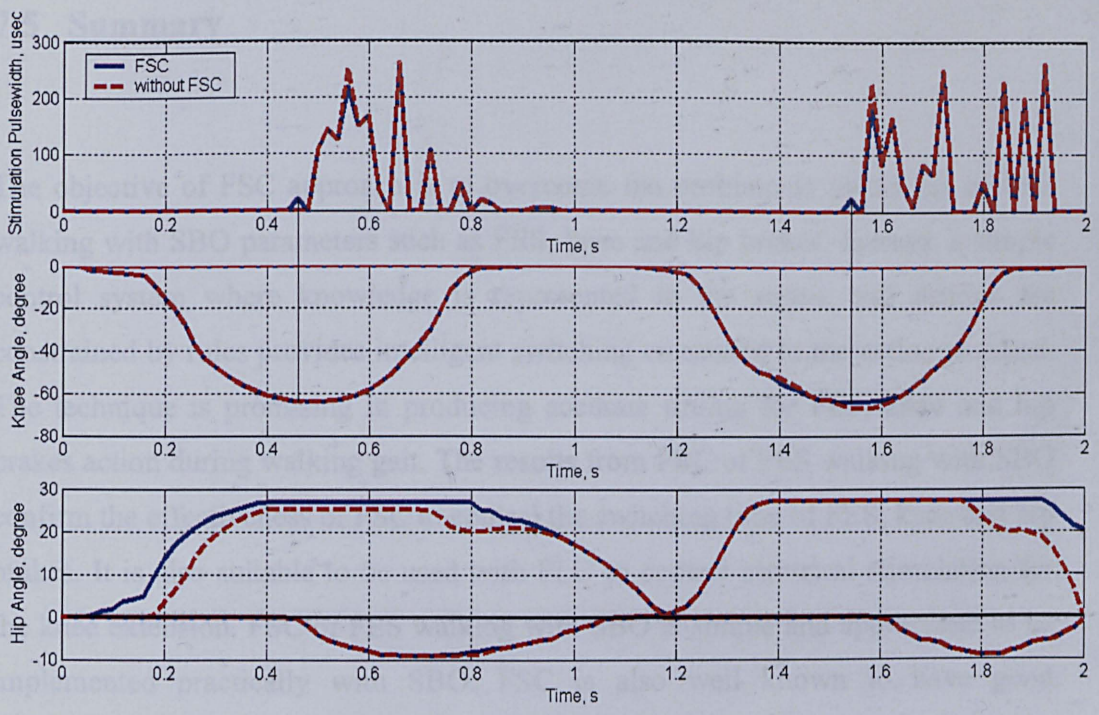


**Figure 7.5: Stimulation pulse-width, knee and hip trajectory for with and without FSC of FES walking with SBO**

Furthermore, results of hip trajectories from FSC system was slightly different compared to the results from system without FSC, but knee trajectories and stimulation pulse-width were almost the same for both systems. This is because using FSC, hip angle at 27° can be catch accurately with the feedback to the FSC. In FSC system also FES stimulation started earlier than without FSC system but the stimulation required was almost the same. As a result, the knee trajectories for both systems were slightly different at the transition between knee flexion and knee extension. Knee trajectory from FSC system was found to be smoother than the system without FSC.

## 7.5 Summary

The objective of FSC approach is to overcome the problem in switching of FES walking with SBO parameters such as FES, knee and hip brakes. Instead, a simple control system where knowledge is represented in the states, and actions are constrained by rules provides intelligent switching command to the action required. The technique is promising in producing accurate timing for FES, knee and hip brakes action during walking gait. The results from FSC of FES walking with SBO confirm the effectiveness of FSC to control the switching time of FES, knee and hip brakes. It is also suitable to be used with FLC to control electrical stimulation for the knee extension. FSC of FES walking with SBO is simple and appropriate to be implemented practically with SBO. FSC is also well known to have good robustness for external and internal disturbances of the system.

# Chapter 8

# Conclusion and Future Work

This chapter presents the relevant conclusions drawn from the work undertaken and attempts to place these in the context of developing an FES system for paraplegic mobility. The main achievements in the area of FES for SCI especially paraplegic mobility are highlighted. Finally, recommendations for future work in these studies are described.

## 8.1 Conclusion

This research has been motivated by the need for a reliable and practical system for paraplegic mobility. Therefore, the main aim for this research has been to develop a reliable, effective, safe and affordable complete system for FES-assisted paraplegic walking with wheel walker. In order to achieve this aim successfully, every aspect from modelling to control to hybrid orthosis have been investigated and analysed vigilantly. This has been to make sure the system developed will be cost and time effective, safe and reliable in helping paraplegic mobility. Furthermore, it is also to ensure that the technology used in this research enhanced the current technology available in the market and contribute the atest FES-assisted walking system for paraplegic.

The most effective method to enhance performance of the FES-assisted paraplegic system is to reduce the electrical stimulation required since the electrical stimulation pulse is proportional to muscle fatigue. Therefore this research aimed to enhance the FES-walking performance by minimising the electrical stimulation required through the development of muscle model, fully utilising the voluntary upper body effort by introducing body weight transfer technique during FES-walking, selection of optimum stimulation parameters, the application of optimal control techniques and the development of hybrid orthosis. The power of this system depends on the accuracy of the modelling parameters. For this thesis, the research work has focused on modelling, analysing and developing a complete system, which may suggest the optimum stimulation pulse-width required for FES-assisted paraplegic walking with wheel walker. The development of a complete FES walking system for paraplegic in this thesis consists of seven levels.

First, an appropriate model of humanoid with wheel walker that replicate the real environment has to be developed in order to simulate the FES-walking precisely. This is one of the critical parts in this thesis where the model has to be as accurate as possible. In this study, the humanoid with wheel walker has been modelled with anthropometric data, based on the subject used in this work, within the MSC.visualNastran4D software environment (vN4D). The leg stiffness and damping parameters have been optimally tuned and incorporated in the humanoid model developed to make sure the humanoid's leg has the same properties as the subject used. The vN4D allows the model to be simulated as a virtual physical environment with the ability of measurement made in real-time. The vN4D is impressive and highly competent software that can replace conventional approaches involving complex mathematical modelling. Moreover, the ability of vN4D to be integrated with Matlab/Simulink environment has given additional advantages in this study where the interaction of the humanoid model with the muscle model and control system has shown real world conditions visually and measurably.

Second level is the development of the muscle models. This is a crucial part in this work where human muscle is known as a highly complex, time-varying and nonlinear dynamic system. Therefore, it is necessary to develop the muscle model using a suitable approach to cope with the complexity and uncertainty of the model and yet represent the actual system accurately. However, most of the current muscle models developed either experimentally or physically are not suitable to be used with control application. This is because those models characterise each muscle features alone and there is no relation between the model features, and this may prevent them from combining as one complete model. Muscle models developed by Riener and Ferrarin are well-known muscle models for FES control application.

The Riener's muscle model is a physiological based muscle model that comprises calcium dynamics and muscle fatigue. Unfortunately, it needs to identify many muscle parameters that require customised experimental procedures and special equipment to be applied to the subject to obtain one complete Riener's muscle model. On the other hand, Ferrarin's muscle model is a first order transfer function obtained by a least squares error method and easy to implement. Moreover, it does not require many individualised muscle parameters to be identified. However, Ferrarin's muscle model does not provide extra information about muscle behaviour including muscle fatigue. In this thesis, new experimental based muscle model has been developed using ANFIS technique. Riener's and Ferrarin's muscle models together with ANFIS muscle model have been compared and investigated. For quadriceps muscle model, the performances of these three models, at their respective most optimally tuned set of parameters, have been evaluated. Of these, the ANFIS quadriceps muscle model has been found to be the most suitable model for use to determine the muscle torque while integrated with FES. The ANFIS hamstrings muscle model has also been developed and it has shown outstanding performance.

Third, muscle fatigue associated with FES is an important topic in this research area. During repetitive activation of FES, muscle fatigue is found to appear more quickly. Therefore increasing either the frequency or the pulse-width of stimulation will be necessary to permit the targeted muscle force to be maintained during a functional task. In this thesis, investigation on the effect of FES stimulation parameters on muscle fatigue has been carried out. The results from this study have shown that high frequencies give rise to faster muscle fatigue while stimulation pulse-width has no significant effect on muscle fatigue but highly affects the maximum muscle force. Therefore, by maintaining the stimulation frequency and controlling the stimulation pulse-width muscle fatigue can be reduced during FES application. The results from this work can serve as guidance for selection of optimum stimulation parameters in FES application. In this thesis also, initial work has been carried out on calculating the paraplegic maximum potential that can be used to avoid or reduce leg spasm or/and leg injury during and after stimulating paraplegic leg. This work needs more investigation and experiment in the future so that FES can be fully utilised.

Fourth, the development of intelligent control techniques in order to deliver the correct amount of stimulation pulse-widths required by the quadriceps and hamstrings muscles sequentially to perform a smooth and safe walking gait. In this thesis, two types of control techniques, namely PID and FL control have been used. The conventional PID controllers have been employed to track predefined walking trajectories by adjusting the knee torque and stimulation pulse-width in two separate studies. The first study is to analyse the torque required for paraplegic walking with wheel walker and to determine optimum stimulation parameters based on the maximum amount of torque while the second study has been to apply control for the stimulation pulse-width to be fed to the muscle model. PID control has been found to be needing more torque and stimulation pulse-width as compared to FLC. Moreover, PID control has achieved poor tracking of the predefined reference trajectories compared to FLC. Thus, while both controllers have been able to track

predefined walking trajectories, FLC has used less electrical stimulation compared to PID control.

Fifth, the introduction of body weight transfer (BWT) will improve the paraplegic walking performance by minimising the electrical stimulation required. BWT is practical technique and applicable to paraplegic walking with wheel walker. Paraplegic still have upper body strength that can be used to compensate for the changes by volitional activity of the trunk and upper extremities acting over the wheel walker on the ground. In this technique, while the left leg is in the position of swing phase, the upper body will tilt to the right and transfer the upper body weight to the right leg. From the hypothesis, this technique will reduce the pressure and weight on the left leg and furthermore the torque required will also decrease. In this thesis, this hypothesis is investigated by applying the same control procedure for FES walking with BWT technique and the performance has been analysed. It has been demonstrated that BWT technique is practical and effective if paraplegic can be train to follow the upper body posture required in BWT technique. The torque required in BWT can be reduced more than 80% of torque required without BWT.

Sixth, a new hybrid orthosis based on exploiting natural dynamics of human gait called spring brake orthosis (SBO) has been employed for further enhancement of FES walking performance. SBO simplifies the control task and results in smooth motion and more natural-like trajectory produced by the flexion reflex for gait in spinal cord injured subjects. SBO first introduced by Gharooni et al. (2001) for leg swing and in this thesis extended work has been done to increase paraplegic walking performance using SBO. During FES walking using SBO, electrical stimulation is required to be applied to the quadriceps muscle for leg extension only, compared to the FES walking without SBO where electrical stimulation is required for both quadriceps and hamstrings muscles. It has been demonstrated that torque required in FES walking with SBO using FLC can be reduced by 11.49% for quadriceps muscles as compared with the torque required for quadriceps muscles in FES walking without SBO. On the other hand, the torque required in FES walking

with SBO for hamstring muscles is totally reduced by 100% as explained above, there is no torque required for hamstring muscle in walking with SBO since spring is used for knee flexion. Therefore, SBO with FES helps spinal cord injured person walking more efficiently, effectively, safely and reliably.

Seventh, the implementation of finite state control (FSC) in FES walking with SBO is to overcome the problem in switching of FES walking with SBO. This technique has been introduced to enhance or improve the switching technique in FES walking with SBO. The technique is promising in producing an accurate timing for FES, knee and hip brakes action during walking gait. This has been shown in the results, where the hip brake catches 0° and 27° in both legs during FES walking with SBO. It is also suitable to be used with FLC to control electrical stimulation for the knee extension. FSC technique is simple and suitable to be applied to FES walking with SBO. Furthermore, FSC technique is appropriate to be implemented practically with SBO.

## 8.2 Recommendation for Further Work

Even though this research has embarked on alternative strategies to improve the FES walking system, this thesis has provided an impetus for future work. The research presented seems to have raised more questions that it has answered. There are several lines of research arising from this work which should be pursued and there are some natural extensions to this work that would help expand and strengthen the results.

1. Although, the use of visual Nastran (vN4D) software environment for modelling part illustrates results visually and measurably, the execution time is demanding. Therefore, alternative software with more effective and less

computational time may increase the efficiency of the virtual investigation in the future for research in this area.

2. In this thesis, novel experimental based quadriceps and hamstrings muscle models have been developed. The performance of the muscle model developed is outstanding. However, it may be improved if more data from various paraplegic subjects can be obtained to enhance the current model to become more generalised muscle model. It will also be more useful model in the future.

3. The investigation on the effect of stimulation parameters on the muscle fatigue is an important part before any experiment can be performed using FES. In this thesis, initial work has been done to obtain the stimulation parameters for the specific functional task to be applied to the paraplegic. Further investigation can be carried out by obtaining more experimental data from a range of paraplegic subjects. This can create comprehensive database for thorough analysis on the muscle fatigue and stimulation parameters.

4. In this research, all the controllers' parameters were obtained by trial and error method. Further improvement can be made by optimising the parameters using evolutionary algorithm or optimisation techniques to enhance the control of the FES walking system.

5. Even though in this thesis, the developments of spring brake orthosis is almost in the final stage, the implementation of SBO was only done in the simulation environment. The development of the intelligent control techniques including finite state control and body weight transfer for FES walking with wheel walker have been carried out and evaluated in the simulation environment. The realisation of the developed approaches in experimental and practical settings need to be carried out.

# References


Abdel-Magid, Y. L. and Abido, M. A. (2003). "Coordinated design of a PSS and a SVC-based controller to enhance power system stability." *International Journal of Electrical Power & Energy System*: 695-704.

Abramson, S. A. (1948). "Bone disturbances in injuries to spinal cord and caude equina (Paraplegia)." *Journal of Bone and Joint Surg* **30**: 982-987.

Acosta-Marquez, C. and Bradley, D. A. (2005). The analysis, design and implementation of a model of an exoskeleton to support mobility. *Rehabilitation Robotics, 2005. ICORR 2005. 9th International Conference on.*

Andrews, A. W., Thomas, M. W. and Bohannon, R. W. (1996). "Normative Values for Isometric Muscle Force Measurements Obtained With Hand-held Dynamometers." *PHYS THER* **76**(3): 248-259.

Andrews, B. J., Kirkwood, C. A., Barnett, R. W., Phillips, G. F. and Baxendale, R. H. (1992). *control of hybrid FES-Orthosis for Paraplegics*. Amsterdam, IOS Press.

Anonymous. (2008). "Pine Discount Pharmarcy." Retrieved 10 June 2008, 2008, from http:// www.onlineservicesidmworkinprogress.com/PinesDiscountPharmacy/Products.html.

Anonymous. (2011). "Gait Analysis." Retrieved 18 April 2011, 2011, from http://www.me.queensu.ca/people/deluzio/GaitAnalysis.php.

Anonymous. (2010). "Skeletal muscle." Retrieved 24 December 2010, 2010, from http://www.shoppingtrolley.net/skeletal%20muscle.shtml.

Apparelyzed. (2010). "What is a spinal cord? [online]." *Apparelyzed.com Spinal Cord Injury Discussion Forum and Support* Retrieved 19 March 2010, 2010, from http://www.apparelyzed.com/spinal_cord_injury.html.

Bailey Bio. (2010). "Muscular system." Retrieved 24 December 2010, 2010, from http://www.baileybio.com/plogger/?level=picture&id=239

Bajd, T., Kralj, A. and Karcnik, T. (1994). Unstable states in four-legged locomotion. Intelligent Robots and Systems '94. 'Advanced Robotic Systems and the Real World', IROS '94. Proceedings of the IEEE/RSJ/GI International Conference on.

Bajd, T., Kralj, A. and Zefran, M. (1992). Improved four-point walking by functional electrical stimulation. Engineering in Medicine and Biology Society, 1992. Vol.14. Proceedings of the Annual International Conference of the IEEE.

Bajd, T., Zefran, M. and Kralj, A. (1995). Timing and kinematics of quadrupedal walking pattern. Intelligent Robots and Systems 95. 'Human Robot Interaction and Cooperative Robots', Proceedings. 1995 IEEE/RSJ International Conference on.

Bavel, Z. (1983). *Introduction of the theory of automata*, Reston Publishing Company (Prentice Hall).

Brandstatter, B. and Baumgartner, U. (2002). "Particle swarm optimization - mass-spring system analogon." *Magnetics, IEEE Transactions on* **38**(2): 997-1000.

BeDell, K. K., Scremin, A. M. E., Perell, K. L. and Kunkel, C. F. (1996). "Effects of functional electrical stimulation-induced lower extremity cycling on bone density of spinal cord-injured patients1." *American Journal of Physical Medicine & Rehabilitation* **75**(1): 29-34.

Besio, W., Tepavec, D., Tarjan, P. and Ozdamar, O. (1997). Command generation for FES enhanced grasping utilizing surface EMG in cervical injured. *Biomedical Engineering Conference, 1997., Proceedings of the 1997 Sixteenth Southern.*

Bigland-Ritchie, B., Zijdewind, I. and Thomas, C. K. (2000). "Muscle fatigue induced by stimulation with and without doublets." *Muscle & Nerve* **23**(9): 1348-1355.

Binder-Macleod, S. A. and Russ, D. W. (1999). "Effects of activation frequency and force on low-frequency fatigue in human skeletal muscle." *J Appl Physiol* **86**(4): 1337-1346.

Binder-Macleod, S. A. and Snyder-Mackler, L. (1993). "Muscle fatigue: Clinical implications for fatigue assessment and neuromuscular electrical stimulation." *PHYS THER* **73**(12): 902-910.

Bjørnstrup, J. (1995). Estimation of human body segment parameters: Historical background. *Internal Technical Report*, Aalborg Univeristy - Faculty of engineering, Science and Medicine - Department of Electronic System (ES).

Bouri, M., Stauffer, Y., Schmitt, C., Allemand, Y., Gnemmi, S., Clavel, R., Metrailler, P. and Brodard, R. (2006). The WalkTrainer: A robotic system for walking rehabilitation. *Robotics and Biomimetics, 2006. ROBIO '06. IEEE International Conference on.*

Brown-Triolo, D., Triolo, R. and Peckham, P. (1997). Mobility issues and priorities in persons with SCI : A qualitative investigation. *Second Annual IFESS Conference.*

CDRF. (2010). "Paralysis and SCI in the U.S [online]." *Christopher and Dana Reeve Foundation* Retrieved 22 March 2010, 2010, from http://www.christopherreeve.org.

Chen, Y. L., Chen, S. C., Chen, W. L., Hsiao, C. C., Kuo, T. S. and Lai, J. S. (2004). "Neural network and fuzzy control in FES-assisted locomotion for the hemiplegic." *Journal of Medical Engineering and Technology* **28**(1): 32-38.

Chipperfield, A., Purshouse, R., Fleming, P. J., Thompson, H. and Griffin, I. (2002). Multi-objective optimisation in control system design: an evolutionary computing approach. *IFAC World Congress*, Barcelona, Spain.

Chizeck, H. J., Chang, S., Stein, R. B., Scheiner, A. and Ferencz, D. C. (1992). "Identification of electrically stimulated quadriceps muscles in paraplegic subject." *IEEE Transactions On Biomedical Engineering* **46**(1): 51-61.

Chizek, H. J., Kobetic, R., Marsolais, E. B., Abbas, J. J., Donner, I. H. and Simon, E. (1988). "Control of functional neuromuscular stimulation systems for standing and locomotion in paraplegics." *Proceedings of the IEEE* **76**(9): 1155-1165.

Clinkingbeard, J. R., Gersten, J. W. and Hoehn, D. (1964). "Energy cost of ambulation in traumatic paraplegia." *Physical and Rehabilitation Medicine* **43**: 157-165.

Cooper, E. B., Scherder, E. J. A. and Cooper, J. B. (2005). "Electrical treatment of reduced consciousness: experience with coma and Alzheimer's disease." *Neuropsyh Rehabilitation* **15**: 389-405.

Côté, F., Masson, P., Mrad, N. and Cotoni, V. (2004). "Dynamic and static modelling of piezoelectric composite structures using a thermal analogy with MSC/NASTRAN." *Composite Structures,* **65**(3-4): 471-484.

Crago, P. E., Peckham, P. H. and Thrope, G. B. (1980). "Modulation of muscle force by recruitment during intramuscular stimulation." *IEEE Trans. Biomed. Eng* **27**: 679–684.

Davoodi, R. and Andrews, B. J. (1999). "Optimal control of FES-assisted standing up in paraplegia using genetic algorithms." *Medical Engineering & Pysics* **21**: 609-617.

Davoodi, R. and Andrews, B. J. (2004). "Fuzzy logic control of FES rowing exercise in paraplegia." *Biomedical Engineering, IEEE Transactions on* **51**(3): 541-543.

Davoodi, R., Andrews, B. J. and Wheeler, G. D. (2002). "Automatic Finite state control of FES-assisted indoor rowing exercise after spinal cord injury." *Neuromudulation: Technology at the Neural Interface* **5**(4): 248-255.

Denaï, M. A., Palis, F. and Zeghbib, A. (2007). "Modeling and control of non-linear systems using soft computing techniques." *Applied Soft Computing* **7**(3): 728-738.

Donaldson, N. and Chung-Huang, Y. (1998). "A strategy used by paraplegics to stand up using FES." *Rehabilitation Engineering, IEEE Transactions on* **6**(2): 162-167.

Drillis, R. and Contini, R. (1966). *Body Segment Parameters*. New York, Office of Vocational Rehabilitation, Department of Health, Education and Welfare.

Durfee, W. K. and Rivard, A. (2005). "Design and Simulation of a Pneumatic, Stored-energy, Hybrid Orthosis for Gait Restoration." *Journal of Biomechanical Engineering* **127**(6): 1014-1019.

Dutta, A., Kobetic, R. and Triolo, R. J. (2008). "Ambulation after incomplete spinal cord injury with emg-triggered functional electrical stimulation." *IEEE Transactions on Biomedical Engineering* **55**(2): 791-794.

Edrich, T., Riener, R. and Quintern, J. (2000). "Analysis of passive elastic joint moment in paraplegics." *Biomedical Engineering, IEEE Transactions on* **47**(8): 1058-1065.

Epstein, M. and Herzog, W. (1998). *Theoretical Models of Skeletal Muscle*. Chichester and New York, Wiley.

Eser, P. C., Donaldson, N. N., Knecht, H. and Stussi, E. (2003). "Influence of different stimulation frequencies on power output and fatigue during FES-cycling in recently injured SCI people." *Neural Systems and Rehabilitation Engineering, IEEE Transactions on* **11**(3): 236-240.

Fee, J. W. (1995). The leg drop pendulum test in spastic cerebral palsy: the addition of active elements to a passive, nonlinear, second order model. *Biomedical Engineering Conference, 1995., Proceedings of the 1995 Fourteenth Southern.*

Fee, J. W., Jr. (1994). A non-linear, passive, model of the leg drop pendulum test: assessing changes in spastic cerebral palsy after vertical accelerations. *Engineering in Medicine and Biology Society, 1994. Engineering Advances: New Opportunities for Biomedical Engineers. Proceedings of the 16th Annual International Conference of the IEEE.*

Fee, J. W. and S, J. M. (1995). "The leg pendulum test in spastic celebral palsy: the addition of active elements to a passive, nonlinear, second order model."

Feng, W. and Andrews, B. J. (1994). Adaptive fuzzy logic controller for FES-computer simulation study. Engineering in Medicine and Biology Society, 1994. Engineering Advances: New Opportunities for Biomedical Engineers. Proceedings of the 16th Annual International Conference of the IEEE.

Ferguson, K., Polando, G., Kobetic, R., Triolo, R. and Marsolais, E. (1999). "Walking with a hybrid orthosis system." *Spinal cord*: 800-804.

Ferrarin, M., Palazzo, F., Riener, R. and Quintern, J. (2001). "Model-based control of FES-induced single joint movements." *Neural Systems and Rehabilitation Engineering, IEEE Transactions on [see also IEEE Trans. on Rehabilitation Engineering]* **9**(3): 245-257.

Ferrarin, M. and Pedotti, A. (2000). "The relationship between electrical stimulus and joint torque: a dynamic model." *Rehabilitation Engineering, IEEE Transactions on [see also IEEE Trans. on Neural Systems and Rehabilitation]* **8**(3): 342-352.

Ferris, D. P., Sawicki, G. S. and Domingo, A. (2005). "Powered lower limb orthoses for gait rehabilitation." *Top Spinal Cord Injury Rehabilitation* **11**(2): 34-49.

FESNW. (2010). "Functional electrical stimulation North West." Retrieved 3 January 2010, 2010, from http://www.fesnorthwest.co.uk/.html.

Franken, H. M., Veltnik, P. H., Tijsmans, R., Nijmeijer, H. and Boom, H. B. K. (1994). "Identification of Passive knee joint and shank dynamics in paraplegics using quadriceps stimulation." *IEEE transactions on rehabilitation engineering* **1**(3): 154-164.

Gharooni, S., Heller, B. and Tokhi, M. O. (2001). "A new hybrid spring brake orthosis for controlling hip and knee flexion in the swing phase." *Neural Systems and Rehabilitation Engineering, IEEE Transactions on [see also IEEE Trans. on Rehabilitation Engineering]* **9**(1): 106-107.

Gharooni, S. C., Tokhi, M. O. and Tavakoli, S. (2007). Energy reduction in paraplegic gait to support weight on treadmill. *International Conference on Biomechanics of the lower limb in health, disease and rehabilitation*, Salford, UK.

Goldberg, D. E. (1989). Genetic algorithms in search optimization and machine learning, Addison-Wesley Publishing company.

Goldfarb, M. and Durfee, W. (1996). "Design of a controlled-brake orthosis for FES-aided gait." *IEEE Trans. Rehab. Eng* **4**(1): 13-24.

Goldfarb, M., Korkowski, K., Harrold, B. and Durfee, W. (2003). "Preliminary evaluation of a controlled-brake orthosis for FES-aided gait." *Neural Systems and Rehabilitation Engineering, IEEE Transactions on [see also IEEE Trans. on Rehabilitation Engineering]* **11**(3): 241-248.

Granham, G. M., Thrasher, T. A. and Popovic, M. R. (2006). "The effect of random modulation of functional electrical stimulation parameters on muscle

fatigue." *Neural Systems and Rehabilitation Engineering, IEEE Transactions on [see also IEEE Trans. on Rehabilitation Engineering]* **14**(1): 38-45.

Graupe, D. and Kohn, K. H. (1998). "Functional neuromuscular stimulator for short distance ambulation by certain thoracic-level spinal cord injured paraplegics." *Surg. Neurol.* **51**: 202-207.

Graupe, D. and Kordylewski, H. (1994). Neural network control of FES in paraplegics for patient-responsive ambulation. *Circuits and Systems, 1994. ISCAS '94., 1994 IEEE International Symposium on.*

Hausdorff, J. and Durfee, W. (1991). "Open-loop position control of the knee joint using electrical stimulation of the quadriceps and hamstrings." *Medical and Biological Engineering and Computing* **29**(3): 269-280.

Hendershot, D. M. and Phillips, C. A. (1988). Improvement of efficiency in a quadriplegic individual using an FES-RGO system. *Engineering in Medicine and Biology Society, 1988. Proceedings of the Annual International Conference of the IEEE.*

Hill, A. V. (1938). "The heat of shortening and the dynamic constants in muscle." *Proceedings of the Royal Society*: 136-195.

Holland, J. (1975). *Adaptation in natural and artificial systems.* Ann Arbor MI, University of Michigan Press.

Hollerbach, J. M. and Flash, T. (1982). "Dynamic interactions between limb segments during planar arm movement." *Biological Cybernetics* **44**(1): 67-77.

Hu, Y., Ming, D., Wang, Y. Z., Wong, Y. W., Wan, B. K., Luk, K. D. K. and Leong, J. C. Y. (2004). Three-dimensional dynamical measurement of upper limb support during paraplegic walking. *Engineering in Medicine and Biology Society, 2004. IEMBS '04. 26th Annual International Conference of the IEEE.*

Huq, M. S. (2009). Analysis and control of hybrid orthosis in therapeutic treadmill locomotion for paraplegia. *Automatic Control and System Engineering*, The University of Sheffield. **PhD**.

Hussain, Z. and Tokhi, M. O. (2008). Modelling of muscle extension and flexion for fes-assisted indoor rowing exercise. *Modeling & Simulation, 2008. AICMS 08. Second Asia International Conference on.*

Huxley, A. F. (1957). "Muscle structure and theories of contraction." *Progress in Biophysics and Biophysical Chemistry*: 255-318.

Huxley, A. F. and Niedergerke, R. (1954). "Structural changes in muscle during contraction: interference microscopy of living muscle fibres." *Nature* **173**(4412): 971-973.

Huxley, H. and Hanson, J. (1954). "Changes in the cross-striations of muscle during contraction and stretch and their structural interpretation." *Nature* **173**(4412): 973-976.

IFESS (2010). "International functional electrical stimulation society " Retrieved 15 December 2010, 2010, from http://www.ifess.org/

Inman, V. T., Ralston, H. J., Todd, F. and Lieberman, J. C. (1981). *Human walking* Williams & Wilkins Baltimore.

Isakov, E., Douglas, R. and Berns, P. (1992). "Ambulation using the reciprocating gait orthosis and functional electrical stimulation." *Paraplegia* **30**: 239-245.

Jantzen, J. (1998). Tuning of Fuzzy, PID controllers. *Technical Report in Department of Automation.* Lyngby, Denmark, Technical University of Denmark.

Jaspers, P., Van Petegem, W., Van der Perre, G. and Peeraer, L. (1996). Design of an automatic step intention detection system for a hybrid gait orthosis. *Engineering in Medicine and Biology Society, 1996. Bridging Disciplines for Biomedicine. Proceedings of the 18th Annual International Conference of the IEEE.*

Karu, Z. Z., Durfee, W. K. and Barzilai, A. M. (1995). "Reducing muscle fatigue in fes application by stimulating with n-let pulse trains." *IEEE Transactions on Biomedical Engineering* **42**(8): 809-817.

Keith, D. (2010). "Simulation with vN4D saves 4 months in Rotary Engine Development [online]." *HTP Company* Retrieved 5 April 2010, 2010, from http://www.htpcompany.com/mscsoftware.html.

Kennedy, J. and Eberhart, R. (1995). Particle swarm optimization. Neural Networks, 1995. Proceedings., IEEE International Conference on.

Kesar, T. and Binder-Macleod, S. (2006). "Effect of frequency and pulse duration on human muscle fatigue during repetitive electrical stimulation." *Journal of Physiology* **91**(6): 967-976.

Kesar, T., Chou, L.-W. and Binder-Macleod, S. A. (2008). "Effects of stimulation frequency versus pulse duration modulation on muscle fatigue." *Journal of Electromyography and Kinesiology* **18**(4): 662-671.

Kobetic, R., To, C. S., Schnellenberger, J. R., Audu, M. L., Bulea, T. C., Gaudio, R., Pinault, G., Tashman, S. and Triolo, R. J. (2009). "Development of hybrid orthosis for standing, walking and stair climbing after spinal cord injury." *Journal of Rehabilitation Research and Development* **46**(3): 447-462.

Kralj, A. and Bajd, T. (1989). Functional electrical stimulation: Standing and walking after spinal cord injury. Florida, CRC Press.

Latiff, I. A. and Tokhi, M. O. (2009). Fast convergence strategy for particle swarm optimization using spreading factor. *IEEE Congress on Evolutionary Computing*, Norway.

Levy, M., Mizrahi, J. and Susak, Z. (1990). "Recruitment, force and fatigue characteristics of quadriceps muscles of paraplegics isometrically activated by surface functional electrical stimulation." *Journal of Biomedical Engineering* **12**(2): 150-156.

Liberson, W., Holmquest, H. and Scott, M. (1961). "Functional electrotherapy: stimulation of the common peroneal nerve synchronized with the swing phase of gait of hemiplegic subjects." *Arch Phys Med Rehabil* **42**: 202-205.

Lin, D. C. and Rymer, W. Z. (1991). "A quantitative analysis of pendular motion of the lower leg in spastic human subjects." *Biomedical Engineering, IEEE Transactions on* **38**(9): 906-918.

Liptak, B. (1995). *Instrument engineers' handbook: Process control.* Radnor, Pennsylvania, Chilton Book Company.

Mahfouf, M. (2004). *Fuzzy logic modelling & control –ACS6112, Theoretical & practical aspects of fuzzy Systems*, Department of Automatic Control And systems Engineering, the University of Sheffield, MSc Control Systems Course Notes. .

Makssoud, H. E., Guiraud, D. and Poignet, P. (2004). "Mathematical muscle model for functional electrical stimulation control strategies." *Proceedings of the 2004 IEEE International Conference on Robotic and Automation*: 1282-1287.

Mamdani, E. H. (1974). "Application of fuzzy algorithms for simple dynamics plant." *Proceedings of IEE* **121**(12): 1585-1588.

Marsolais, E. B. and Mansour, J. M. (1992). "Hip and trunk stability in paraplegic electrically augmented gait." *Engineering in Medicine and Biology Magazine, IEEE* **11**(4): 64-67.

Matsunaga, T., Shimada, Y. and Sato, K. (1999). "Muscle fatigue from intermittent stimulation with low and high frequency electrical pulses." *Archives of Physical Medicine and Rehabilitation* **80**(1): 48-53.

McGhee, R. B. (1968). "Some finite state aspects of legged locomotion." *Mathematical Biosciences* **2**(1-2): 67-84.

Mikelberg, R. and Reid, S. (1981). "Spinal cord lesions and lower extremity bracing: An overview and follow up study." *Paraplegia* **19**: 379-385.

Mizrahi, J. (1997). "Fatigue in muscle activated by functional electrical stimulation." *Physical and Rehabilitation Medicine* **9**(2): 93-129.

Mourselas, N. and Granat, M. H. (1998). "Evaluation of patterned stimulation for use in surface functional electrical stimulation systems." *Medical Engineering & Physics* **20**(5): 319-324.

MSC visualNastran (2011). "MSC visualNastran 4D." Retrieved 18 April 2011, 2011,from http://www.mae.virginia.edu/meclab/images/visualNastran4D.pdf

Mulder, A. J. (1991). Finite state control in functional neuromuscular stimulation. Netherlands, Drukkeriji FEBO.

Mulder, A. J., Veltink, P. H., Boom, H. B. K. and Zilvold, G. (1992). "Low-level finite state control of knee joint in paraplegic standing." *Journal of Biomedical Engineering* **14**(1): 3-8.

Nene, A. V. and Jennings, S. J. (1989). "Hybrid paraplegic locomotion with the parawalker using intramuscular stimulation: A single subject study." *Paraplegia* **27**: 125-132.

Nene, A. V. and Patrick, J. H. (1990). "Energy cost of paraplegic locomotion using the parawalker: electrical stimulation hybrid orthosis." *Archives of Physical Medicine and Rehabilitation* **71**: 116-120.

NINDS. (2010, 20 March 2010). "Spinal Cord Injury: Hope hrough research [online]." *National Institute of Neurological Disorders abd Stroke (NINDS)*, from http://www.ninds,gov/disorders/sci/detail_sci.html.

Panda, S. and Padhy, N. P. (2007). "Comparison of particle swarm optimization and genetic algorithm for tcsc-based controller design." *International Journal of Computer Science and Engineering*: 41-49.

Passino, K. M. and Yurkovich, S. (1998). *Fuzzy Control*. USA, Addison Wesley Longman Inc.

Pedotti, A., Ferrarin, M., Quintern, J. and Riener, R. (1996). *Neuroprosthetics - from basic research to clinical application*, Springer-Verlag Berlin.

Pheasant, S. (1886). *Bodyspace: Anthropometry, Ergonomics and design*. London, Taylor and Francis.

Philips, C. A. and Hendershot, D. M. (1991). "Functional electrical stimulation and reciprocating gait orthosis for ambulation exercise in a tetraplegic patient: A case study." *Paraplegia* **29**: 268-276.

Popovic, D. (1987). Hybrid systems for motion restoration. *Artificial Organs*, New York, VCH Publisher.

Popovic, D. and Joni, S. (1999). Control of bipedal locomotion assisted with functional electrical stimulation. *American Control Conference, 1999. Proceedings of the 1999.*

Popovic, D., Tomovic, R. and Schwirtlich, L. (1989). "Hybrid assistive system-the motor neuroprosthesis." *Biomedical Engineering, IEEE Transactions on* **36**(7): 729-737.

Popovic, D. B. (1990). "Dynamics of the self-fitting modular orthosis." *Robotics and Automation, IEEE Transactions on* **6**(2): 200-207.

Popovic, M. R., Dietz, V., Keller, T., Pappas, I. and Morar, M. (1999). Grasping and walking neuroprostheses for stroke and spinal cord injured subjects. *American Control*, San Diego.

Popovic, M. R., Keller, T., Papas, I. P. I., Dietz, V. and Morari, M. (2001). "Surface-stimulation technology for grasping and walking neuroprostheses." *Engineering in Medicine and Biology Magazine, IEEE* **20**(1): 82-93.

Qiu, J. (2009). "China spinal cord injury network: Changes from within." *Lancet Neuro* **8**(7): 606-607.

Quigley, M. J. (1977). "Should functional ambulation be a goal for paraplegic persons?" *Clincal Prosthetics and Orthotics* **1**(4): 4-6.

Rabischong, E. and Guiraud, D. (1993). "Determination of fatigue in the electrically stimulated quadriceps muscle and relative effect of ischaemia." *Journal of Biomed Engineering* **15**(6): 443-450.

Riener, R. and Edrich, T. (1997). Significant of passive elastic Joint Moments in FES. 2nd Annual Conference: International Functional Electrical Stimulation Society and 5th Triennial Conference: Neural Prostheses: Motor Systems V, Simon Fraser University, Burnaby, British Columbia, Canada.

Riener, R. and Edrich, T. (1999). "Identification of passive elastic joint moments in the lower extremities." *Journal of Biomechanics*: 539-544.

Riener, R. and Fuhr, T. (1998). "Patient-driven control of FES-supported standing up: a simulation study." *IEEE Transactions on Rehabilitation Engineering* **6**(2): 113-124.

Riener, R., Quintern, J. and Schmidt, G. (1996). "Biomechanical model of the human knee evaluated by neuromuscular stimulation." *Journal of Biomechanics* **29**(9): 1157-1167.

Routh, G. R. and Durfee, W. K. (2003). Doublet stimulation to reduce fatigue in electrically stimulated muscle during controlled leg lifts. *Engineering in Medicine and Biology Society, 2003. Proceedings of the 25th Annual International Conference of the IEEE.*

Sau Kuen, N. and Chizeck, H. J. (1994). Fuzzy vs. non-fuzzy rule base for gait event detection. Engineering in Medicine and Biology Society, 1994. Engineering Advances: New Opportunities for Biomedical Engineers. Proceedings of the 16th Annual International Conference of the IEEE.

Scheiner, A., Ferencz, D. C. and Chizeck, H. J. (1994). The effect of joint stiffness on simulation of the complete gait cycle. *Engineering in Medicine and*

*Biology Society, 1994. Engineering Advances: New Opportunities for Biomedical Engineers. Proceedings of the 16th Annual International Conference of the IEEE.*

Schwirtlich, L. and Popovic, D. (1984). Hybrid orthoses for deficient locomotion. *VIII Advances in External Control of Human Extremities* Beograd.

Shaw, I. S. (1998). *Fuzzy control of industrial systems: theory and applications.* Norwell, USA, Luwer Academic Publisher.

Sisto, S. A., Forrest, G. F. and Faghri, P. D. (2008). Technology for mobility and quality of life in spinal cord injury, analyzing a series of options available. *IEEE Engineering in Medicine and Biology* 56-68.

Solomonow, M., Aguilar, E., Reisin, E., Baratta, R. V., Best, R., Coetzee, T. and D'Ambrosia, R. (1997). "Reciprocating gait orthosis powered with electrical muscle stimulation (RGO II). Part I: Performance evaluation of 70 paraplegic patients." *Orthopedics* **20**(4): 315-324.

Solomonow, M., Lu, Y., Best, R., Baratta, R. V., Shoji, H. and D'Ambrosia, R. (1990). The RGO generation ii:high efficiency FES Powered orthosis as a practical walking system for paraplegics. *Engineering in Medicine and Biology Society, 1990., Proceedings of the Twelfth Annual International Conference of the IEEE.*

Stallard, J. and Major, R. E. (1995). "The influence of orthosis stiffness on paraplegic ambulation and its implications for functional electrical stimulation (FES) walking systems." *Int. Prosthet. Orthot* **19**: 108-114.

Thrasher, A., Graham, G. M. and Popovic, M. R. (2005). "Reducing muscle fatigue due to functional electrical stimulation using random modulation of stimulation parameters." *Journal of Artificial Organs* **29**(6): 453-458.

Tinazzi, M., Zanette, G., La Porta, F., Polo, A., Volpato, D., Fiaschi, A. and Mauguière, F. (1997). "Selective gating of lower limb cortical somatosensory evoked potentials (SEPs) during passive and active foot movements." *Electroencephalography and Clinical Neurophysiology/Evoked Potentials Section* **104**(4): 312-321.

Tomovic, R. (1972). Hybrid actuator for orthotic systems: Hybird assistive systems. *IV advances in external control of human Extremities*, Beograd.

Tomovic, R. and Karplus, W. J. (1961). Land Locomotion-simulation and control. *International Symposium External Control of Human Extreameties*, Dubrovnik, Yugoslavia.

Tomovic, R. and McGhee, R. B. (1966). "A finite state approach to the synthesis of bioengineering control systems." *Human Factors in Electronics, IEEE Transactions on* **HFE-7**(2): 65-69.

Veltink, P. H. and Donaldson, N. (1998). "A perspective on the control of FES-supported standing." *Rehabilitation Engineering, IEEE Transactions on* **6**(2): 109-112.

Vignes, R. M. (2004). Modelling muscle fatigue in digital humans. *University of Iowa.*

Wang, H., Xiu-Hua, C., Lin, G. X. and Fa, R. M. (2001). "Strength investigation of composite honeycomb structure after repair." *Acta Aeronautica et Astronautica Sinica* **22**(3): 270-273.

Wartenberg, R. (1951). "Pendulousness of the leg as a diagnostic test." *Journal of Neurology* **1**: 8-24.

Winter, D. A. (1990). *Biomechanics and motor control of human movement.* New York, Willey-Interscience.

Yu-Luen, C., Shih-Ching, C., Weoi-Luen, C., Chin-Chih, H., Te-Son, K. and Jin-Shin, L. (2004). "Neural network and fuzzy control in FES-assisted locomotion for the hemiplegic " *Journal of Medical Engineering & Technology* **28**(1): 32-38.

Zadeh, L. A. (1965). "Fuzzy sets." *Information and Control* **8**: 338-353.

Zahalak, G. I. (1990). *Modeling muscle mechanics (and energetics).* Heidelberg, New York, Springer-Verlag.

Zajac, F. E., Topp, E. L. and Stevenson, P. J. (1986). A Dimensionless Musculotendon Model. *Conference of IEEE Engineering, Medical Biology Society*, Dallas-Ft Worth, Texas.

Zefran, M., Bajd, T. and Kralj, A. (1996). "Kinematic modeling of four-point walking patterns in paraplegic subjects." *Systems, Man and Cybernetics, Part A, IEEE Transactions on* **26**(6): 760-770.

Zhaojun, X., Dahai, W., Dong, M. and Baikun, W. (2006). New gait recognition technique used in functional electrical stimulation system control. *Intelligent Control and Automation, 2006. WCICA 2006. The Sixth World Congress on.*